Roles of Programmed Cell Death in Ototoxicity

（薬剤性内耳障害におけるプログラム細胞死の役割）

By

Dalian Ding

April, 2014

A thesis/dissertation for a Doctoral Degree submitted to the Faculty of the

Graduate School of Agricultural and Life Sciences

University of Tokyo

Department of Applied Biological Chemistry

Doctoral Supervisor: Masaru Tanokura

ABSTRACT

Roles of Programmed Cell Death in Ototoxicity

Dalian Ding

University of Tokyo

2014

Ototoxic drug- or chemical-induced cochlear cell death is thought to occur through two major and distinct cell death mechanisms: necrosis and/or apoptosis[1,2]. Necrosis is a disorganized and unprogrammed breakdown of cells with the appearance of denaturation of intracellular proteins and enzymatic digestion in injured cells. In contrast, apoptosis is a death process that is mediated by a predefined intracellular death program in response to stress or cell death signals by various causes, such as aging, ischemia, toxic chemicals, intense noise, irradiation, blast wave, heavy metals and etc. [3-23]. The overall goal of my dissertation study is to provide new basic knowledge of the molecular basis for the programmed cell death in ototoxicity.

First, I show how administration of kanamycin damages cochlear cells in guinea pigs. Kanamycin is an aminoglycoside bacteriocidal antibiotic which causes severe damage to the kidney as well as inner ear. When guinea pigs received an intramuscular injection of kanamycin sulfate with a dose of 400 mg/kg of body weight per day for 10 days, kanamycin induced both necrotic cell death and apoptotic cell death in the cochlea. Long-term treatment with kanamycin also caused severe swelling of mitochondria and expansion and rupture of lysosomes. This in turn triggered lysosome-mediated necrosis leading to the release of acid hydrolase into the cytoplasm and eventually to digestion of all the organelles[9,24]. In contrast, a short-term

administration of another aminoglycoside antibiotic chemical, gentamicin with a dose of 40 mg/ml induced acute apoptosis in mice. *In vitro,* treatment for 24 hours with gentamicin at 0.1 mM ~ 3 mM also induced acute apoptosis in the cultured cochlear organs[25].

Most toxic foreign chemicals cannot enter into the cochlea because of the blood-cochlear barrier. The diuretics, drugs that treat high blood pressure, glaucoma and edema, can selectively break the blood-cochlear barrier by reducing the blood supply to or causing ischemia in the cochlear lateral wall. Hence, widely used diuretics such as ethacrynic acid and furosemide can be used to open the blood-cochlea barrier allowing ototoxic chemicals to enter into the cochlea [4,9,26-32]. Next, I show how co-administration of gentamicin and ethacrynic acid damages cochlear cells: When chinchillas were treated by co-administration of gentamicin and ethacrynic acid, the concentration and accumulation of gentamicin increased in the cochlear liquid due to the temporal rupture of the blood-cochlea barrier. In the middle and basal turns of the cochlea, massive hair-cell loss, including destruction of the stereocilia and cuticular plate, occurred 12 hours after gentamicin and ethacrynic acid treatment. Condensation and fragmentation of DNA, a morphological feature of apoptosis, were also observed 5–6 hours post-treatment in the hair cells in the basal turn of the cochlea. Moreover, succinate dehydrogenase levels significantly decreased in the basal turn of the cochlea 4 hours following gentamicin and ethacrynic acid treatment; these early changes were accompanied by the release of cytochrome *c* from the mitochondria into the cytosol, and increased levels of caspase-9 and caspase-3. Collectively these results suggest that mitochondrial apoptotsis may play a major role in gentamicin induced acute cochlear damage.

Third, I show that cisplatin, a widely used chemotherapy agent, causes cell death in the cochlea[3,28,33-39]. Previous studies have shown that cisplatin alone fails to induce significant

cochlear damage in experimental animal models due to the blood-cochlear barrier. However, when cisplatin is co-administered with ethacrynic acid, ethacrynic acid significantly enhances the ototoxic effects of cisplatin by temporarily disrupting the blood-cochlear barrier. In agreement with those reports, co-administration of cisplatin at a dose of 0.8 mg/kg and ethacrynic acid at a dose of 40 mg/kg caused extensive outer hair cell and inner hair cell damage in chinchillas. Nuclei of the hair cells appeared relatively normal 6 hours after cisplatin and ethacrynic acid treatment. At 12 hours post-treatment, nuclei were condensed and fragmented. At 48 hours post-treatment, a large number of nuclei were missing. The apoptosis initiator caspase 8 and the membrane cell death receptor TRADD were detected in the hair cells at 6~ hours post-treatment. Caspase 8 levels increased at 24 hours post-treatment, but dramatically diminished at 48 hours post-treatment. The apoptosis executioners, caspase 3 and caspase 6, which act downstream of caspase 8, were also detected in the hair cells at 12–24 hours post-treatment. Together, these results suggest that cisplatin and ethacrynic acid treatment induces an apoptosis pathway that is initiated by TRADD and caspase 8, followed by caspase-3 and caspase-6, leading to hair cell loss.

Fourth, I show that the antimalarial drug mefloquine induces cochlear cell death through apoptosis [7,40-43]. Mefloquine is a widely used anti-malarial drug. However, clinical reports suggest that mefloquine is ototoxic and neurotoxic. I found that mefloquine caused cochlear hair cell loss in a dose-dependent manner in rats; hair cell loss progressed from the base to the apex and from the outer hair cells to the inner hair cells as mefloquine concentration increased. Mefloquine also rapidly damaged spiral ganglion neurons and auditory nerve fibers in a dose-dependent manner. Shrunken and/or fragmented nuclei, morphological features of cells undergoing apoptosis, were observed in the hair cells, spiral ganglion neurons and supporting

cells. Moreover, caspase 8, caspase 9, and caspase 3, were heavily expressed in the hair cells and spiral ganglions 24 hours after mefloquine treatment. These results indicate that mefloquine damages both the sensory and neural cells in postnatal rat cochlea by activating caspases 8, caspases 9, and caspases 3.

Numerous drugs and chemicals have long been known to be ototoxic. Yet, they are still used extensively worldwide, particularly in developing countries because of their low costs. Unfortunately, there is currently no treatment for drug- or chemical-induced hearing loss. Moreover, precisely how these drugs or chemicals cause cochlear damage remains unknown. My thesis study results convincingly demonstrate that all of the commonly used drugs, kanamycin, gentamicin, cisplatin, and mefloquine, can cause cochlear hair cell and/or neuron damage through specific programmed cell death pathways. Because kanamycin, gentamicin, cisplatin, and mefloquine continue to be used as antibiotics, anticancer, or anti-malaria agents, there is an urgent need to understand the cellular and molecular mechanisms underlying ototoxicity and to develop a treatment for drug-induced hearing loss. The data presented in my thesis will provide an enhanced understanding of the fundamental mechanisms underlying cochlear damage and hearing loss induced by ototoxic chemicals and my hope is to contribute to ending this terrible side effect.

ACKNOWLEDGEMENTS

In 1968, during the Great Proletarian Cultural Revolution in China, I was exiled to a rural farm camp when I was just 16 years old. I was one of the millions of Chinese students who were denied the opportunity to attend high school or college during the Revolution. Since all the universities in China were closed for more than ten years during the Cultural Revolution, I was forced to work as a peasant farmer in southeast China with no opportunity to get a formal education for two years. Shortly after I returned from the farm camp, I obtained a job in the Union Hospital as a cleaner. During those years, I went to an evening nursing school. After two-years of training, I obtained a job in the Department of Otolaryngology in the Union Hospital first as a nurse and then as a laboratory technician. In 1978, I moved to Shanghai and sought to reclaim my education. There, I worked full-time as a laboratory technician in the Otology laboratory in the Shanghai Second Medical University, while spending nights and weekends going to a middle school, high school, and college. After spending more than ten long years, I finally graduated from the Fudan University in Shanghai, China.

In 1995, I moved to the United States to work as an assistant research fellow. In 2003, I was promoted to associate professor and then to full professor in July of 2007.

Today, I have more than 43 years of experience studying anatomy, pathology, and physiology of inner ears. My areas of expertise also include anatomy and physiology of the vestibular system, neurotoxic and ototoxic chemicals and drugs, presbycusis, cochlear microcirculations, blood-cochlea barrier, endolymphatic hydrops, and noise- and/or blast wave- induced inner ear damage. I have published over 300 scientific articles, 20 book chapters, and books in the field of auditory research. I have taught more than 20 training courses, and trained more than 1,000 medical

doctors or graduate students in the fields of inner ear anatomy and histology and otolaryngology not just in China and the U.S.A., but all over the word. Today, there are over 1,000 of my former students who are training their students and staffs to dissect out cochlear and vestibular organs from various species, including rats, mice, chinchillas, guinea pigs, rabbits, and monkeys. However, because of the lost years during the Cultural Revolution, and because I had to work to raise a family, I did not have the opportunity to obtain a Ph.D degree until I met Dr. Shinichi Someya in the summer of 2011. It was Dr. Someya who encouraged me to apply for a PhD program at the University of Tokyo and has supported my PhD studies since 2011. Therefore, I would like to first gratefully thank Dr. Someya for his encouragement, help and support in countless ways. I would also like to express my greatest appreciation to my primary advisor, Dr. Masaru Tanokura, for accepting me into the Ph.D. program and for supporting me throughout my Ph.D. studies. His encouragement, advice, and guidance helped me to achieve my academic dream. I would like to thankfully acknowledge Dr. Richard Salvi, Director of Center for Hearing and Deafness at The University at Buffalo for his intimate friendship, valuable suggestions, and crucial aid to my PhD studies. Finally I would like to thank my wife, Haiyan Jiang, for her love and support throughout my entire academic career.

Dalian Ding

August 18, 2014

CONTENTS

LIST OF FIGURES

TABLE

CHAPTER 1: INTRODUCTION

1. Classification of cell death

Cell death can be divided into two major classifications, apoptosis (programmed cell death) and necrosis (unprogrammed cell death) (Figure 1-1) [1,2]. Apoptosis is a form of programmed cell death that is mediated by a predefined intracellular death program. Programmed cell death can be triggered by a wide range of stimuli, such as trauma, hypoxia, irradiation, blast waves, intense noise, and toxic chemicals. In response to these stimuli, the body removes damaged and/or unnecessary cells through a network of proapoptotic and antiapoptotic proteins. There are several major characteristics of apoptosis: blebbing (formation of blebs in the plasma membrane in a cell), cell shrinkage, nuclear fragmentation, chromatin condensation, and chromosomal DNA fragmentation.[4,9,28,33,44-68].

In contrast to apoptosis, necrosis is a form of accidental or unprogrammed cell death that is caused by cell injury, trauma, toxins, and/or infections. In necrosis, in response to injury, various death receptors are activated, which results in the loss of cell membrane integrity followed by unregulated digestion of cell components. The key morphological characteristics of necrosis include intracellular swelling and cell membrane rupture. For example, necrosis involves the rupture of lysosome membranes that release degrading enzymes to digest the cell components[9,23,24,69,70]. Although the term "necrosis" is commonly used, accidental or unprogrammed cell death is also called "oncosis" instead of "necrosis," because the term of oncosis refers specifically to cellular swelling [71,72].

Figure 1-1

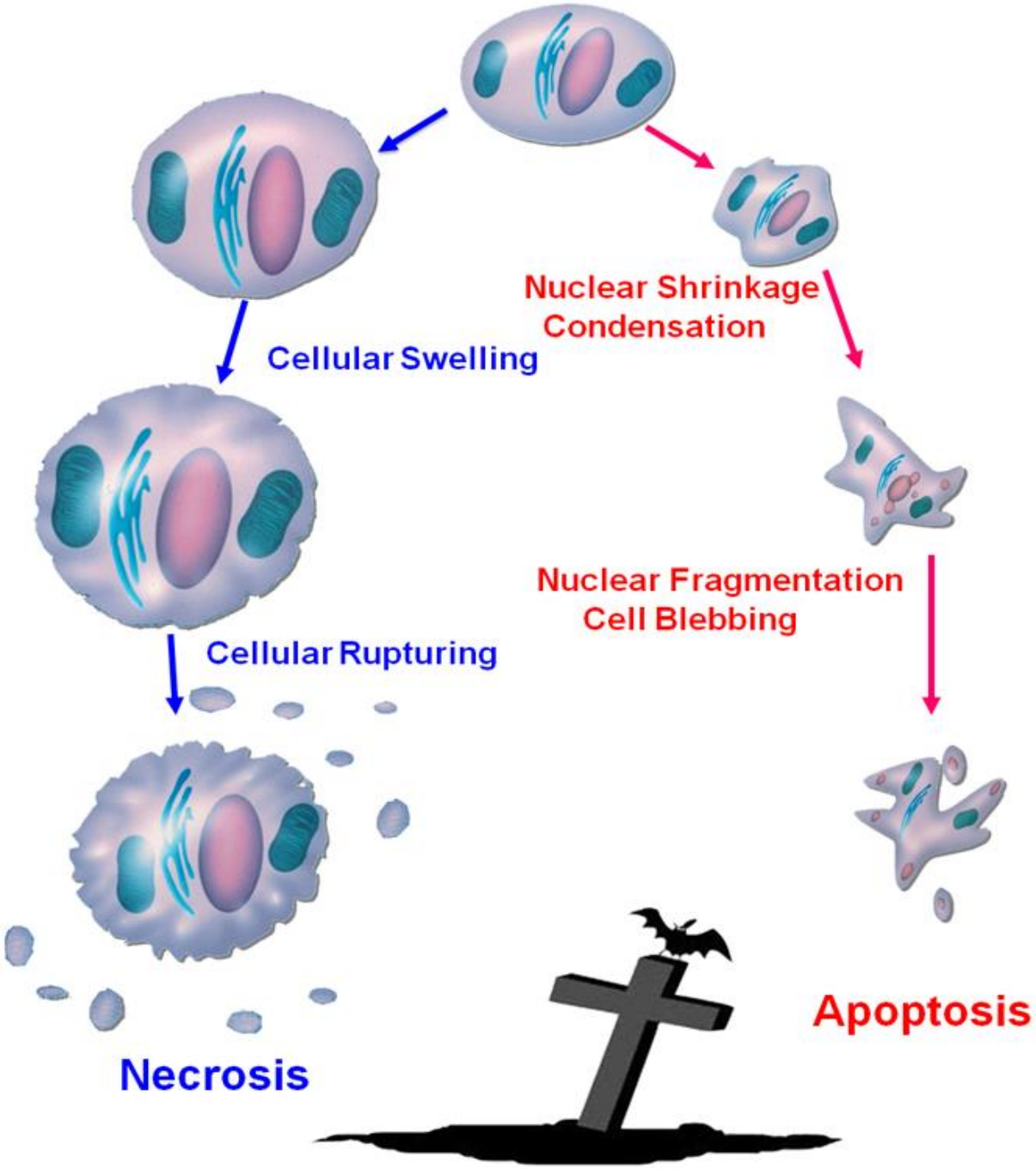

Figure 1-1. Classification of cell death can be divided into two major classifications: Apoptosis and necrosis. Apoptosis is a form of programmed cell death that involves blebbing, cell shrinkage, nuclear fragmentation, chromatin condensation, and chromosomal DNA fragmentations. Necrosis is a form of accidental or unprogrammed cell death that involves intracellular swelling and cell membrane rupture.

2. Inner ear cell death caused by ototoxic chemicals

As stated above, ototoxic chemicals are known to causes necrosis, a form of cell injury that results in an unregulated digestion of cell components. Previous studies have shown that necrotic cell death, characterized by cellular swelling and cellular rupturing, occurs only in chronic ototoxicity, particularly by aminoglycoside antibiotics, but not in acute ototoxicity [5,9,24,73]. Ototoxic chemicals are also known to cause apoptotic cell death, a programmed cell death that leads to self-destruction. Previous studies have shown that acute ototoxicity usually induces apoptotic cell death, characterized by nuclear shrinkage or condensation, followed by nuclear fragmentation or cell blebbing [4,5,9,23,28,33,35-37,40-42,48,58,67,74-78].

3. Ototoxic effects of aminoglycoside antibiotic compounds

Aminoglycoside antibiotics were developed in the 1940s for treating gram negative infections; however, their use is constrained by their toxic effects on the kidneys and inner ears [79-83]. Despite these side effects, aminoglycosides continue to be used extensively worldwide because of the low costs, effectiveness in treating certain types of infections [84] and ability to suppress premature stop codons in muscular dystrophy and cystic fibrosis [85-91].

The bactericidal effects of aminoglycosides arise from their ability to inhibit protein synthesis. Aminoglycosides preferentially bind to prokaryotic and mitochondrial ribosomes at the A (adenosine) decoding region of the 16S ribosomal RNA (rRNA), which results in codon misreading and suppression of translation[92-94].

Bacterial diseases occur not only in humans, but also in agricultural plants and livestock. Accordingly, there are a large number of agricultural antibiotics and veterinary antibiotics, including aminoglycoside antibiotics, developed over the past 50 years[95-118]. Fortunately, there is

an increasing awareness of food safety issues regarding the use of antibiotics, and there are several legislations that control antibiotic residual levels in livestock so that local and state governments can pay close attention to food safety for agricultural crops and livestock meats. Up to today, to our knowledge, there is no report of crop- or livestock meat-induced ototoxicity in humans [104,105,112].

In eukaryotic cells, aminoglycosides antibiotics are thought to bind weakly to the cytoplasmic rRNA due to an A to G (guanosine) substitution in the 16S rRNA [77,119,120]. However, in mitochondria, cell components are more susceptible to aminoglycosides because the mitochondrial 16S rRNA has A at the 1408 position in an eukaryotic cell [121]. These observations are consistent with the endosymbiosis theory which states that mitochondria arose from ancient prokaryotic organisms [122]. Because eukaryotic mitochondria have A at the same position on the 16S rRNA as that of prokaryotic rRNAs, mitochondria are thought to be a major target for aminoglycoside antibiotics [5,9,23,123-125].

In an experimental model of acute ototoxicity by co-administration of ethacrynic acid and kanamycin or gentamicin *in vivo*, aminoglycoside antibiotic accumulates in the cochlear perilymph in a short period of time due to the destruction of the blood-cochlea barrier in the stria vascularis on the cochlear lateral wall by ethacrynic acid treatment [4,5,9,23,29,30,32,124-126]. The aminoglycoside antibiotic then enters the hair cell and accumulates in the mitochondria. This in turn damages the mitochondrial membrane, leading to cytochrome *c* release from the cracked mitochondrial membrane, resulting in the activation of Apaf-1, caspase-9, and caspases-3, and hair cell destruction.

In contrast, aminoglycoside ototoxicity develops slowly under treatment with kanamycin or gentamicin alone due to the existence of the blood-cochlea barrier [5,9,23,24,29,73,123,126-128]. In an

experimental model of chronic ototoxicity, the cell destruction process is complex and varies with drug dose and drug treatment duration, and those damaged cells usually show pathological features of both necrosis (enlarged nuclei) and apoptosis (shrunken nuclei) [5,9,23,24,29,73,123,125,128,129]: hair cell death occurs through the combination of mitochondrial apoptosis initiated by mitochondrial membrane damage, and necrotic cell death by lysosomal membrane damage and/or cell membrane rupture [5,9,23,24,73,123,130].

4. Ototoxic effects of platinum anti-tumor compounds

Platinum-based compounds are widely used for chemotherapy. Cisplatin, carboplatin, oxaliplatin, and nedaplatin are widely used platinum agents currently approved for cancer treatment[131-138]. However, platinum chemicals have side effects and are also environmentally hazardous. Evidence indicate that platinum chemicals, including platinum, palladium, and rhodium from automobile catalytic converters, water supplies, medical facilities waste water could pollute the environment [139-142]. To monitor platinum pollution in the environment, duckweed is utilized as a bioindicator of platinum pollution. Duckweed is also considered as remediation for cisplatin polluted water supplies to enhance thiol synthesis[139,143,144].

The antitumor effects of platinum agents arise from intra or interstrand cross-linking of DNA and/or protein-DNA cross-linking that inhibits DNA replication and RNA transcription, thereby blocking tumor proliferation through the induction of apoptosis [36,74,145-151]. However, platinum agents also cause nephrotoxicity, neurotoxicity, ototoxicity, and vestibulotoxicity through damaging sensory cells and/or neurons[3,47,136,152-158]. Indeed, one third of cisplatin-treated patients develop hearing loss and vestibular dysfunction [3,5,28,31,33,36-38,47,69,74,77,153,154,158-168]. In laboratory animals, cisplatin-induced hair cell damage usually begins in the base of the cochlea

and spreads toward the apex, promoting the progression of hearing loss[169-172]. Cisplatin damages cochlear outer hair cells (OHCs) first before damaging the inner hair cells (IHCs), while in vestibular organs, cisplatin damages the type-I hair cells first before damaging the type II hair cells [28,36,74,173,174]. In contrast, in *in vitro* systems, cisplatin damages the OHCs and IHCs evenly through the entire length of the cochlea[36,38,158,162]. Carboplatin, generally considered to be less ototoxic than cisplatin, is however, highly ototoxic in chinchillas as it produces an unusual pattern of damage that begins in the IHCs and type I spiral ganglion neurons (SGN) [3,5,11,17,69,74,124,158,164,166-168,175-184]. On the other hand, oxaliplatin, known to be highly neurotoxic to the dorsal root ganglion, does not cause ototoxicity in rats [185], although we have shown previously that oxaliplatin is highly toxic to both hair cells and SGN in neonatal cochlear organotypic cultures, [3,5,154,158,186]. The differences in the degrees of ototoxicity and cochlear cell damage patterns between *in vitro* and *in vivo* systems for cisplatin, carboplatin or oxaliplatin might be due to the different uptake levels for each platinum compound: the low ototoxicity of oxaliplatin relative to cisplatin is thought to be attributed to a lower uptake of oxaliplatin in cochlea tissues[187]. Nevertheless, the precise mechanisms remain unclear [158].

As stated earlier, the major targets of platinum compounds in the cochlea are sensory hair cells, spiral ganglion neurons, and the stria vascularis, and apoptosis is thought to play a role in platinum agent-induced cell death in both *in vivo* or *in vitro* systems [5,33,36,37,41,47,74,154,169,170,172,188-194]. Under platinum agent treatment, a death signal in the cell membrane is thought to initiate apoptosis by activating caspase-8, followed by the activation of caspase-3, caspase-6, and p53 to stimulate a wide network of apoptosis signaling pathways [5,28,33,36,37,47,48,195].

5. Ototoxic effects of antimalarial mefloquine

Malaria is a mosquito-borne infectious disease caused by plasmodium[196-200]. Malaria produces recurrent attacks of shaking, chills, headaches; muscle aches, tiredness, nausea, vomiting, and high fever, and is one of the most painful sicknesses with a high death rate. It is one of the leading causes of death worldwide in the tropical and subtropical regions of developing countries in Africa, Asia, and America. Approximately 300-500 million people develop malaria and 1.5-3 million people, mostly children, die each year[196-200]. Though malaria is a fatal sickness, it can be cured or treated by antimalarial drugs such as mefloquine and quinine. Mefloquine (Lariam ®), developed in the 1960's, is a widely used antimalarial drug because mefloquine is less toxic compared to quinine, even though the therapeutic effects and adverse side effects are similar in mefloquine and quinine [201]. Because of its long half-life, mefloquine is often used at a moderate and prophylactic dose for travelers and military personnel. However, a higher dosage of mefloquine is known to cause adverse side effects. These adverse effects include anxiety, panic attacks, nightmares, dizziness, tremors, headaches, fatigue, grand mal seizures, and suicidal ideation[202-210]. In addition, mefloquine treatment causes hearing and balance disturbances by damaging the cochlear and vestibular hair cells and spiral ganglion neurons through an apoptosis program [211]: in postnatal cochlear and vestibular organotypic cultures, mefloquine treatment at <10 μM induces apoptotic cell loss of cochlear and vestibular hair cells and spiral ganglion neurons in a dose dependent manner by initiating an intrinsical and/or extrinsical death signal [40,41,67,212]. This cell death pathway/process is in contrast to that of aminoglycosides, whose cell degeneration typically starts from inside the cell or initiates apoptosis from the cell membrane. Therefore, mefloquine-induced cell death appears to involve apoptotic cell death initiated by simultaneous extracellular and intracellular signals[5,7,40-43,67,212]. Yet, precisely how anti-malaria agents cause ototoxicity remains unclear.

6. Ototoxic effects of other chemicals

In addition to the ototoxic antibiotics, antineoplastics, and antimalarials discussed above, there are many other chemicals that are known to have severe ototoxic effects, including diuretics [4,9,26-32,195,213], analgesic-antipyretics [75,214,215], heavy metals [8,21,216,217], organic solvents [19], cardiac glycosides [12,218-220], analogs of glutamate [154,221-223], herbicides [224-227], and insecticides [228-231]. These chemicals damage inner ear cells through different cell death mechanisms. For example, diuretics block the blood supply to the cochlear lateral wall and damage the cochlear cells by causing ischemia and anoxia [26,27,29-31,213,232,233]. This is followed by free radical-induced damage during reperfusion. Analgesic-antipyretics such as sodium salicylate, cause apoptotic cell death in the spiral ganglion neurons by generating free radicals, while in cochlear organotypic culture systems, sodium salicylate does not cause sensory hair cell damage or death [75,214]. Heavy metals such as manganese, lead, and cadmium are also known to trigger apoptotic death signals in the spiral ganglion neurons, although those heavy metals do not cause cochlear sensory hair cell damage, suggesting that heavy metals are specifically toxic to the auditory neurons [8,21,23,216,217]. Paraquat, a herbicide, induces oxidative stress and associated apoptosis in the cochlear tissue through superoxide generation[224-227]. In contrast, organic solvents such as dimethyl sulfoxide appear to cause both apoptotic and necrotic cell death since dimethyl sulfoxide-induced cell death displays the activation of apoptotic signal proteins and swelling of the cell body [19]. Currently the specific cell death mechanisms by which analgesic-antipyretics, heavy metals, organic solvents, cardiac glycosides, analogs of glutamate, herbicides, and insecticides cause inner ear cell damage remain unclear. In this dissertation, I investigated how the ototoxic aminoglycoside antibiotics, diuretics, platinum antitumor, or antimalarial compounds discussed above cause sensory hair cell, spiral ganglion neuron, or stria vascularis

cell death at the molecular levels in cochlear organotypic cultures or cochlear tissues from rats, mice, or chinchillas. Understanding the mechanisms of action of ototoxic compounds may define novel therapeutic approaches for hearing loss caused by chemical toxins or drugs.

CHAPTER 2: MATERIALS AND METHODS

1. Subjects

All procedures regarding the use and care of animals in this study were reviewed and approved by the Institutional Animal Care and Use Committee at the State University of New York at Buffalo (NY, USA).

2. Principal reagents

Primary reagents and chemicals used for this research project are listed below. Kanamycin sulfate (K400, Sigma, USA). Gentamicin sulfate (G1914, Sigma, USA). Ethacrynic acid (Sodium Edecrin, Merck, USA). Furosemide (F4381, Sigma, USA). Carboplatin (C2538, Sigma, USA). Cisplatin (P4394, Sigma, USA). FITC-conjugated phalloidin (77415, Sigma, USA). Hank's Balanced Salt Solution (14175, Psisley, U.K). Basal Medium Eagle (B9638, Sigma, USA). Bovine Serum Albumin (A4919, Sigma, USA). Serum-Free Supplement (I1884, Sigma, USA). Glucose (G-2020, Sigma, USA). Penicillin G (P-3414, Sigma, USA). Glutamine (G-6392, Sigma, USA). BME (B-1522, Sigma, USA). Alexa Fluor 488 hydrazide (A 10436, Invitrogen, USA). Formalin (HT5014, Sigma, USA). EDTA (34H0285, Sigma, USA). Osmium Tetroxide (419494, Sigma, USA). Ethanol (G8303, Aaper, USA). Epon 812 (10902, EMS, USA). Toluidine blue (89640, Sigma, USA). Hematoxylin (K4350, Sigma, USA). Glycerin (G2289, Sigma, USA). Propidium iodide (P4170, Sigma, USA). Topro-3 (642661, Invitrogen, USA). Silver nitrate (209139, Sigma, USA). Triton X-100 (T8787, Sigma, USA). Dimethyl formamide (DMF) (D4551, Sigma, USA). Glutaraldehyde (G5882, Sigma, USA). Caspase-8 inhibitor (CaspaTag 8, Invitrogen, USA). Caspase-9 inhibitor (CaspaTag 9, Invitrogen, USA).

Caspase-3 inhibitor (CaspaTag 3, Invitrogen, USA). Caspase-6 inhibitor (CaspaTag 6, Invitrogen, USA). Methanol (34860, Sigma, USA). TRADD antibody (H-278, Santa Cruz, USA). Neurofilament -200 antibody (N0142, Sigma, USA). Neuronal class III b-tubulin antibody (MMS-435P, Covance, USA). APO-BrdU TUNEL Assay Kit (A-23210, Molecular Probes, USA). Dihydroethidium (37291, Sigma, USA). Oligo GEArray (GEA) Apoptosis Series Kit (Superarray, USA). RNeasy Mini Kit (74104, Qiagen, Germany). Truelabeling -AMP linear RNA amplification kit (1005, SuperArray, USA). ArrayGrade cRNA Cleanup Kit (GA-012, SuperArray, USA). Chemiluminescent Detection Kit (D-01, Superarray, USA). RNeasy Mini Kit (74104,Qiagen, Germany). RNase-free DNase set (79254, Qiagen, Germany). Oligo -dT15 (Ambion, USA). DyNAmo SYBR Green I PCR Kit (F-400S, Finnzymes, Finland). PBS (P5368, Sigma, USA).

3. Treatment with ototoxic chemicals

For the chronic ototoxic animal model of long-term treatment with aminoglycoside antibiotics, such as kanamycin or gentamicin, guinea pigs or chinchillas received an intramuscular injection of kanamycin sulfate (500mg/kg) each day for a period of 7-10 days, or an intramuscular injection of gentamicin sulfate (125mg/kg) each day for a period of 7 days. These chemicals were used daily because these ototoxic compounds can be blocked by the blood-cochlea barrier [9,24,27,29,31,33,39,69,73,123,127,234,235].

To avoid obstruction of the blood-cochlea barrier, loop diuretics such as ethacrynic acid and furosemide were used to break the blood-cochlea barrier on the cochlear lateral wall, because they exert their transient ototoxic effects by suppressing blood flow through the capillaries of the stria vascularis. The ischemia and anoxia on the cochlear lateral wall induced by loop diuretics

caused severe strial edema, enlargement of the extracellular spaces and a large decrease in the endolymphatic potential. These histopathological changes on the cochlear lateral wall disrupted the blood-cochlea barrier, and greatly enhanced the entry of ototoxic drugs into the cochlea. Therefore, when a loop diuretic was co-administrated with other ototraumatic agents such as aminoglycoside antibiotics or platinum antitumor drugs, it exacerbated the hearing loss and cochlear pathology rapidly, simply by co-administration [3,4,9,28-33,36,126,195,218].

4. Cochlear organotypic cultures

The detailed process of preparing cochlear organotypic cultures is described in our earlier publications [7,12,25,40,41,43,125,162,186,225,236-238]. Sprague Dawley rat pups (either sex) at postnatal day 3 or adult chinchillas age 12 to 18 months were decapitated. For cochlear organotypic cultures of rat pups, the cochlea was carefully removed in Hank's Balanced Salt Solution (1X GIBCO, Psisley, U.K.). The lateral wall was dissected away and the whole basilar membrane containing the organ of Corti and spiral ganglion neurons was taken as a flat surface preparation for examination under a microscope. A drop (12μl) of rat tail collagen (Type 1, BD Biosciences, 4236 Bedford, MA), 10×basal medium eagle (BME, Sigma, 2% sodium carbonate, 9:1:1 ratio) was placed in the center of a 35mm diameter culture dish (Falcon 1008, Becton Dickinson) and allowed to gel at room temperature. When gelled, 1.2ml of serum-free medium consisting of 2g bovine serum albumin (BSA, Sigma A-4919), 2ml Serum-Free Supplement (Sigma I-1884), 4.8ml of 20% glucose (Sigma G-2020), 0.4ml penicillin G (Sigma P-3414), 2ml of 200mM glutamine (Sigma G-6392), 190.8ml of 1X BME (Sigma B-1522) was placed in the dish. The cochlear tissues were placed on the surface of the collagen gel (Figure 2-1).

Figure 2-1

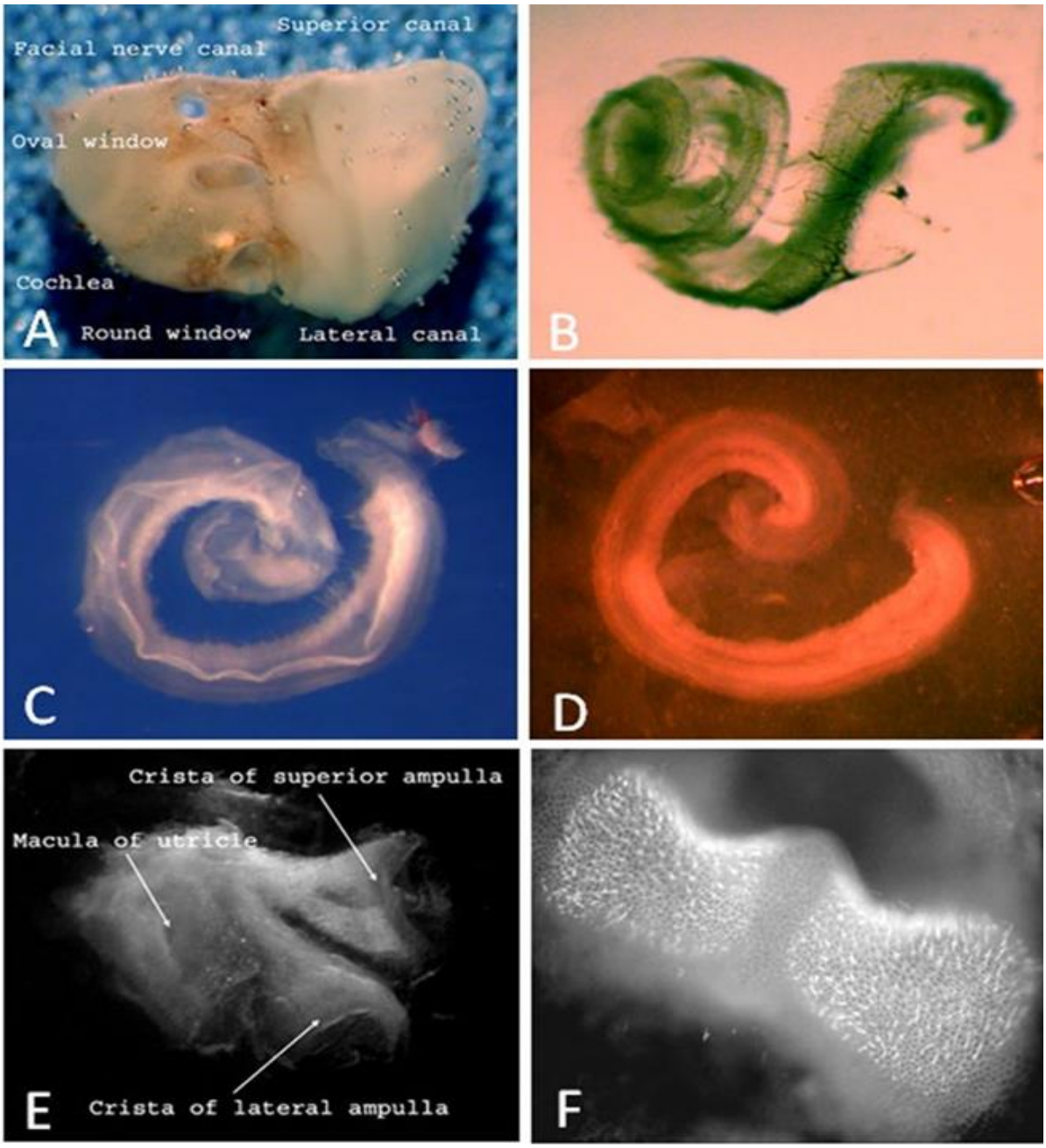

Figure 2-1. Sample preparations of cochlear and vestibular organotypic cultures. (A) Temporal bone was removed by micro-dissection. (B) The cochlear membranous labyrinth was dissected out. (C) The basilar membrane of cochlea was prepared after removing the spiral ligament. (D) The cochlear basilar membrane was placed on the surface of collagen gel. (E) The macula of utricle and crista of lateral and superior semicircular canals were micro-dissected. (F) A surface preparation of crista of superior semicircular canal was growing on the collagen gel.

For cochlear cultures of adult chinchillas, twelve chinchillas aged 12 to 18 months were used for this study. The cochlear basilar membrane was microdissected out, and embedded into collagen gel in dishes prepared as described above. The cochlear explants were placed in an incubator (Forma Scientific,) and maintained at 37℃ in 5% CO2 overnight. On the second day, the cochlear tissue was treated with various concentrations of platinum in culture medium for 24 or 48h.

5. Labeling of ototoxic chemicals

To determine the intracellular action site of ototoxic chemicals, fluorescent compounds or radioactive isotopes were used to label aminoglycoside antibiotics or cisplatin [5,9,23,162,239-241]. To label cisplatin, dye-conjugated cisplatin derivative was obtained by conjugating Alexa Fluor 488 hydrazide (Invitrogen) to carbohydrate-linked platinum (II) complex cis-dichloro [(2-b-D-glucopyranosidyl) propane-1, 3-diamine] platinum. The carbohydrate-linked cisplatin derivative was obtained according the methods described by Chen and colleagues [242] whereas the labeling of Alexa Flour 488 was performed according the manufacturer's instructions. The carbohydrate-linked cisplatin derivative was first converted into an aldehyde, which could readily react with hydrazines, hydroxylamines or primary amine-containing compounds, such as Alexa Fluor 488 hydrazine [162]. To observe gentamicin uptake, rhodamine was conjugated to gentamicin by methods similar to those used to label cisplatin. Rhodamine-labeled gentamicin was applied to a cochlear organotypic culture system to evaluate the time course of gentamicin uptake and to measure differences in uptake rates between cochlear outer hair cells and inner hair cells, and between cochlear hair cells in the apical turn and the basal turn[5,9,23]. To detect the exact cellular binding organelles of kanamycin, kanamycin molecules were conjugated with the radioactive

isotope, tritium, provided by the Chinese Institute of Physics. Guinea pigs were placed under deep anesthesia and the cochlea was surgically exposed. Small holes were made, one each in the scala vestibuli and the scala tympani in the basal turn of the cochlea. A micropipette (tip diameter 50μm) was inserted into the hole in the scala tympani. 0.25% kanamycin in Konishi's artificial perilymph containing ^{3}H-labeled kanamycin (4.4μC$_i$/mg) was perfused into the cochlea with a perfusion rate of 8μl/minute into the scale tympani for 60 minutes. The perfusion drained through the hole in the scala vestibule. After the perfusion, the animals were decapitated. The cochlear tissue was fixed with 2.5% glutaraldehyde, sectioned by ultramicrotome, processed for autoradiography and viewed with a transmission electron microscope [5,9,23,239-241]. Using a subcellular organelle isolation technique, tissue was homogenized and organelles separated by density gradient to detect ^{3}H-labeled kanamycin for further calculation of kanamycin concentrations in various organelles [5,239,241].

6. Histology of the inner ear

6.1 Cochlear and vestibular surface preparations and quantifications

The detailed process of cochlear and vestibular surface preparations is noted in our previous descriptions[5,128,243-246]. In brief, animals were deeply anesthetized with carbon dioxide and then decapitated. The temporal bone was quickly removed, and the round and oval windows were opened. 10% formalin in PBS was slowly perfused through the round window for approximately 1 minute. The temporal bone was then immersed in the fixative overnight. The cochlear basilar membrane, the spiral ligament, and vestibular end-organs including macula of saccule, macula of utricle, and crista of three semicircular canals were micro-dissected out under a dissection

microscope. For surface preparations of cochlear labyrinth, the spiral ligament was separated from basilar membrane, and the basilar membrane was dissected out along the spiral lamina. For surface preparations of vestibular end-organs, the superior, horizontal and posterior portions of the vestibular cavity were opened and the saccule was carefully removed from the underlying bone. The utricle was separated from surrounding tissue by disconnecting the nerves and blood vessels. The otoconia of the saccule and utricle were removed to expose the two maculae. The ampullae were separated from their semicircular canals by cutting the attached nerve fibers, blood vessels and connective tissue. The ampullae were opened to expose the cristae. The cochlear tissue and vestibular labyrinth were then mounted in glycerin on a glass slide (Figure 2-2).

To quantify the cochlear hair cells, specimens were examined under a light microscope (400X) along the entire length of the basilar membrane frame-by-frame from the apical turn to the base to determine the number of missing inner hair cells (IHC) and outer hair cells (OHC). Cochleograms summarizing the percent of hair cells missing as a function of cochlear location, normalized as percent distance from the apex, were constructed for each animal and averaged across animals within a group for statistical analysis [3,5,7,9,29,33,35,41,69,123,125,162,166,236,247].

To quantify the vestibular hair cells, the flat surface preparations of vestibular end-organs were examined under a light microscope (1000X). The number of hair cells was counted in a small region of 0.0067 mm^2 to determine hair cell density[5,33,34].

6.2 Cochlear and vestibular sections

In order to observe the cochlear and vestibular system, temporal sections were prepared for pathological evaluation. The angle of temporal bone sections was along the horizontal section

Figure 2-2

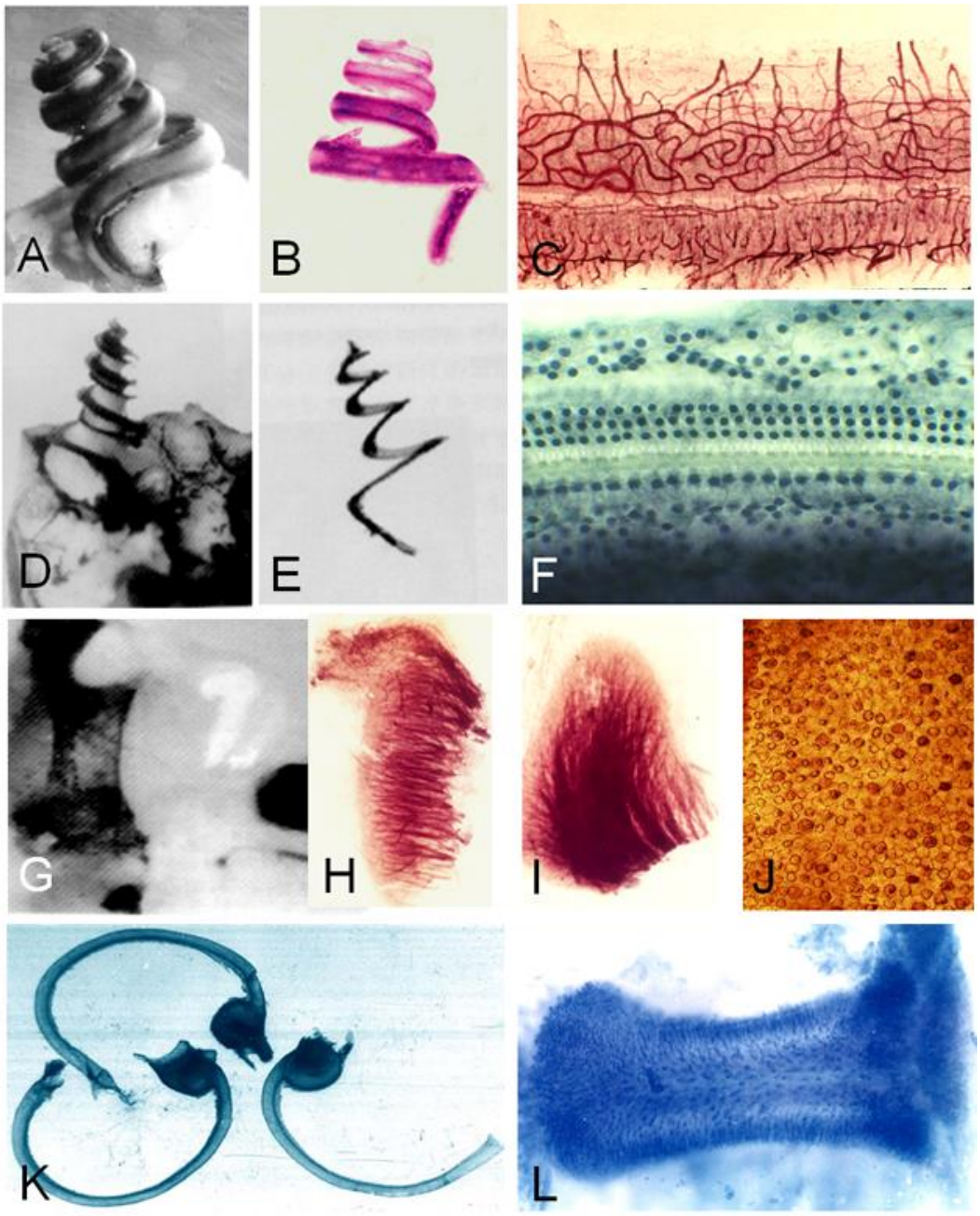

Figure 2-2. Surface preparations of the inner ear. (A) The osseous cochlea was removed to expose the spiral ligament. (B) The spiral ligament was dissected out. (C) Surface preparation of spiral ligament. (D) Cochlear basilar membrane was exposed. (E) Cochlear basilar membrane was dissected out. (F) Surface preparation of cochlear basilar membrane. (G) Vestibular cavity was opened to expose macula of saccule and macula of utricle. (H) Macula of saccule was dissected out. (I) Macula of utricle was dissected out. (J) Surface preparations of macula of utricle. (K) Three semicircular canals were dissected out. (L) Surface preparations of ampullary crest.

parallel to the cochlear modiolus, cochlear and vestibular sections were performed routinely as described in our previous publications [5,10,69,128,153,164-166,248,249] (Figure 2-3). For example, to embed tissues in plastic for sectioning, the cochlea was fixed with 2% glutaraldehyde in 0.1M PBS, and decalcified with 10% EDTA for 5 days. After rinsing with PBS, the sample was immersed in 2% osmium tetroxide in PBS for 2 hours, dehydrated through a graded series of ethanol solutions ending with 100%, and embedded in Epon 812. After polymerization, Epon 812-embedded cochlear tissue was cut at a thickness of 1.5 μm and collected on glass slides. Sections were stained with toluidine blue, examined under a light microscope (Zeiss Axioskop) and photographed. The number of auditory nerve fibers (ANF) in Habenula Perforata and the number of spiral ganglion neurons (SGNs) in Rosenthal's canal was counted for quantitative analysis.

6.3 Evaluation of cochlear pathology:

To observe the pathological changes during ototoxicity, numerous staining techniques were used for this research project. These results undoubtedly provide important clues for understanding the apoptotic pathways activated by various ototoxic chemicals.

Hematoxylin was one of the first "dyes" used for histological purposes. This compound is actually a natural dye derived from the logwood tree. When oxidized, it forms hematein, which is the active agent that labels the nuclei. Since nuclear swelling or nuclear condensation is characterized as necrosis or apoptosis respectively, observations of nuclear morphological changes by hematoxylin staining are the easiest way to evaluate the cell death pattern. In the hematoxylin staining protocol, stain is applied to the tissue sample for a very brief duration until the staining is easily observed while checking under a microscope. This prevents excessive

Figure 2-3

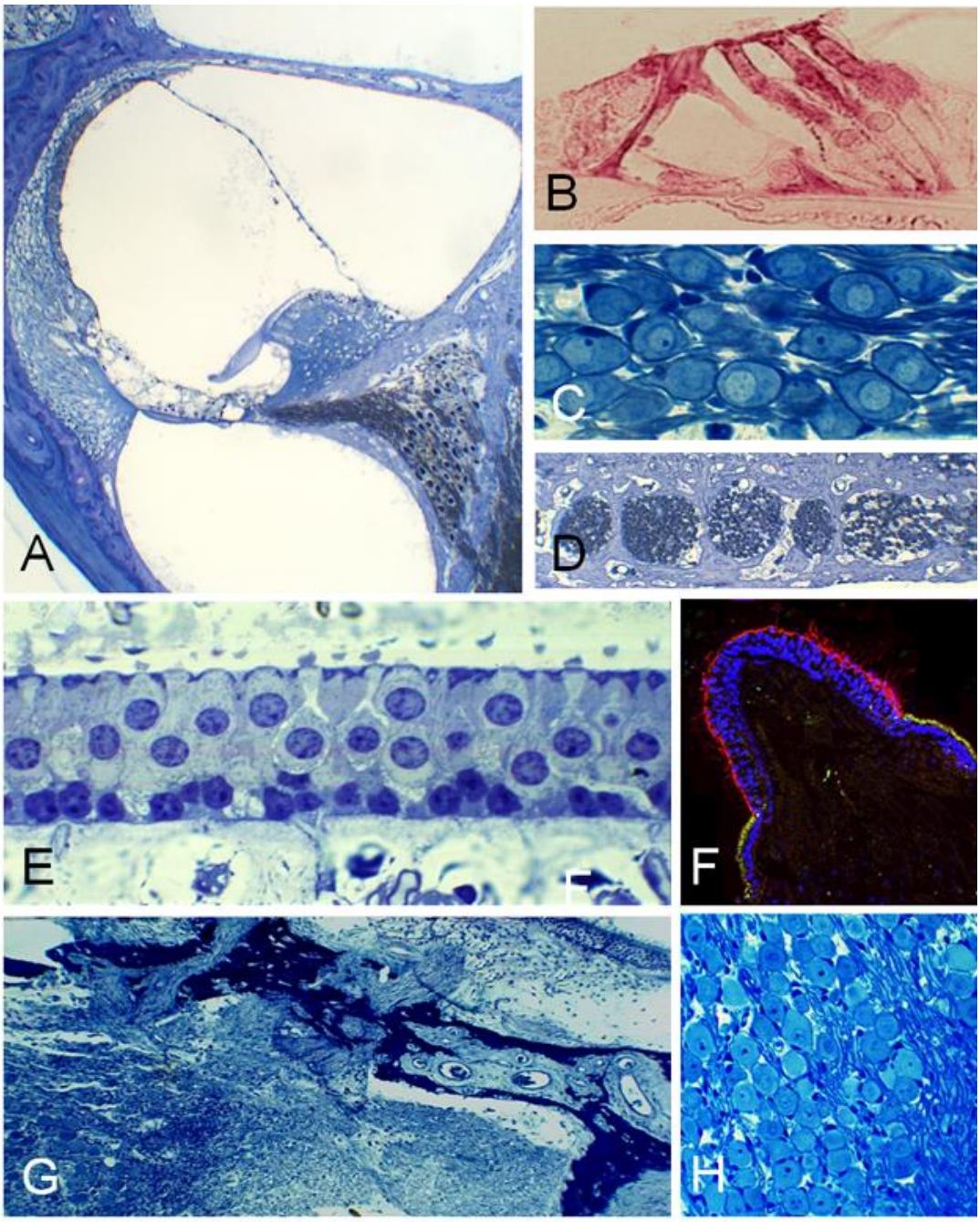

Figure 2-3. Sections of the inner ear. (A) Section of the cochlea. (B) Section of the organ of Corti. (C) Section of spiral ganglion neurons in Rosenthal's canal. (D) Section of auditory nerve fibers in Habenula Perforata. (E) Section of macula of utricle. (F) Section of ampullary crest. (G) Section of utricle and its vestibular ganglion neurons. (H) Section of vestibular ganglion neurons.

staining of the tissue. If over-staining has occurred, the tissue can be de-stained by washing in a dilute acid-alcohol mixture until the appropriate reduction in staining is obtained. After the staining, the cochlear basilar membrane is mounted on a slide as a flat surface preparation in glycerin (Figure. 2-4A) [5,29,31,32,39,127,128,162,239,243,245,246,250-252].

Propidium iodide and Topro-3 are dyes often used to label the nuclei of cells in order to determine the status of the cell cycle or cell degeneration. Propidium iodine is a red dye, prepared by dissolving in de-ionized water at a concentration of 10 mg/mL to make a 1000X stock solution and is stored as aliquots below 0°C. It should be diluted into buffer immediately prior to use and used to stain specimens for 10 to 30 minutes. PI will bind to DNA and RNA, so there is an additional step that should be performed when using this dye to stain nuclei. Following fixation and permeabilization, samples must be treated with RNAse (10 U/mL diluted into buffer for 30 minutes at 37°C in a humidified chamber) in order to avoid background staining of the cytoplasm. Topro-3 is a carbocyanine monomer nucleic acid stain with far-red fluorescence similar to Alexa Fluor®647 or Cy®5 dyes. It is useful as a nuclear counterstain and dead cell indicator, and preferentially stains the nuclear DNA. Therefore, Topro-3 is among the highest-sensitivity probes for nucleic acid detection with low background and bright fluorescent signal. After fixation and dissection, cochlear tissue is simply stained with Topro-3 working solution for 20 minutes according to the manufacturer's protocol (Figure. 2-4B) [4,5,7,9,23,28,33,43,225,238].

Silver nitrate provides auditory researchers with a convenient and useful method for labeling the stereocilia and cuticular plate of cochlear hair cells. The epithelium of the cochlear basilar membrane is a thin sheet of connective tissue covered by sensory epithelium and supporting epithelium. The silver atoms are deposited along the border of the cells and outline

Figure 2-4

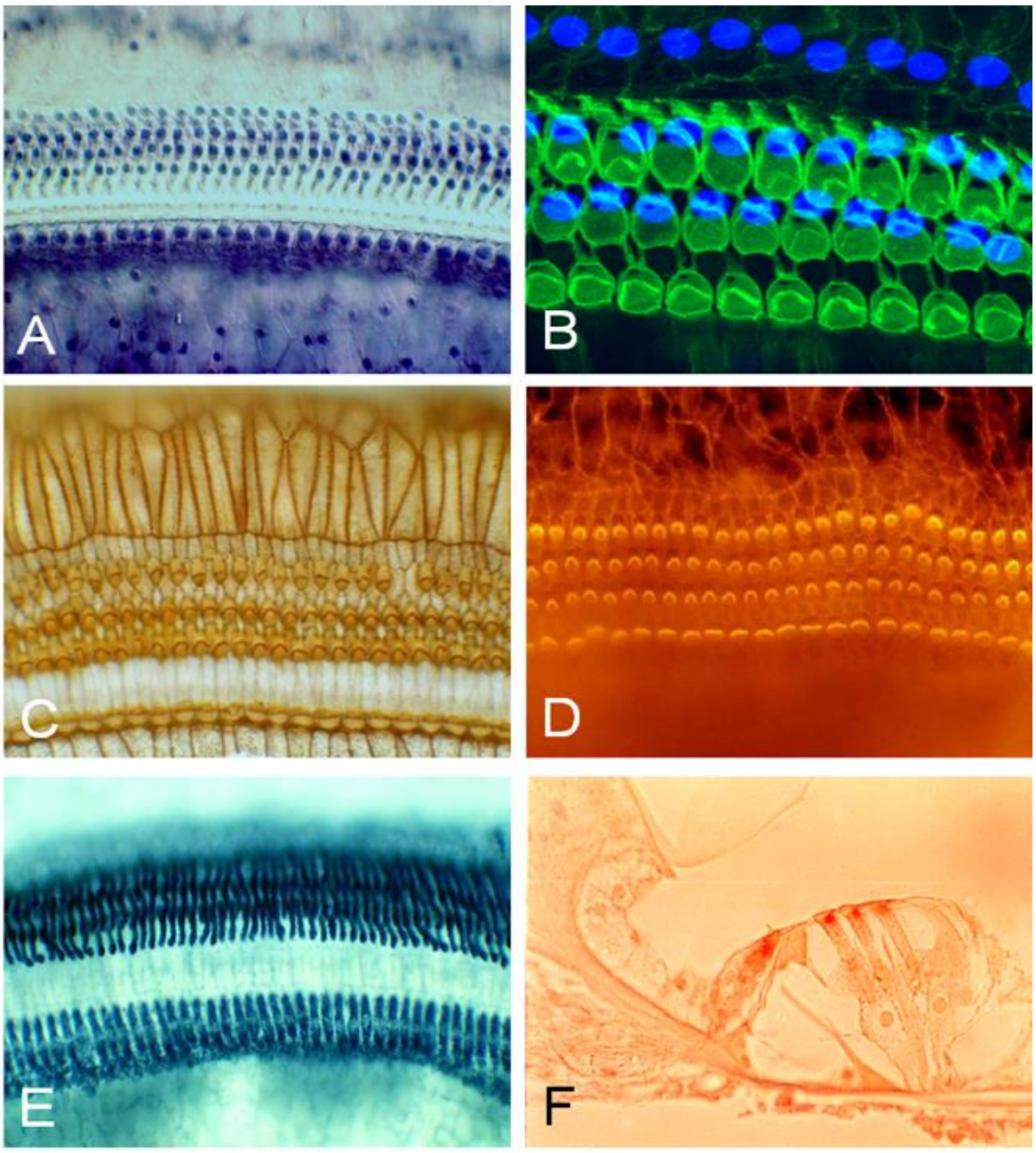

Figure 2-4. Cochlear histological staining. (A) Cochlear surface preparation with hematoxylin staining. (B) Cochlear surface preparation with Topro-3 staining. (C) Cochlear surface preparation with silver nitrate staining. (D) Cochlear surface preparation with phalloidin staining. (E) Cochlear surface preparation with succinate dehydrogenase staining. (F) Cochlear section with acid phosphatase staining.

the epithelium in brown-black. Therefore, the silver nitrate labeling on epithelium is actually a metal precipitation, but does not look like other colorings which bind specific organelles or proteins. To perform the silver nitrate labeling, a hole was drilled in the cochlear apex, and the round and oval windows were opened. 0.5% silver nitrate solution was perfused three times into the cochlear cavity through the hole in the apex. After silver nitrate perfusion, the cochlea was then fixed with 10% formalin, and immersed in the fixative overnight. On the second day, the cochlear basilar membrane was dissected out, and mounted on a slide as a flat surface preparation in glycerin, exposed to sunlight for 30 minutes, examined under a light microscope and photographed (Figure. 2-4C) [4,5,235,244].

Fluorescence conjugated phalloidin. Phalloidin is a bicyclic peptide that belongs to a family of toxins isolated from the deadly Amanita phalloides "death cap" mushroom and is commonly used in fluorescent imaging applications to selectively label F-actin in cells. The stereocilia and cuticular plate of cochlear hair cells are rich in F-actin which can be specifically labeled by phalloidin, therefore phalloidin is commonly used to mark the hair cells in the inner ear. After fixation, the cochlear basilar membrane was immersed into 0.25% Triton X-100 for 5 min and then placed in fluorescence-conjugated phalloidin (1:200 dilutions) in PBS for 30 minutes. After rinsing with PBS, specimens were mounted on glass slides in 50% glycerol and coverslipped. Samples were then examined under a confocal microscope using appropriate filters to detect the phalloidin labeled F-actin on the surface of hair cells (Figure. 2-4D) [4,7,12,25,28,38,41,125,162,220,237,238,253].

Succinic dehydrogenase (SDH) is an enzyme complex, bound to the mitochondria. SDH is a soluble iron flavoprotein that catalyzes the reversible oxidation of succinic acid to fumaric acid. It is the only enzyme that participates in both the citric acid cycle and the electron transport chain. Therefore, SDH is a marker enzyme of mitochondria, and can be used to reflect the aerobic respiration chains of mitochondria and the energy supplies in the cell. In addition, cochlear hair cells contain high numbers of mitochondria, much more numerous than the surrounding supporting cells due to their energy metabolism requirement. Therefore, SDH staining can be considered to reveal the higher density of mitochondria in hair cells and distinguish them from surrounding supporting cells which have far fewer mitochondria. The histochemical demonstration of the activity of this enzyme is achieved by incubation with a succinate substrate in the presence of a tetrazolium compound. Tetrazoliums are water-soluble compounds employed in histochemistry as redox indicators. Under appropriate conditions, enzymatic activity removes hydrogen from the substrate and the hydrogen is transferred to the tetrazolium reducing it to the insoluble purple-blue formazan which is deposited at the site of enzyme activity. Nitro blue tetrazolium is the most commonly used of the tetrazolium compounds due to the intense color and fine precipitate of the formazan. SDH staining solution is mixed with 0.2M sodium succinate, 0.2M phosphate buffer, and 0.2M nitro-BT (tetranitro blue tetrazolium) in a ratio of 1:1:2. The process for SDH staining is below. 1. Open the round and oval windows and drill a hole on the apical turn of the cochlea. 2. Gently perfuse SDH staining solution through the opening on the apex, and immerse specimens in SDH solution for 45 minutes at 37^{o}C. 3. Fix specimens in 10% formalin overnight. 4. Microdissect out the cochlear basilar membrane and mount it on a glass slide as a surface preparation (Figure. 2-4E), or make sections for observation under the light microscope [4,5,11,33,123,126-128,166,244,247,254].

Acid phosphatase is a marker enzyme for lysosomes; its alteration can reflect the active stages of lysosomes. As a cellular digestive system, lysosomes are membrane-enclosed organelles of the cell, serving both to degrade material taken up from the extracellular environment and to digest obsolete components of the cell. Therefore, lysosomes are very important in maintaining the metabolism of the cell. To detect the changes of lysosomes during ototoxicity, acid phosphatase is an ideal object for observation. The enzymatic histochemistry for acid phosphatase staining using azo dyes was applied to normal and kanamycin treated animal models. The procedures of acid phosphatase staining are as described previously [5,9,23,73,128,243]. In brief, at the end of experiment, animals were decapitated. The cochlea was fixed with 10% formalin in PBS. After fixation, the cochlear cavity was opened, and the staining solution containing 5 mg of naphthol AS-BI phosphate, sod.salt, 0.2 ml of Dimethyl formamide (DMF) and 10 ml of Hexazonium-p-rosaniline buffer was perfused into the cochlea, and incubated for 30 minutes at 37^{o}C. Afterwards, cochlear surface preparations or cochlear frozen sections were prepared and observed under a light microscope (Figure. 2-4F). In order to observe more detailed microstructure and ultrastructure, the products of histochemical reactions from acid phosphatase were labeled by lead sulfide and relabeled by osmium tetroxide to provide the high electron density necessary to identify ultrastructure using a transmission electron microscope. The preparation of specimens for transmission electron microscopy is as described in our previous publications [5,9,23,128,241]. The cochlear basilar membrane was fixed with 2% glutaraldehyde in buffered sodium arsenate for 3 hours, and then micro-dissected out and incubated in Gomori medium containing Na-beta-glycerophosphate as substrate. The cochlear basilar membrane was then post-fixed in 1% osmium tetroxide, followed by routine procedures to dehydrate and embed in Epon 812 [5,11,69,128,153,167,168,243]. Ultrathin sections were cut with glass knives at a

thickness of 70 nm and collected on thin-bar nickel grids. Ultrathin sections were stained with uranyl acetate and examined on a Hitachi H-7000 electron microscope at an accelerating voltage of 15 kV.

Caspases, or cysteine-aspartic proteases or cysteine-dependent aspartate-directed proteases, are a family of cysteine proteases that play essential roles in apoptosis. There are two types of apoptotic caspases: initiator caspases and effector (executioner) caspases. Initiator caspases (caspase 2, caspase 8, caspase 9, and caspase 10) cleave inactive pro-forms of effector caspases, thereby activating the effector caspases (caspase 3, caspase 6, and caspase 7), and in turn cleave other protein substrates within the cell and trigger the apoptotic process. Caspase 4 and caspase 5 work in concert with caspase 1, and are associated with autoimmune diseases caused by NALP1 variants, but they are not yet classified as initiators or effectors. In contrast, Caspase 14 is not involved in apoptosis or inflammation, but instead it is involved in skin cell development. As mentioned above, two initiator caspases (caspase 8 and caspase 9) were detected in the current research project. Caspase 8 is a component of the tumor necrosis factor receptor type 1 (TNF-R1) and Fas signaling complexes that are involved in TNF-R1- and Fas-induced apoptosis. Caspase 8 activation was evaluated to determine whether platinum-induced apoptosis started from the cell death receptors on the cell membrane. Another initiator, caspase 9, occurs only in response to the mitochondrial death pathway which is activated by a complex of cytochrome C and apaf-1. Therefore, caspase 9 was evaluated in the current study to confirm whether or not the platinum-induced apoptosis started from cytochrome C release. Executioner caspases, (caspase 3 and caspase 6) were also evaluated in this study to determine the downstream activations of effector caspases. To evaluate the different caspases, cochleas were labeled with fluorescently-labeled caspase-8 inhibitor (CaspaTag 8, 1:30 in solvent, Intergen), caspase-9 inhibitor

(CaspaTag 9, 1:30 in solvent, Intergen), caspase-3 inhibitor (CaspaTag 3, 1:30 in solvent, Intergen) or caspase-6 inhibitor (CaspaTag 6, 1:30 in solvent, Intergen) using procedures similar to those in our earlier publications. Briefly, fluorescently-labeled inhibitors for caspase 8, caspase 9, caspase 3, or caspase 6 were perfused into the cochlear cavity in vivo or added to cochlear explants in culture medium in vitro for 30 minutes. After fixation, the cochlear basilar membrane was double stained with PI or phalloidin, and mounted as a flat surface preparation [3-5,7,12,28,33,41,48,225,238].

Tumor necrosis factor receptor-associated death domain (TRAAD) is encoded by the gene which is a death domain containing an adaptor molecule that interacts with TNFRSF1A / TNFR1 and mediates programmed cell death signaling and NF-kappaB activation. This protein binds adaptor protein TRAF2, reduces the recruitment of inhibitor-of-apoptosis proteins (IAPs) by TRAF2, and thus suppresses TRAF2 mediated apoptosis. This protein can also interact with receptor TNFRSF6/FAS and adaptor protein FADD/MORT1, and is involved in the Fas-induced cell death pathway. To further prove if TRADD was the initiator to start the apoptotic signaling in platinum-induced apoptosis, TRADD immunocytochemistry was detected in the early stage of apoptosis. After fixation, TRADD immunolabeling was performed. Specimens were incubated in 0.3% H_2O_2 in methanol for 1 hour to block endogenous peroxidases. After washing in PBS for 20 minutes, samples were incubated for 30 minutes in a mixture containing Triton X-100 (0.3%) plus normal horse serum (10%) in PBS. The specimens were incubated overnight at 4 ^{o}C with a rabbit polyclonal TRADD antibody (Santa Cruz Biotechnology, Inc., H-278, sc-7868) in PBS. Samples were rinsed in PBS three times, and then incubated in FITC-conjugated goat anti-rabbit IgG (1:100) for 1 hour. After three rinses in PBS, the specimens were double stained with PI (10

ug/ml) for 10 minutes, and mounted on glass slides in 50% glycerol containing antifade solution as described in our previous publications [3,5,28,33].

Neurofilaments are an intermediate filament occurring with neurotubules in the neurons and are part of the cytoskeletal structure. In the auditory system, neurofilament immunostaining is widely used for the evaluation of auditory nerve fibers and spiral ganglion neurons. Cochlear explants were fixed for 2 hours in 4% formalin and subsequently washed with 0.1 M phosphate buffered saline (PBS). As described in our previous publications, the specimens were immunolabeled with a primary monoclonal antibody against neuronal class III b-tubulin (Covance, MMS-435P), which was detected using a secondary antibody labeled with Cy3 (goat antimouse IgG, Jackson ImmunoResearch; #115-165-206). After rinsing with 0.1 M PBS and double staining, specimens were mounted on glass slides in glycerin, coverslipped, and examined using a confocal microscope (Zeiss LSM-510 meta, step size 0.5 mm per slice) with appropriate filters to detect the fluorescence of Cy3-labeled product in nerve fibers and spiral ganglion neurons (SGN) (excitation 550 nm, emission 570 nm) and green fluorescence of Alexa 488-labeled phalloidin (excitation 488 nm, emission 520 nm) that labels the bundles of stereocilia and the cuticular plate of the hair cells. Confocal images were stored on disk and processed using Confocal Assistant, ImageJ and Adobe Photoshop 5.5 software [3,5,7,12,25,33,35,36,41,125,154,162,236].

TUNEL is the abbreviation for Terminal deoxynucleotidyl transferase dUTP nick end labeling (TUNEL). The TUNEL method for detecting DNA fragmentation by labeling the terminal end of nucleic acids originally was described by Garvrieli Sherman and Ben-Sasson in 1992 [255]. After several modifications and improvements, it became an ideal method for detecting DNA fragmentation at the last phase of apoptosis by labeling the terminal end of nucleic acids.

At the end of the experiment, cochlear explants were fixed with 10% formalin in PBS for 4 hours. The APO-BrdU TUNEL Assay Kit (Molecular Probes A-23210) was used to evaluate nuclear DNA fragmentation, according to the manufacturer's protocol. Briefly, the fixed cochlear explants were transferred to ethanol overnight (4^{o}C), rinsed in Wash buffer from the kit, and then incubated with DNA-labeling solution overnight (4^{o}C). Afterwards, specimens were rinsed twice in Rinse buffer and then incubated in 100 µl of freshly prepared antibody labeling solution by mixing 5 µl of the Alexa Fluor 488-labeled anti-BrdU antibody with 95 µl of Rinse buffer for 60 minutes. The specimens were routinely double stained with mouse anti-neurofilament 200 kD antibody (Sigma N0142, clone N52) followed by secondary anti-mouse IgG TRITC (Sigma T5393) to label the spiral ganglion neurons, and/or fluorescent conjugated phalloidin to label the stereocilia of cochlear hair cells. The nuclei were also stained with Topro-3 as described above. Images were collected with a confocal microscope (Zeiss LSM-510) with appropriate filters for red fluorescence of hair cells by TRITC-phalloidin or spiral ganglion neurons by TRITC-neuronfilament labeling, green fluorescence of positive TUNEL labeling, and blue fluorescence of Topro-3 nuclei labeling, and stored in a computer and evaluated with software (Zeiss LSM Image Examiner, Adobe Photoshop) [7,12,19,238].

Superoxide is an unavoidable byproduct of the cellular electron transport chain where electrons inadvertently pass directly to oxygen forming the extremely toxic oxygen radical O^{2-}. As an initiator and a promoter of chain reactions that convert target molecules to radical species, superoxide plays an important role causing cell death in most ototoxic chemical-induced cell apoptosis. One way of explaining this is that activation of apoptosis is associated with generation of reactive oxygen species. The role of free radicals during apoptosis was initially proposed based upon the observation of Bcl-2, an inhibitor of apoptosis with apparent antioxidant function

[256-259]. Therefore, detection of free radicals is useful to understand whether reactive oxygen is involved in initiating the cell death mechanisms. Here, dihydroethidium is used as the superoxide indicator. To measure superoxide levels in living cochlear cells, specimens were stained with 100 nM dihydroethidium for 30 minutes in the typical culture conditions. After 2 hours of fixation with 10% formalin in PBS, hair cells were stained with Alexa Fluor® 488 phalloidin for 30 minutes, while nuclei were stained with 0.75 µM Topro-3 for 20 minutes. The stained sections were examined with a confocal microscope (Zeiss LSM-510) using red fluorescence for superoxide (absorption: 544 nm, emission: 572 nm), green fluorescence for steriocilia of cochlear hair cells (excitation 495 nm, emission 519 nm), and blue fluorescence for nuclei (excitation 642 nm, emission 661 nm). Images were stored on a computer and evaluated with Zeiss LSM Image Examiner and Adobe Photoshop. Red fluorescent signals were quantified using ImageJ (ver. 1.46j). The image files were split to three images (Green, Red and Blue) using Image/split channels. Oxygen radical levels were evaluated by selecting the red image and the measure function was selected from the analyze menu to get values of integrated density in the designated area. In order to get more exact values of integrated density, mean values of background density were subtracted. Mean values of integrated density/area from each group (N=3) were represented as superoxide level [5,7,43,224-226,238].

7. Molecular Biology

7.1 PCR gene array.

The Oligo GEArray (GEA) Apoptosis Series Kit (Superarray Inc., Frederick, MD) was used according to the manufacturer's instructions. An Oligo GEA designed to profile the expression

of 96 key rat genes involved in apoptosis was used for cochlear tissue examination [5,37,42]. In the array, the genes were grouped into 11 categories, according to their functional and structural features, including the TNF ligands, TNF receptors, bcl -2 related genes, caspases, IAP, TRAF, CARD, death domain family members, death effector domain family members, and CIDE domain family members, as well as genes involved in the p53 and ATM pathways. In brief, total RNA was prepared using the RNeasy Mini Kit (74104, Qiagen Inc., Valencia, CA). Synthesis of cDNA and amplification of cRNA were performed using a Truelabeling-AMP linear RNA amplification kit (SuperArray Inc., catalog number 1005). 1.5-3.5 ug total RNA were mixed with GEA primers in RNase-Free H2O, to a final volume of 10 µl, and incubated at 70ºC for 10 minutes. Afterwards, a 10 µl Synthesis Master Mix (containing 4 µl RNase-free H2O, 4 µl 5 X cDNA synthesis buffers, 1 µl RNase inhibitor, and 1 µl cDNA synthesis enzyme mix) was added to initiate reverse transcription. The tube was incubated at 42 ºC for 50 minutes and then at 37 ºC for 5 minutes. A 20 µl Amplification Master Mix (containing 2 µl 10 mM of Biotinylated-UTP, 16 µl of 2.5X RNA Polymerase Buffer, and 2 µl of RNA Polymerase Enzyme) was added to the tube which was then incubated overnight at 37 ºC. cRNA was purified using a SuperArray ArrayGrade cRNA Cleanup Kit (GA-012). Hybridization was performed by adding 0.75 ml of the hybridization buffer supplied by the manufacturer. Arrays were incubated overnight at 60 ºC in hybridization cylinders with Superarray Hybridization Solution containing 5-20 µg biotin labeled cRNA. Arrays were washed and chemiluminescence was imaged using alkaline phosphatase conjugated streptavidin and CDP -Star chemiluminescent substrate (Chemiluminescent Detection Kit (D-01, Superarray Inc.). Images were captured and analyzed using a Kodak Image 2000 and Kodak 1D software (Rochester, NY). Data were normalized to background-corrected levels from the housekeeping gene, glyceraldehyde 3 -phosphate

dehydrogenase (GAPDH). The experiments were repeated 8 times. Genes were subjected to further analysis if they demonstrated either an increase or a decrease in 6 of the 8 experiments.

7.2 Semi-quantitative Real-Time PCR.

All RNA was isolated from cochlea cultures using the RNeasy Mini Kit (Qiagen) and RNase-free DNase set (Qiagen). The total RNA recovered was dissolved in water, and the concentration was determined by measuring absorbance at 260 nm on a spectrophotometer (Beckman Coulter, DU 640). RNA integrity was verified by electrophoresis on 1% agarose gels. First-strand complementary DNA was synthesized by priming with oligo-dT15 (Ambion, Foster City, CA). This primer has the advantage of cDNA synthesis starting at the boundary poly-A-tail adjacent to mRNA. Reverse transcription was performed in 20 µl reactions. Initially, 2 µg RNA and 2 µl (2.5 µm) oligo-dT primer were mixed to a 12 µl volume, heated to 83^{o}C for 3 minutes and placed on ice; then 2 µl 5X buffer, 1 µl (10 units) RNase inhibitor, 4 µl (2 mM stock) dNTP, and 1 µl (100 units) reverse transcriptase were added (all components manufactured by Ambion). The solution was incubated at 42 ^{o}C for 60 minutes and the reaction was terminated by heating the solution at 95 ^{o}C for 10 minutes. Polymerase chain reaction: Quantitative RT-PCR was performed on an Opticon II (MJ Research) instrument using a DyNAmo SYBR Green I PCR Kit (Finnzymes, F-400S, Miami, FL). The PCR reaction mixture consisted of 10 µl of Master SYBR Green I mix, 5 µl of forward and reverse primers (1.2 mM stocks), and cDNA (5 µl, 100 ng). The primers for GAPDH, MCl-1, GADD45a, and BNIP3 were provided by Superarray Inc. (PPR06557A-24, PPR0641A-24, PPR06489A-24, and PPR06513A -24). Cycling started with denaturation at 95 ^{o}C for 10 minutes, followed by 45 cycles of denaturation at 94 ^{o}C for 30 seconds, annealing at 55 ^{o}C for 30 seconds, and extension at 72 ^{o}C for 60 seconds. The

fluorescent signals were acquired from 72-88 ^{o}C for 1 second after each cycle. The GAPDH mRNA level, determined under identical conditions in each RNA sample, was used as an internal control to normalize the RNA levels from different samples. Data analysis: A standard curve was generated by plotting the threshold cycle (Ct) value versus the log of input RNA equivalent (0.1-100 ng calculated from the dilution factor of the RT products). The fold changes between control and test cultures, normalized to GAPDH, were determined using the following equation: Fold change = 2-Δ (ΔCt), where ΔCt = Ct(target) – Ct (gapdh) and Δ (ΔCt)=ΔCt (treated) -ΔCt (untreated). PCR products were visualized on 1% agarose gels to ensure a single product of the correct length. Statistical analysis: All data are presented as mean ± 1 standard error of the mean. Differences were analyzed using one-way ANOVA (Sigma Stat. 2.03) with $p < 0.05$ considered statistically significant [5,37,42].

7.3 Western blotting

The western blot technique was used to assess the level of specific protein expression from cochlear explants exposed to the various experimental conditions [3,5,7,33,35,36,38,128,162,260]. To provide sufficient protein for analysis, 20 cochlear explants were used for each treatment condition. Cultures were harvested at various time points after treatment. Cochlear tissues were washed with cold PBS, homogenized and lysed in three times their volume of ice-cold buffer (50 mM Tris–HCl, pH 7.4, 150 mM NaCl, 10% glycerol, 1% Nonidet P-40, 1 mM orthovanadate, 1 mM phenylmethylsulfonyl fluoride, 1 ng/ml leupeptin and 1 ng/ml aprotinin). The samples were then centrifuged for 3 minutes at 12,000 x *g* and the supernatants removed for analysis. Protein concentrations were measured by the Bradford assay [261]. Aliquots of the crude lysate containing 40 µg of protein were mixed with sodium dodecylsulfate (SDS) sample loading buffer, boiled,

and then electrophoresed on 10% SDS-polyacrylamide gels. The proteins were transferred to nitrocellulose membranes (Schleicher and Schuell). After blocking with 5% non-fat dry milk in phosphate-buffered saline–Tween (PBST; 0.05% Tween 20 in PBS), the membrane was incubated overnight with a specific antibody (1:1000), washed six times for 10 min each with PBST, incubated for 45 minutes at room temperature with HRP-conjugated secondary antibody (1:2000; ICN Biomedicals, Inc., Irvine, CA, USA) in 5% non-fat dry milk. Immunoreactions were visualized by enhanced chemiluminescence according to the manufacturer's instructions (Amersham Pharmacia Biotech). From each blot, several X-ray films were prepared by exposing for different lengths of time. Afterward, the images were scanned into a computer. To quantify the changes in protein expression, we calculated the ratio of the relative density of protein bands compared to the GAPDH. The relative density ratio of protein:GAPDH in the control condition was set at 1.0, and the ratios of densities corresponding to the other treatment conditions were normalized accordingly.

CHAPTER 3: RESULTS

1. Long-term treatment with kanamycin induces both necrosis and apoptosis in the cochlea of guinea pigs and chinchillas

To investigate whether kanamycin causes cell death through apoptosis or necrosis in the cochleas of laboratory animals, five adult chinchillas (12–18 months of age and weighing between 475 and 610 g) were injected with kanamycin (400 mg/kg of body weight) for eight consecutive days. Following dissection and histological preparation, it was confirmed that the hair cells displayed large and round nuclei when stained with Propidium Iodide (red) in the control/untreated cochleas (Figure. 3-1A). In contrast, after eight days treatment with kanamycin, some of the hair cells appeared swollen or enlarged and displayed pale nuclei, a key feature of a cell undergoing necrosis (dashed rings) (Figure. 3-1B). Interestingly, some of the other hair cells displayed shrunken or fragmented nuclei (arrows), a typical characteristic of apoptosis (Figure. 3-1B). Together, these observations suggest that both apoptosis and necrosis are involved in hair cell death in chronic ototoxicity induced by long term treatment with kanamycin.

Lysosomes are cellular organelles that function as a digestive or disposal system in the cell and contain acid hydrolase enzymes that can digest proteins, macromolecules, waste materials and cellular debris [9,24,73,82,262-264]. The membrane composition of the lysosome is thought to allow its digestive enzymes to work in an acid environment. Lysosomes can also digest old or damaged organelles as part of the autophagy system. However, lysosomes are not inexhaustible: once lysosomes are overloaded with macromolecules, the membranes of lysosomes break up, causing

the release of the acid hydrolase enzymes into the cytoplasm, which in turn leads to digestion of all the organelles inside the cell and eventually to cell autolysis. To investigate if lysosomes play a role in hair cell death induced by long term treatment with kanamycin, 25 adult guinea pigs (3–5 months of age and weighing between 300 and 450 g) were treated with kanamycin at the dose of 500 mg/kg per day for 7 days. To visualize lysosomes, acid phosphatase (a marker enzyme for lysosomes) was stained with azo dye using light microscopy, while acid phosphatase was stained with lead sulfide using transmission electron microscopy. I first confirmed that strong staining of the azo dye-labeled acid phosphatase (arrows) was present beneath the cuticular plate of the cochlear hair cells under normal conditions (Figure. 3-2A and B). The primary lysosomes (arrows) (large lysosomes with few or no vesicles) were also observed in the cytoplasm beneath the cuticular plate of the hair cells in normal cochlea (Figure. 3-2A and B). Under kanamycin treatment (500 mg/kg of body weight) for seven consecutive days, the primary lysosomes (arrows) were observed in the cytoplasm near the base of the hair cells and encompassing swelling mitochondria, indicating that lysosomes arrested the damaged and nonviable mitochondria (Figure. 3-2C). After swallowing foreign matter substances, primary lysosomes are known to transform into secondary lysosomes with many small membrane-bound vesicles [9,23,24,73,239,241]. Figure 3-2D shows that two secondary lysosomes (arrows) appeared to swallow two damaged mitochondria (Figure. 3-2D). In normal mammalian cells, the length or diameter of a primary lysosome is about 50-500nm [265], which is 10 to 20 times smaller than the length or diameter of a healthy mitochondrion (0.5-10μm) [266]. However, under kanamycin treatment, the length/diameter of the secondary lysosomes (arrows) was greatly enlarged and was 3 times bigger than that of the mitochondria (Figure. 3-2B and E). Figure 3-2F indicates that the

Figure 3-1.

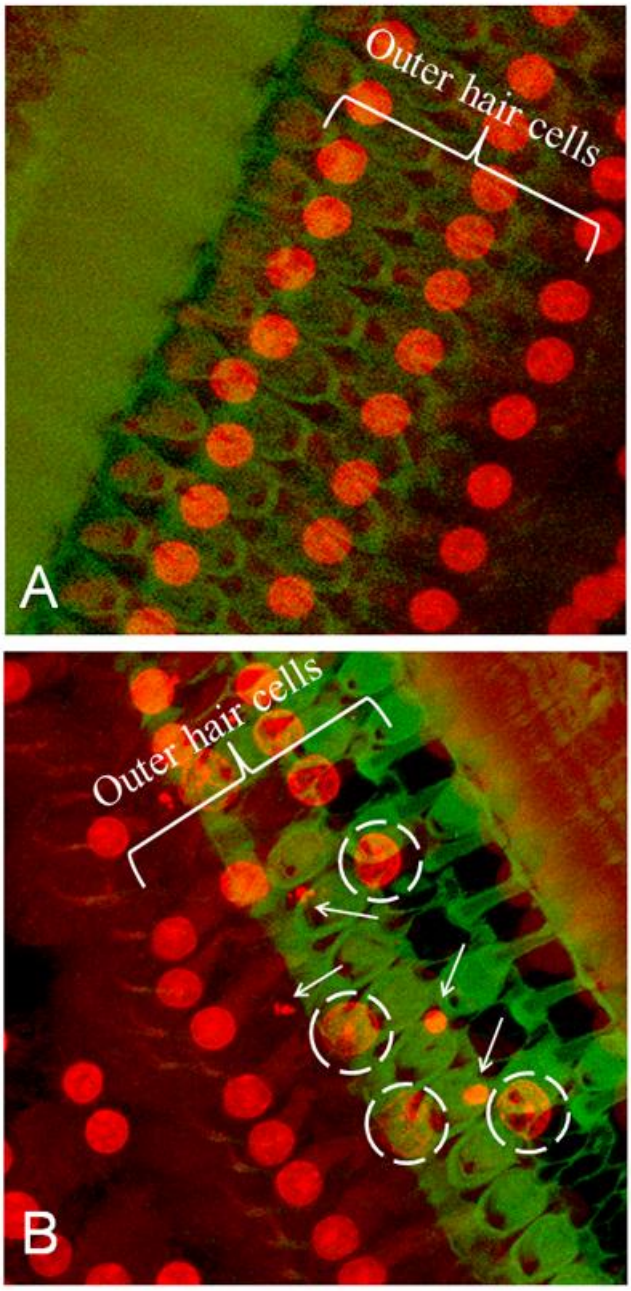

Figure 3-1. Pathological changes of outer hair cells induced by kanamycin treatment in chinchillas. (A) Surface preparation of a normal chinchilla cochlea. Nuclei of the outer hair cells were stained with PI (red) and the cuticular plate was stained with FITC-conjugated phalloidin (green). (B) Surface preparation from a chinchilla treated with kanamycin with a dose of 400 mg/kg per day for 8 days. Note that some outer hair cells had shrunken or fragmented nuclei (arrows), features consistent with apoptosis, while several outer hair cells displayed swollen nuclei (dashed rings), which are morphologic features characteristic of necrosis. The remaining hair cells showed normal morphologic features.

Figure 3-2.

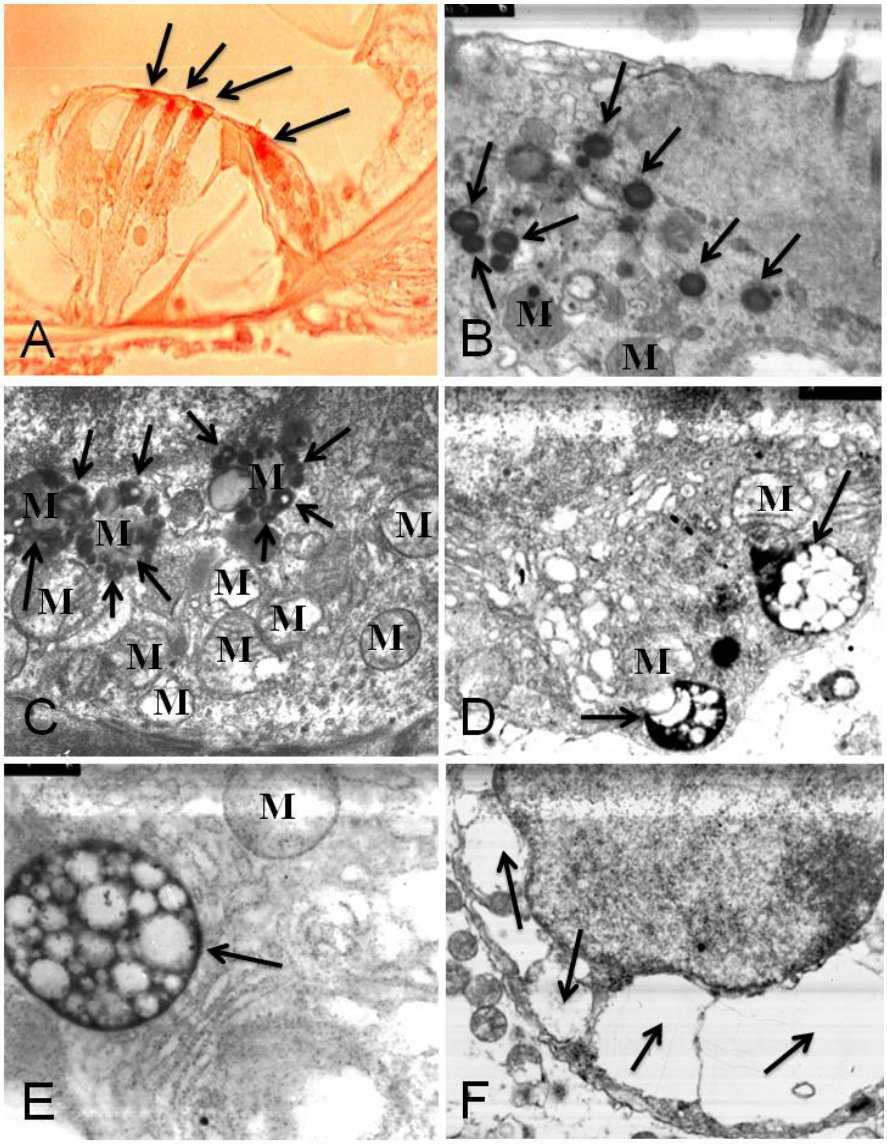

Figure 3-2. Role of lysosomes in kanamycin-induced hair cell degenration in the cochleae of guinea pigs. (A) Guinea pigs were treated with kanamycin with the dose of 500 mg/kg per day for 7 days. Viewed by light microscope, azo dye acid phosphate-labeled lysosomes (arrows) were localized beneath the cuticular plate in the normal cochlear hair cells. (B) Viewed by transmission electron microscope, primary lysosomes with high electron density (arrows) were localized under the cuticular plate. M indicates mitochondria. (C) Primary lysosomes (arrows) were translocated from the original location to the lower part of outer hair cells, and encompassed the damaged mitochondria. M indicates mitochondria. (D) Two nonviable mitochondria appeared to be swallowed by two secondary lysosomes (arrows). M indicates mitochondria. (E) Secondary lysosome (arrows) was expanded after overloading. M indicates mitochondria. (F) The lysosome membrane (arrows) appeared ruptured.

lysosome membranes (arrows) were eventually ruptured, and degrading enzymes were released into the cytoplasm, which perhaps digested all the organelles into large cavities. Together, these observations indicate that necrosis plays a key role in lysosome-associated hair cell death under chronic ototoxic conditions or long term kanamycin treatment.

2. Accumulation of gentamicin and kanamycin in the mitochondria and lysosomes of cochleas

To determine the subcellular localization of gentamicin in the hair cells of cochleas, cochlear organotypic cultures from rat pups at postnatal day 3 were treated with gentamicin labeled with Rhodamine. Gentamicin damaged hair cells in cochlear cultures in a dose dependent manner (Figure. 3-3A-H) with all hair cells remaining intact in control cultures without gentamicin (Figure. 3-3A). Under 0.1 mM gentamicin treatment for 24 hours, no hair cell damage was observed in the middle of the cochlear basilar membrane (Figure. 3-3B). However, at 0.5 mM, gentamicin caused severe hair cell destruction in the middle of the cochlea (Figure 3-3C). Most hair cells were completely damaged 24 hours after 1.0 mM gentamicin treatment (Figure 3-3D). To confirm the above pathological observations, I conducted cochleograms in the cochlear organic cultures treated with gentamicin at 0.1, 0.5, 1.0, and 3.0 mM for 24 hours. Approximately 50 % of outer hair cell loss in the hook region was detected 24 hours after 0.1 mM gentamicin treatment (Figure 3-3E). Outer hair cell loss was spread into the middle turn of the cochlea 24 hours after 0.5 mM gentamicin treatment (Figure 3-3F). Outer hair cell loss was further spread into the apical turn 24 hours after 1.0 mM gentamicin treatment (Figure 3-3G).

Nearly 100% percent of outer hair cells were missing through the entire length of the cochlea 24 hours after 3.0 mM gentamicin treatment (Figure 3-3H).

To investigate the uptake of gentamicin in the hair cells, cochlear organic cultures from rat pups at postnatal day 3, were treated with 0.5 mM gentamicin labeled with rhodamine (red fluorescence) for 12, 24, 36 or 48 hours. First, I confirmed that fluorescence-conjugated gentamicin (red) appeared only in the outer hair cells in the basal turn, while gentamicin was absent in the inner hair cells 12 hours after gentamicin treatment (Figure. 3-4A). Under gentamicin treatment for 24 hours, gentamicin (red) was taken up by both the outer hair cells and inner hair cells (Figure. 3-4B). After 36 hours in culture, both outer hair cells and inner hair cells were completely destroyed (Data not shown). These observations indicate that gentamicin uptake progressed from base to apex and from outer hair cells to inner hair cells.

Next, to investigate the subcellular localization of kanamycin in the hair cells of cochlea, kanamycin was labeled with tritium, which can be detected by autoradiography having high electron density when viewed under the transmission electron microscope [9,241,266]. Tritium-labeled kanamycin with a concentration of 1.25% was perfused into the scala tympani and released from scala vestibule of the cochleae in guinea pigs for 30 minutes or 60 minutes. After fixation, ultrathin sections, and radiation detection, I found that tritium-labeled kanamycin (black, red arrows) was mostly localized in the mitochondria of the cochlear hair cells (Figure 3-4C, D and E). To measure the amount of kanamycin uptake by each organelle, I perfused radio-labeled kanamycin into the scala tympani of the cochleae of guinea pigs for 60 minutes. After the cochlear tissues were harvested and homogenized, lysosomal, mitochondrial, and nuclear /membrane fractions were isolated by density gradient centrifugation and the radioactive intensity was determined using a liquid scintillation counter. The concentration of kanamycin

Figure 3-3.

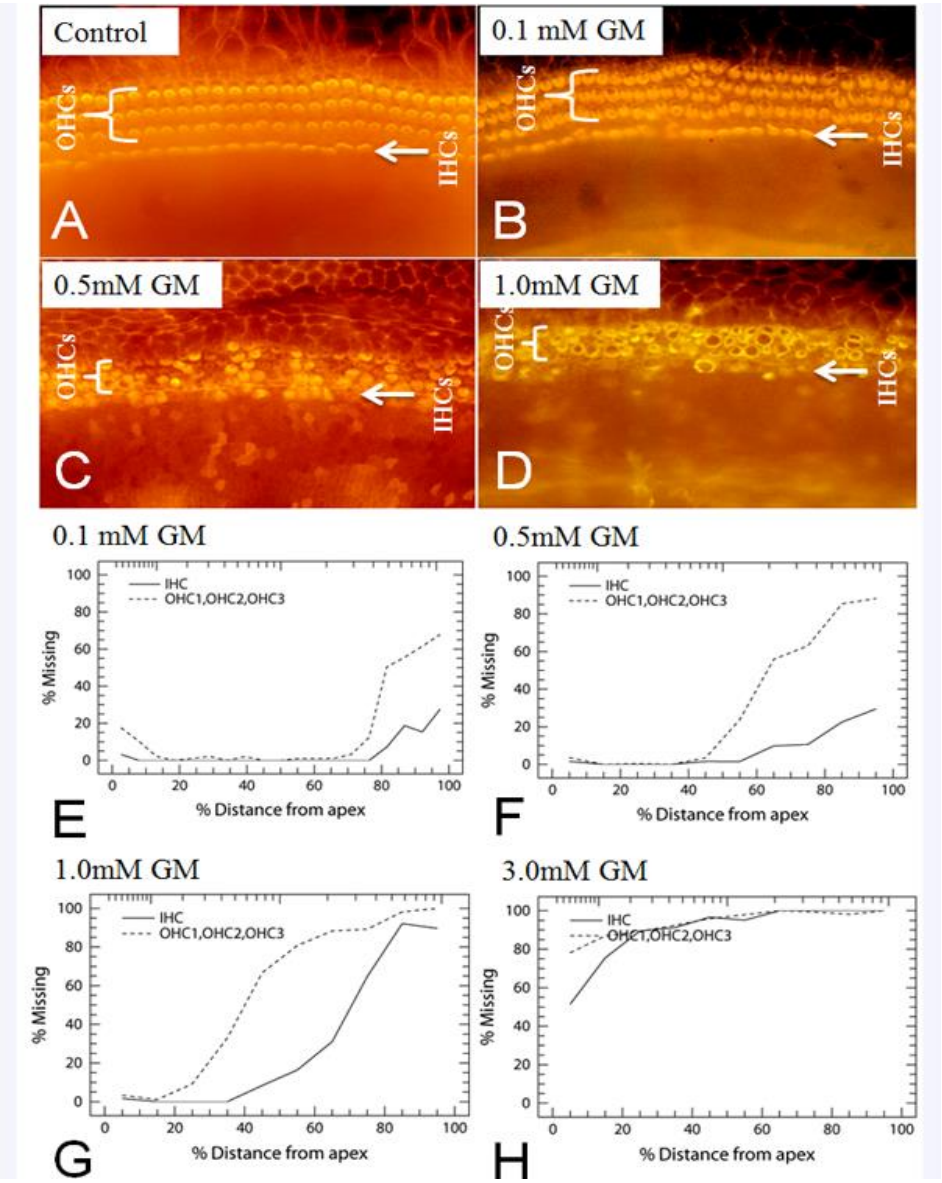

Figure 3-3. Gentamicin damages hair cells in a dose dependent manner in cochlear organotypic cultures from guinea pigs. Bracket and arrow indicate outer and inner hair cells, respectively. (A) All hair cells were intact in the control cochlear cultures without gentamicin. (B) Treatment with 0.1 mM gentamicin did not cause damage in the middle of the cochlear basilar membrane. (C) Severe hair cell destruction was observed in the middle of cochlea after 0.5 mM gentamicin treatment. (D) Most hair cells were completely damaged after 1.0 mM gentamicin treatment. (E) Approximately 50 % of outer hair cells were missing particularly in the hook region after 0.1 mM gentamicin treatment. (F) Outer hair cell loss was spread into the middle turn of the cochlea after 0.5 mM gentamicin treatment. (G) Outer hair cell loss extended into the apical turn after 1.0 mM gentamicin treatment. (H) Nearly 100% of hair cells were missing through the entire length of the cochlea after 3.0 mM gentamicin treatment.

was calculated according to the radiation specific activity of tritium-labeled kanamycin. I found that the mean concentration of kanamycin in the lysosomes was about seven times higher than that of kanamycin in the nuclei/membrane, while the mean concentration of kanamycin in the mitochondria was about three times higher than that of kanamycin in the nuclei/membrane (Figure. 3-4F). Given that the length/diameter of a nucleus is significantly larger than that of a mitochondrion or lysosome, these results indicate that kanamycin selectively accumulates in the lysosomes and mitochondria. Our findings also suggest that both lysosomes and mitochondria are likely the major targets of aminoglycoside antibiotics such as gentamicin and kanamycine.

3. Free radicals play a role in gentamicin-induced hair cell damage

Although evidence suggests that oxidative stress or free radicals play a role in cochlear cell death induced by aging, noise exposure or drugs, precisely how an aminoglycoside antibiotic agent induces oxidative stress and causes hair cell damage is still unclear or controversial. To determine if gentamicin treatment increases levels of superoxide, one of the major free radical species in the cochlear hair cells, cochlear explants of rat pups at postnatal day 3 were untreated or treated with 0.5mM gentamicin for 12 hours or 24 hours, and stained with dihydroethidium (red fluorescence) to visualize superoxide (dihydroethidium is known to be oxidized to ethidium in the presence of superoxide radicals and to bind to nuclear DNA) [7,267,268]. As shown in Figure 3-5A, I first confirmed that the staining of dihydroethidium (red) was very weak in hair cells under control conditions. However, in cochlear cultures treated with 0.5 mM gentamicin for 12 hours, ethidium-labeled nuclei (arrows) were detected in the hair cell region, although the morphology of the hair cells appeared normal (Figure 3-5B). In the cochlear cultures treated with 0.5mM gentamicin for 24 hours, strong ethidium-labeling (arrows) was seen in the condensed nuclei in the damaged hair cells, indicating superoxide-induced hair cell damage (Figure. 3-5C).

Figure 3-4.

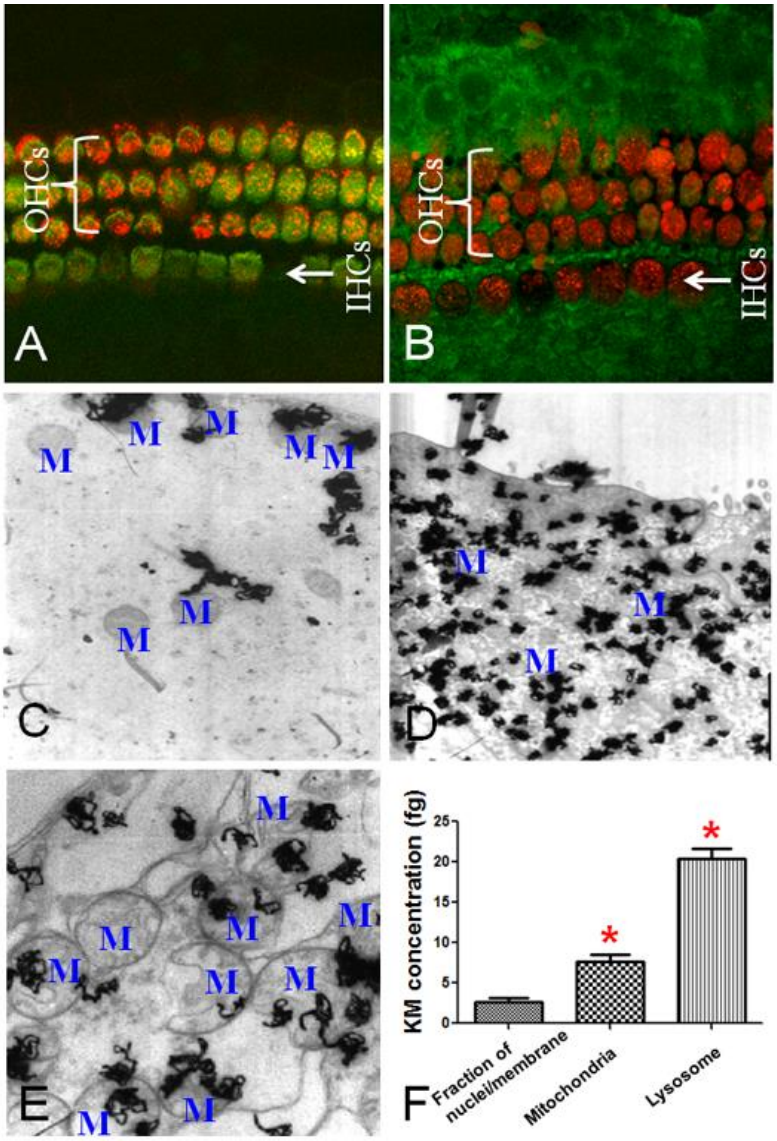

Figure 3-4. Time dependent accumulation of gentamicin or kanamycin in the hair cells. (A) Rhodamine labeled gentamicin (red) was first incepted by the outer hair cells 12 hours after treatment in the cochlear culture system. Bracket and arrow indicate outer and inner hair cells, respectively. (B) Rhodamine labeled gentamicin (red) was found in both the outer hair cells and inner hair cells 24 hours after treatment. (C) Thirty minutes after cochlear perfusion, tritium-labeled kanamycin (black) accumulated in the mitochondria of the hair cells. M indicates mitochondria. (D) Strong labeling of kanamycin (black) was found in the hair cells 60 minutes after cochlear perfusion. M indicates mitochondria (E) Kanamycin labeling was predominately observed in the mitochondria of the hair cells 60 minutes after cochlear perfusion. M indicates mitochondria (F) Femtograms of tritium-labeled kanamycin per organelle fraction obtained from guinea pig cochlea perfused with kanamycin for 60 minutes (*Significantly different from nuclei / membrane fraction $P<0.05$. Error bars indicate S.D.).

Figure 3-5.

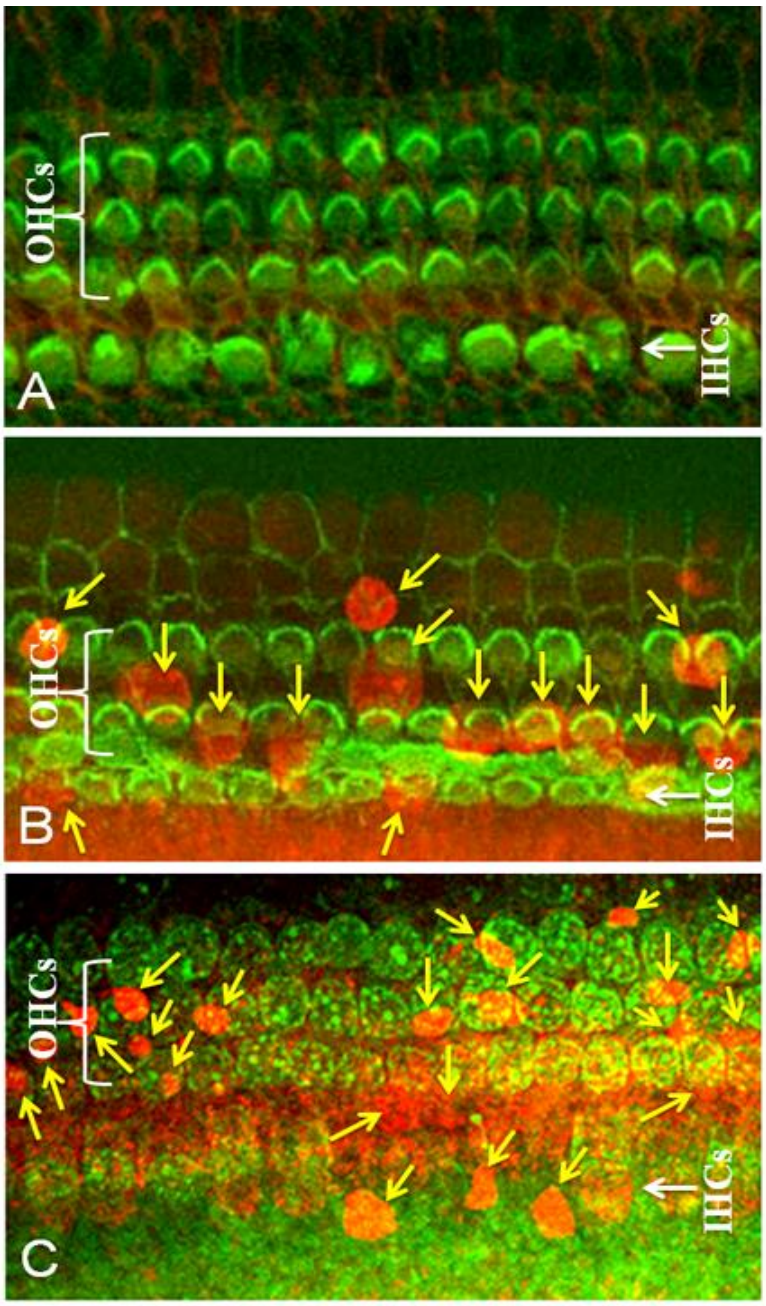

Figure 3-5. Role of superoxide in gentamicin-induced hair cell damage. (A) Weak staining of superoxide (red) was observed in the cochlear hair cells (green) under control conditions. White bracket and arrow indicate outer and inner hair cells, respectively. (B) Superoxide staining (yellow arrows, red) was detected in the outer hair cells 12 hours after 0.5 mM gentamicin treatment. White bracket and arrow indicate outer and inner hair cells, respectively. (C) Strong staining of superoxide (yellow arrows, red) in the nuclei with nuclear condensation was detected in the damaged outer hair cells 24 hours after 0.5 mM gentamicin treatment. White bracket and arrow indicate outer and inner hair cells, respectively.

4. Acute treatment with gentamicin induces apoptotic hair cell death in the cochlea of chinchillas

To investigate if apoptosis plays a role in gentamicin-induced hair cell damage under acute gentamicin treatment, thirty adult chinchillas at 1–3 years of age and weighing between 560 and 670 g were treated with concurrent administration of gentamicin (125 mg/kg, i.m.) and ethacrynic acid (40 mg/kg, i.v., right jugular vein). The drug treatments were terminated after 4, 5, 6, 12, or 24 hours. As described earlier, ethacrynic acid is known to break the blood-cochlear barrier by reducing the blood supply and to open the blood-cochlea barrier for ototoxic chemicals to enter into the cochlea [4, 9, 27-33]. Under co-administration of gentamicin and ethacrynic acid for 6 hours, the stereocilia bundles (brown, black arrows) and apical surface of the organ of Corti appeared relatively normal (Figure 3-6A): the surface structure of the cochlear hair cells in the lower-middle turn of the cochlea appeared normal, and the stereocilia on the three rows of outer hair cells (brown) appeared in a V-shape, consistent with those seen in normal cochleae. However, under co-administration of gentamicin and ethacrynic acid for 12 hours, the stereocilia and the cuticular plate of the outer hair cells and inner hair cells in the lower-middle turn of the cochlea were completely missing (Figure 3-6B). These results indicate that the surface structure of the cochlear hair cells in the lower-middle turn of the cochlea were morphologically intact 6 hours after gentamicin and ethacrynic acid treatment, but not 12 hours after the treatment. These results were consistent with the previous hair cell counting results that 100% of the hair cells were missing 24 hours following co-treatment with gentamicin and ethacrynic acid [4,9,23,26,126,162,269].

Nuclear condensation and fragmentation are anatomical hallmarks of apoptosis[4,7,9,28,270-273]. To determine if acute or rapid destruction of the hair cells following gentamicin and ethacrynic

Figure 3-6.

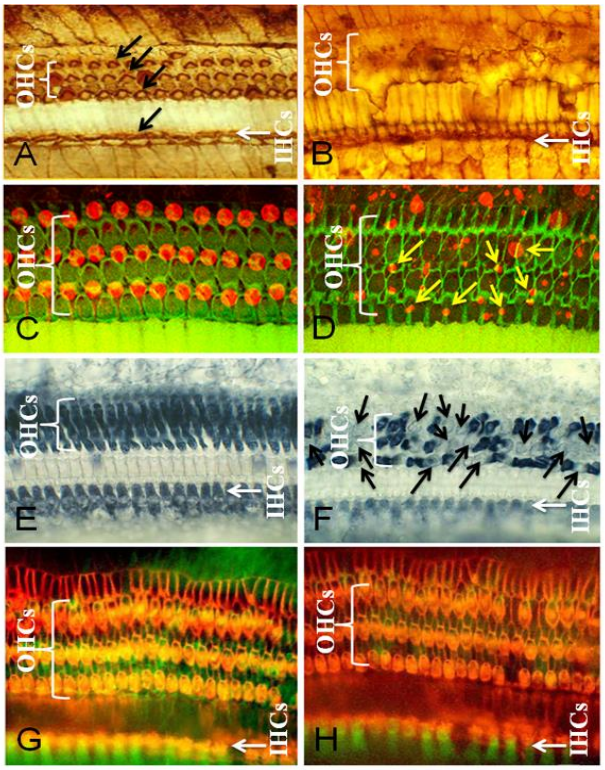

Figure 3-6. Acute treatment of gentamicin and ethacrinic acid induces apoptotic hair cell death in the cochlea of chinchillas. (A) Six hours after gentamicin and ethacrynic acid treatment, the stereocilia bundles (black arrows) and apical surface of the organ of Corti appeared normal. White bracket and arrow indicate outer and inner hair cells, respectively. (B) The stereocilia and cuticular plate of most of the outer hair cells were missing or severely damaged 12 hours after gentamicin and ethacrynic acid treatment. White bracket and arrow indicate the original region of outer and inner hair cells, respectively. (C) A control cochlea showing outer hair cells with large, round PI-labeled nuclei (red). White bracket indicates the region of outer hair cells. (D) 12 hours after gentamicin and ethacrynic acid treatment, the nuclei (red) of outer hair cells were condensed (yellow arrows), fragmented or completely missing. White bracket indicates the region of outer hair cells. (E) Organ of Corti from a control ear showed intense staining of SDH, a mitochondrial marker (dark blue) in the outer hair cells and inner hair cells. White bracket and arrow indicate outer and inner hair cells, respectively. (F) Four hours after gentamicin and ethacrynic acid treatment, SDH staining was absent from some outer hair cells (black arrows). In the inner hair cells, SDH staining was also notably less intense than in the control cochlea. Bracket and arrow indicate outer and inner hair cells, respectively. (G) Cochlear surface preparations stained with MitoTracker (green) and phalloidin (red) in the control cochleas. White bracket and arrow indicate outer and inner hair cells, respectively. (H) Four hours after gentamicin and ethacrynic acid treatment, MitoTracker labeling (geen) intensity was greatly reduced relative to controls in the cytoplasm of outer hair cells (green); MitoTracker staining in the cytoplasm of inner hair cells (green) was moderately reduced relative to controls. White bracket and arrow indicate outer and inner hair cells, respectively.

acid treatment occurs through apoptosis or necrosis, cochlear specimens were stained with propidium iodide (red) to label the nuclei and counterstained with FITC-conjugated phalloidin (green) to visualize the cuticular plate of the hair cell. The propidium iodide-labeled nuclei (red) of the outer hair cells were large, round, evenly stained and arranged in three orderly rows in the control cochlea (Figure 3-6C). The phalloidin staining (green) also shows an intense, thin green ring at the boundary between the outer hair cells and adjacent supporting cells, and the pale green cuticular plate (Figure. 3-6C). In contrast, under gentamicin and ethacrynic acid treatment for 12 hours, the nuclei of the outer hair cells (arrows) appeared shrunken, condensed, and fragmented (Figure 3-6D). Nuclei appeared to be completely missing from several of the outer hair cells (arrows), and thin green bands of actin surrounding the outer hair cells were also observed. However, there was little or no green phalloidin labeling of the apical surface due to the severe damage to the cuticular plate. These morphological observations suggest that apoptotic cell death may occur in the hair cells 12 hours following gentamicin and ethacrynic acid treatment.

Because I found that kanamycin accumulates in the mitochondria of the hair cells, I hypothesized that co-administration of gentamicin and ethacrynic acid may cause mitochondrial dysfunction, leading to acute destruction of hair cells. To test this hypothesis, cochlear specimens were stained for a mitochondrial marker enzyme, succinic dehydrogenase (SDH) following gentamicin and ethacrynic acid treatment. SDH is a mitochondrial enzyme involved in energy and aerobic metabolism, and known to be highly expressed in the OHCs and IHCs, but not in the surrounding supporting cells of the organ of Corti [4,9,23,239,241,247,274]. I first confirmed that concentrated and dark blue SDH staining was observed in the IHCs and OHCs of control cochleae (Figure 3-6E). SDH staining (dark blue, arrows) was also uniformly observed

throughout the cytoplasm of the hair cells. Four hours after gentamicin and ethacrynic acid treatment, SDH staining was mostly absent in some outer hair cells (Figure 3-6F, black arrows), suggesting mitochondrial damage or dysfunction in the hair cells. To investigate if gentamicin and ethacrynic acid treatment affects mitochondrial function, specimens were stained with MitoTracker M-7514 (green) (mitochondrial fluorescent marker/probe that concentrates in functionally active mitochondria) and TRITC-conjugated phalloidin (red) (cuticular plate marker). In the control cochlea, strong MitoTracker (green) and phalloidin (red) staining were observed throughout the cytoplasm of outer hair cells and inner hair cells (Figure. 3-6G), indicating that normal mitochondria were present throughout the hair cells. However, 4 hours after gentamicin and ethacrynic acid treatment, less intense or absent staining of MitoTracker (green) was observed in the outer hair cells, although the cuticular plate of hair cells was observed by TRITC-phallodin (red) (Figure. 3-6H), suggesting a rapid decline in mitochondrial function or mitochondrial damage, which is known to trigger the release of cytochrome *c* into the cytoplasm of the hair cells, leading to apoptotic cell death.

To investigate whether gentamicin and ethacrynic acid treatment triggers cytochrome *c* release, cochleas from normal and gentamicin and ethacrynic acid treated chinchillas were immunolabeled with an antibody against cytochrome *c* (green). In control cochleas, cytochrome *c* immunolabeling (green) was detected along the lateral wall of the outer hair cells where most mitochondria are usually located in the cochlear hair cells (Figure. 3-7A). Four hours after gentamicin and ethacrynic acid treatment, there was a notable increase of intensity in cytochrome *c* staining in the hair cells; labeling appeared to be more granular and was no longer lining the lateral walls but was dispersed throughout the cytoplasm (Figure. 3-7B, white arrows), suggesting cytochrome *c* release into the cytoplasm. Consistent with this observation, the nuclei

Figure 3-7.

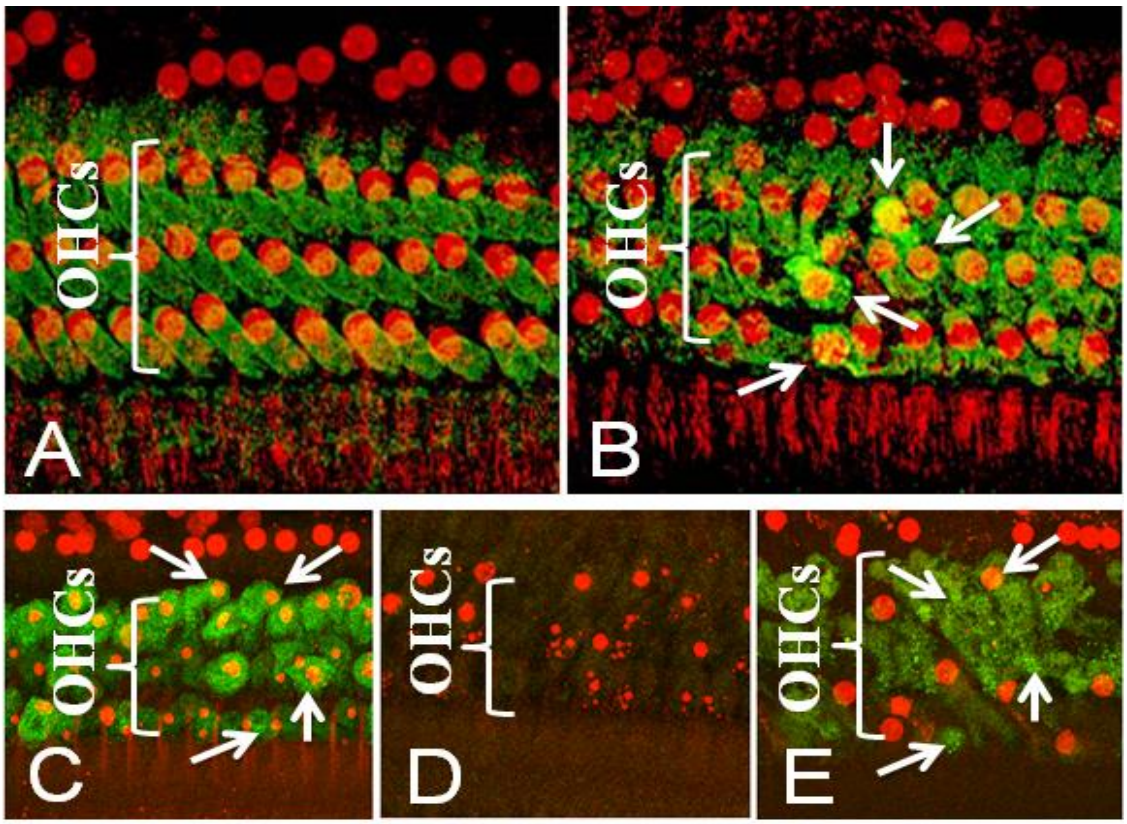

Figure 3-7. Gentamycin-induced hair cell damage through mitochondrial apoptosis. (A) Surface preparations of the cochlea stained with PI to label the nuclei (red) and an antibody against cytochrome *c* (green) in the control cochlea. Note the distinct band of cytochrome *c* labeling (green) along the body of the hair cells. White bracket indicates outer hair cells. (B) Four hours after gentamicin and ethacrynic acid treatment, cytochrome c staining (arrows, green) was more intense and dispersed within outer hair cells compared to controls. White bracket indicates outer hair cells. (C) Five hours after gentamicin and ethacrynic acid treatment, caspase-9 staining (arrow, green) was heavily expressed in the hair cells with condensed and fragmented nuclei. Bracket indicates outer hair cells. (D) Five hours after gentamicin and ethacrynic acid treatment, caspase-8 staining (green) was absent in hair cells with condensed and fragmented nuclei. White bracket indicates outer hair cells. (E) Five hours after gentamicin and ethacrynic acid treatment caspase-3 staining (arrows, green) was heavily expressed in hair cells with condensed and fragmented nuclei. White bracket indicates outer hair cells.

of some of the hair cells with strong cytochrome *c* staining appeared shrunken, indicative of apoptosis. To determine whether apoptotic caspase-8, caspases-9, and/or caspases-3 play a role in gentamicin and ethacrynic acid induced hair-cell apoptosis, cochleas were stained with fluorescently-labeled caspase-8, caspase-9, or caspase-3 inhibitors specific to each caspase protease. I also stained the organ of Corti with PI to evaluate the pathological status of the nuclei. I first confirmed that control cochleas displayed no staining of caspase-8, caspase-9 or caspase-3 fluorescence (data not shown). However, 5 hours post-gentamicin/ethacrynic acid treatment, intense caspase-9 fluorescence staining (green) was evident in nearly all the outer hair cells in the basal turn of the cochlea (Figure. 3-7C). The nuclei of the caspase-9 positive labeled outer hair cells were condensed and considerably smaller than those in control cochleas (Figure 3-7C). In contrast, caspase-8 staining was completely absent in the hair cells (Figure. 3-7D) despite the fact that the nuclei of the OHCs were condensed and in some cases fragmented. Caspase-3 fluorescence staining was present in most of the outer hair cells (Figure 3-7E). The PI-labeled nuclei of caspase-3 positive outer hair cells were condensed or fragmented (Figure. 3-7E). Collectively, these observations suggest that gentamicin and ethacrynic acid cause hair cell loss by rapidly damaging mitochondria, which in turn leads to cytochrome *c* release into the cytoplasm, activating caspase-9 and caspase-3, promoting mitochondrial apoptotic hair cell death.

5. Delayed neuron degeneration following complete hair cell loss by gentamicin and ethacrynic acid treatment in chinchillas

Previous studies indicate that gentamicin selectively destroys the sensory hair cells in the inner ear of laboratory animals, but not the spiral ganglion neurons: Spiral ganglion neuronal degeneration usually occurs following hair cell loss in a well-defined time course after gentamicin treatment [5,9,23,249]. Following complete hair cell degeneration, cochlear peripheral neurons are known to degenerate due to the lack of electrical stimulations and neurotropic factors [275,276]. This process is known as "delayed ganglion neuron death" [5,9,23,249]. To investigate how a single co-administration of gentamicin and ethacrynic acid induce cochlear efferent degeneration, fifteen chinchillas were treated with gentamicin and ethacynic acid, and then cochlear tissues were dissected out after 3 days or 1, 2, 3, or 4 weeks (N = 15, three animals at each time point). After fixation, cochlear basilar membranes were micro-dissected out and stained with acetylcholinesterase to visualize cochlear efferent nerve fibers (brown). I first confirmed that there was no cochlear efferent nerve fiber damage or loss (white arrows) in the control chinchilla cochleas (Figure 3-8A). However, 3 days after gentamicin and ethacrynic acid injection, moderate degeneration of efferent nerve fibers (white arrows) was observed (Figure 3-8B). Severe degeneration of the efferent nerve fibers (white arrows) was observed at 1 week (Figure 3-8C), 2 weeks (Figure 3-8D), 3 weeks (Figure 3-8E), and 4 weeks (Figure 3-8F) under one treatment with gentamicin and ethacrynic acid. To confirm that the degenerative pattern of cochlear efferent fibers occurred along the entire length of the cochlea, I conducted mean cochleograms to quantify losses of cochlear hair cells and cochlear efferent fibers in the cochlea. I found that gentamicin and ethacrynic acid treatment damaged all cochlear hair cells first, the degeneration of cochlear efferent fibers occurs afterwards, while cochlear efferent fiber damage begins at the base of the cochlea and progresses toward the apex in a time dependent manner

(Figure 3-8G-J). These observations suggest that cochlear efferent terminals may degenerate quickly once the targeted hair cells are lost or degenerated.

Figure 3-8.

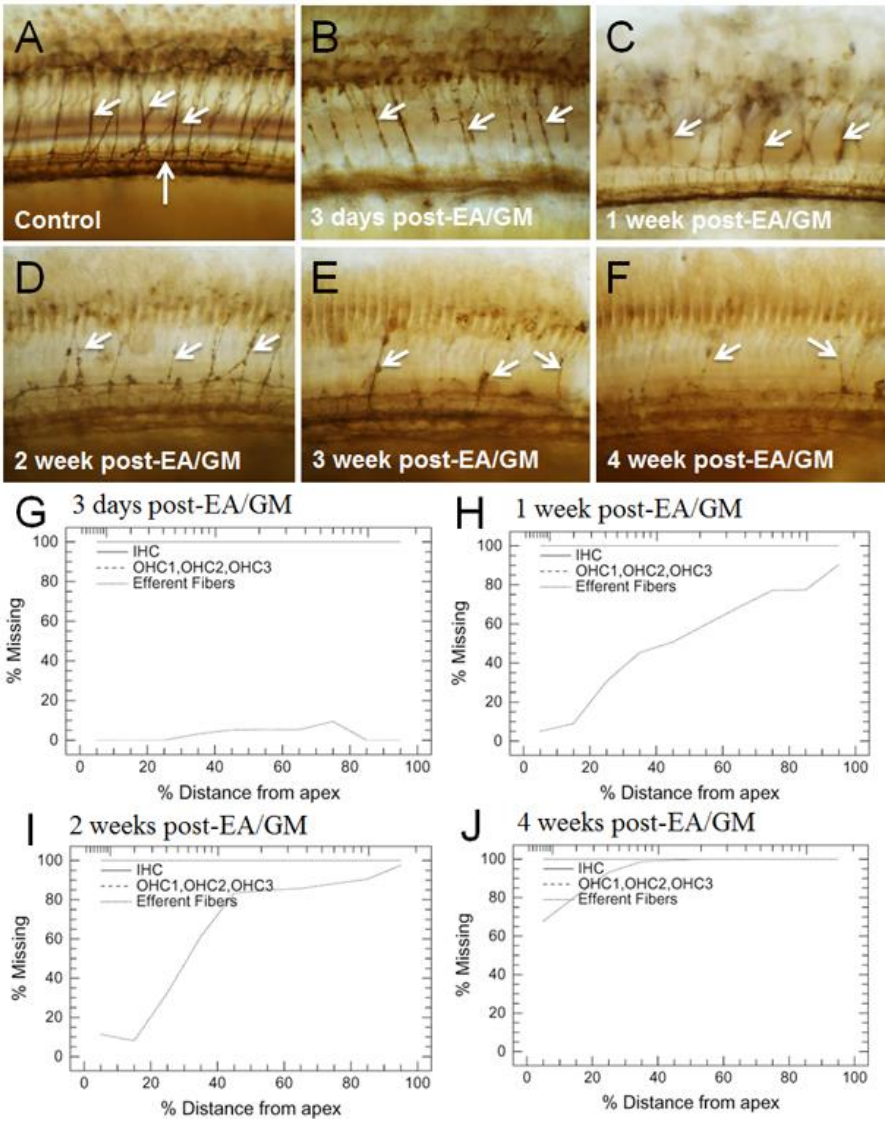

Figure 3-8. Degeneration of cochlear efferent nerve fibers following hair cell loss. (A) Cochlear surface preparations with acetylcholinesterase staining show normal cochlear efferent nerve fibers (arrows). (B) Efferent nerve fibers (arrows) degenerated 3 days after a single injection of gentamicin and ethacrynic acid. Severe degeneration of efferent nerve fibers (arrows) was observed at 1 week (C), 2 weeks (D), 3 weeks (E), and 4 weeks (F) after gentamicin and ethacrynic acid treatment. (G-J) Mean cochleograms show that gentamicin and ethacrynic acid treatment-induced degeneration of cochlear efferent fibers in a stereotypic pattern that secondary degeneration of efferent fibers begins at the base of the cochlea and progresses toward the apex in a time dependent manner.

To further investigate how delayed spiral ganglion neuron and nerve fiber death occur following hair cell destruction, 12 chinchillas were injected with a single gentamicin (125 mg/kg, IM), followed immediately by a single ethacrynic acid (40 mg/kg, IP). Animals were sacrificed after 15 days or 1, 2, or 4 months (N = 3, three animals at each time point). Epon 812-embedded temporal bone was cut at a thickness of 1.5 μm and collected on glass slides. Sections were stained with toluidine blue to visualize spiral ganglion neurons, examined under a light microscope and photographed. The auditory nerve fibers in habenula perforata and the spiral ganglion neurons in Rosenthal's canal were observed under light microscope. I first confirmed that there was no cochlear spiral ganglion neuron damage or loss (dark blue, arrows) in the control chinchilla cochleas (Figure 3-9A). However, most spiral ganglion neurons (dark blue, arrows) were irregularly shaped with fluid filled vacuoles 15 days after a single injection of gentamicin and ethacrynic acid (Figure 3-9B). Severe destruction of spiral ganglion neurons (dark blue, arrows) was observed 1 month (Figure 3-9C), 2 months (Figure 3-9D), 3 months (Figure 3-9E), and 6 months (Figure 3-9F) after treatment with gentamicin and ethacrynic acid and after complete hair cell loss. Furthermore, I confirmed that there was no cochlear auditory nerve fiber damage (dark blue, arrows) in the habenula perforate in the control chinchilla cochleaes (Figure 3-9G). However, auditory nerve fibers (dark blue) were missing 15 days (Figure 3-9H), 1 month (Figure 3-9I), and 2 months (Figure 3-9J) after treatment with gentamicin and ethacrynic acid and after complete hair cell loss. The remaining empty habenula perforate suggest that degeneration of spiral ganglion neurons may begin from the terminals and spread towards the neuron body.

6. Delayed spiral ganglion neuron death following complete hair cell loss *in vitro*

Figure 3-9.

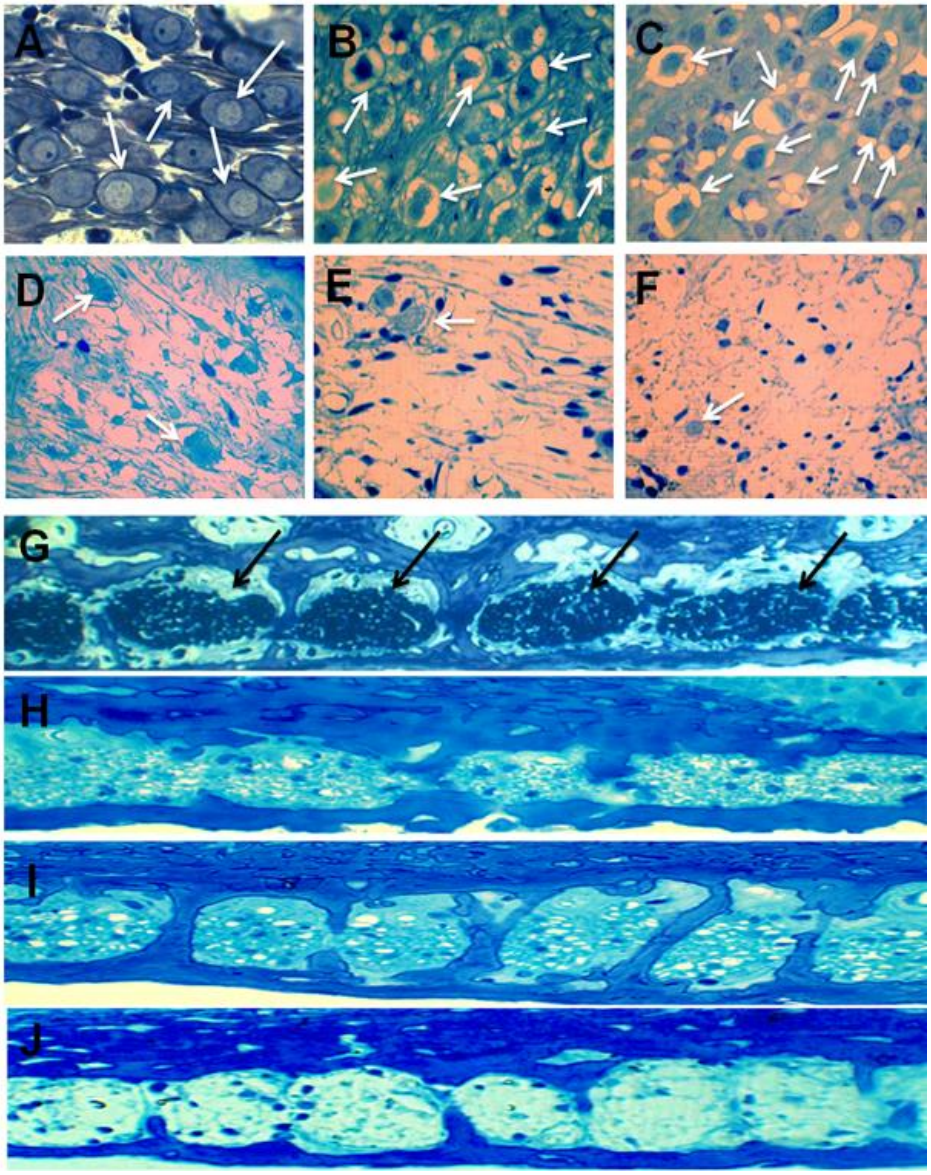

Figure 3-9. Delayed spiral ganglion neuron death following hair cell loss induced by gentamicin and ethacrynic acid treatment. (A) Spiral ganglion neurons were observed in the control chinchilla cochleae (arrows). (B) Most spiral ganglion neurons (arrows) were irregularly shaped with fluid filled vacuoles 15 days after gentamicin and ethacrynic acid treatment. Severe destruction of the spiral ganglion neurons (arrows) were observed 1 month (C), 2 months (D), 3 months (E) or 6 months (F) following hair cell destruction after gentamicin and ethacrynic acid treatment. Auditory nerve fibers (arrows) were observed in the habenula perforate (arrows) in the control cochlea from chinchilla (G). Severe degeneration of auditory nerve fibers (arrows) following hair cell destruction 15 days (H), 1 month (I), or 2 months (J) after gentamicin and ethacrynic acid treatment.

As shown in the previous literatures, it takes several months or longer for delayed spiral ganglion neuron death to develop *in vivo*[5,9,23,249]. This long cell death process can be shortened to several days in *in vitro* cochlear organotypic culture conditions. We have previously shown that in the cochlear culture system, all the cochlear hair cells can be completely destroyed, while all the spiral ganglion neurons and their auditory nerve fibers remain intact under 2 mM gentamicin treatment for 24 hours [5,9,23,275,277]. To investigate whether and how gentamicin treatment induces delayed spiral ganglion neuron degeneration and auditory nerve fiber regression, cochlear organotypic cultures from rat pups at postnatal day 3 were grown in culture medium containing gentamicin for 24 hours treatment. The culture medium containing gentamicin was replaced with fresh standard serum-free medium without additional neurotrophic factors and then incubated for 1, 3, 5, 7 or 14 days. I first found that spiral ganglion neurons (white arrows) and auditory nerve fibers (yellow arrows) were intact in the cochleas 24 hours after 2 mM gentamicin treatment (Figure 3-10A). However, in the culture condition without neurotrophic factors, spiral ganglion neurons (white arrows) and auditory nerve fibers (yellow arrows) degenerated rapidly 3 days (Figure 3-10B) and 5 days (Figure 3-10C) after gentamicin treatment and hair cell loss. After 7 days (Figure 3-10D) or 14 days (Figure 3-10E), most surviving ganglion neurons (white arrows) were degenerated or lost after complete hair cell destruction. To validate these observations, I counted the numbers of spiral ganglion neurons and auditory nerve fibers. I found that gentamicin treatment of cochlea without neurotrophic factors in the cultures decreased spiral ganglion neuron and auditory nerve fiber numbers in a time dependent manner (Figure 3-10F). We have previously shown that transfecting cochlear supporting cells with adenovirus mediated neurotrophin genes results in secretion of neurotrophins and increases the numbers of surviving

Figure 3-10.

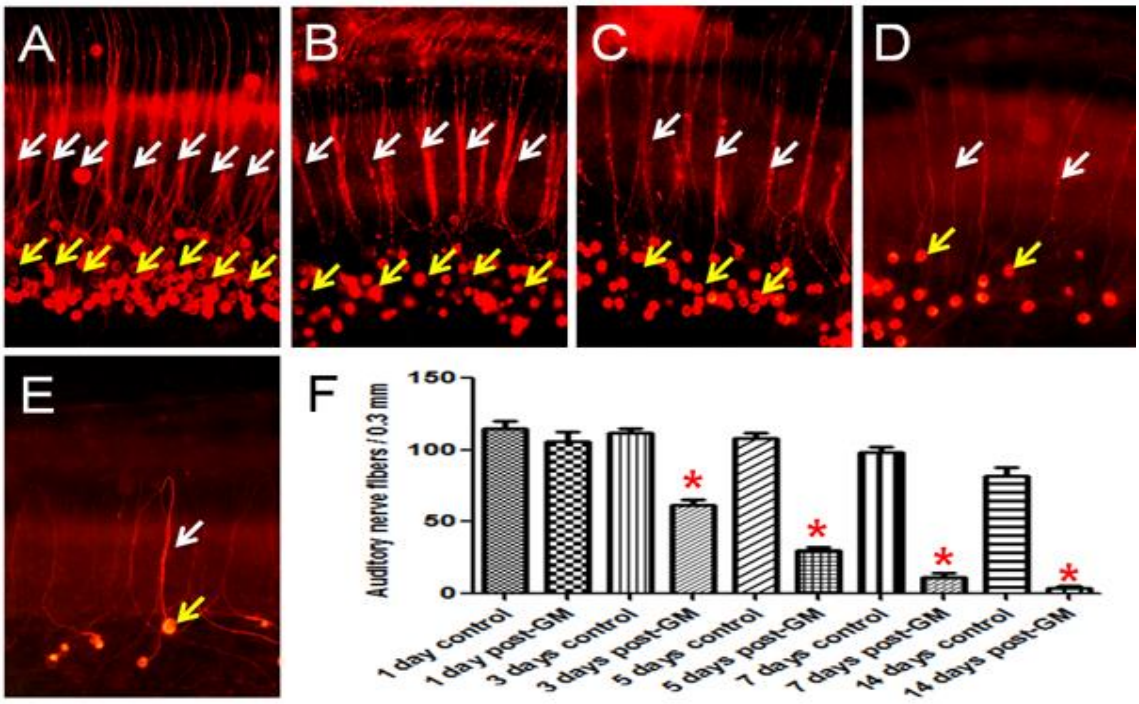

Figure 3-10. Secondary degeneration of spiral ganglion neurons and auditory nerve fibers in cochlear cultures. (A) Auditory nerve fibers (white arrows, red) and spiral ganglion neurons (yellow arrows, red) were intact 24 hours after 2 mM gentamicin treatment. (B) Spiral ganglion neurons (yellow arrows) and auditory nerve fibers (white arrows) degenerated 3 days after gentamicin treatment. (C) More spiral ganglion neuron loss (yellow arrows) was observed 5 days after gentamicin treatment. Most spiral ganglion neurons (yellow arrows) and auditory nerve fibers (white arrows) were degenerated or lost 7 days (D) or 14 days (E) following hair cell loss. (F) Numbers of spiral ganglion neurons and auditory nerve fibers under gentamicin treatment for various numbers of days of incubation (*Significantly different from control $P<0.05$. Error bars indicate S.D.).

spiral ganglion neurons and auditory nerve fibers [5,126]. Therefore, the spiral ganglion neuron deathmodel developed in this study could provide enhanced understanding of how ototoxic aminoglycoside antibiotics induce delayed neuron death in the cochlea.

7. Cisplatin-induced apoptotic cell death in cochlear cultures

Previous studies show that cisplatin treatment with or without ethacrynic acid causes apoptotic dell death, but not necrotic cell death, in the cochlear sensory hair cells and spiral ganglion neurons in cochlear organotypic cultures or cochlear tissues [5,28,31,33,34,36,37,39,48,68,195]. To investigate the molecular mechanisms by which cisplatin causes apoptotic cell death, cochlear and vestibular organotypic cultures from rat pups at postnatal day 3 were treated for 24 hours with 50 μM cisplatin conjugated to Alexa Fluor 488 (green) to visualize cisplatin. I first confirmed that there was no hair cell degeneration (arrows) in the control cochleas (Figure 3-11A). However, cisplatin (green) accumulated selectively in the outer hair cells and caused destruction of the outer hair cells after 24 hours of treatment with 50 μM Alexa Fluor 488 conjugated cisplatin (Figure 3-11B). Next, cochlear and vestibular organotypic cultures were stained with fluorescence-labeled caspase-3 inhibitor (green), which detects active caspase-3, under treatment with 10 μg/ml cisplatin for 48 hours. I first confirmed that there were no caspases-3-positive cells (green) in the cochlear hair cells of the control cochleas (Figure 3-11C). However, caspases-3-positive cells (green) were detected in the damaged hair cells under 10 μg/ml cisplatin treatment for 48 hours (Figure 3-11D). I also confirmed that there were no caspases-3-positive cells in the control vestibular hair cells (Figure 3-11E). However, caspases-3-positive cells (green) were detected in the severely damaged vestibular hair cells under 10 μg/ml cisplatin treatment for 48 hours (Figure 3-11F). To investigate if p53, a major regulator of

Figure 3-11.

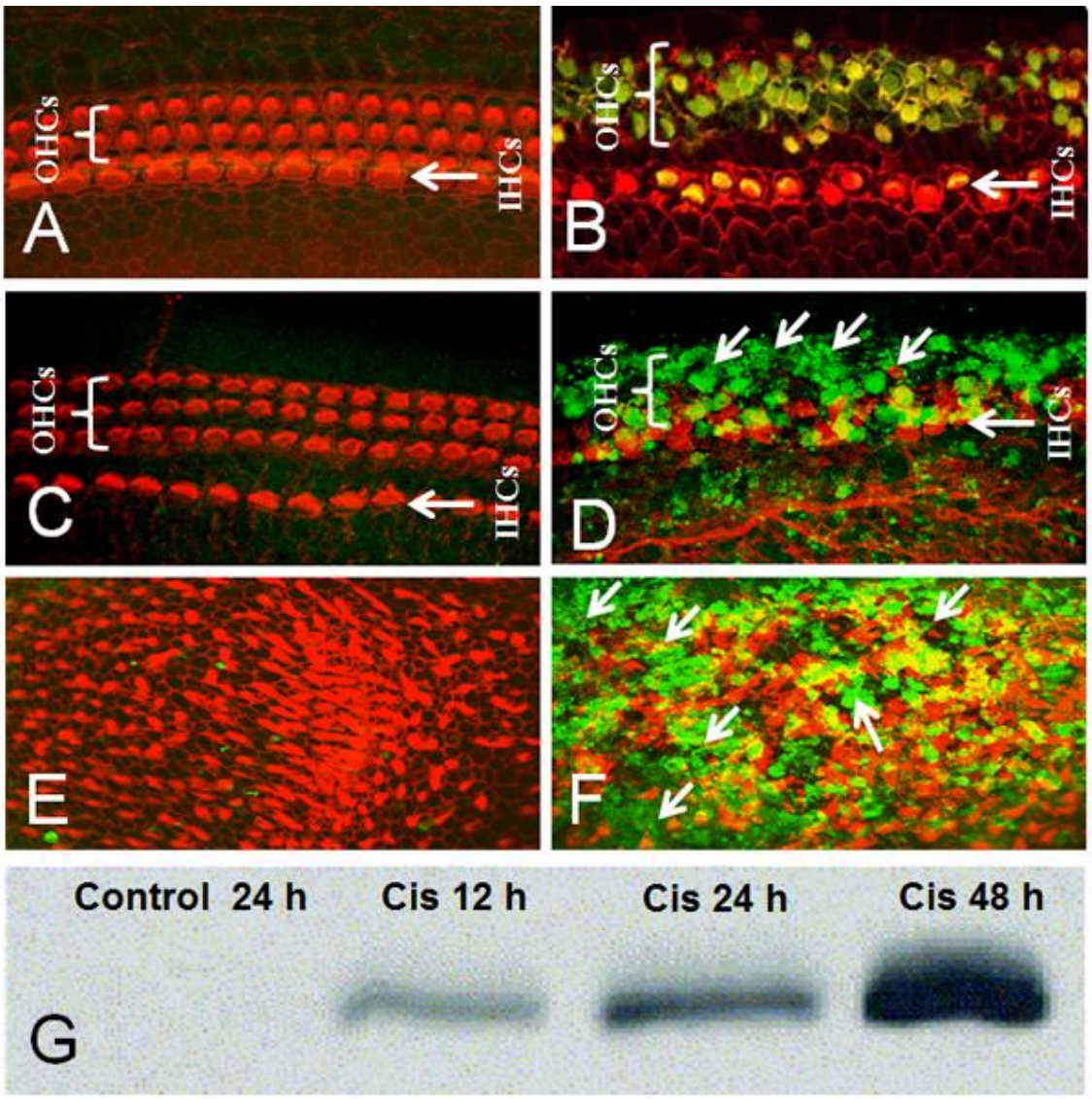

Figure 3-11. Roles of caspases-3 and p53 in cisplatin-induced hair cell death. (A) Hair cells were intact in control cochlea. Bracket and arrow indicate outer and inner hair cells, respectively. (B) Cisplatin (arrows, green) accumulated selectively in the outer hair cells and damaged the outer hair cells after treatment with 50 μM of cisplatin for 24 hours. (C) No caspase-3 staining (green) was detected in the control cochlea. (D) Caspase-3-positive cells (arrow, green) were detected in the severely damaged hair cells after 48 hours of 10 μg/ml cisplatin treatment. (E) No caspase-3 staining (green) was detected in the control vestibular hair cells. (F) Caspase-3-positive cells (arrow, green) were detected in the severely damaged vestibular hair cells after 48 hours of 10 μg/ml cisplatin treatment. (G) Western blot showing cisplatin treatment increased phosphorylated p53 protein levels in a time-dependent manner.

apoptosis, plays a role in cisplatin-induced apoptotic cell death, levels of phosphorylated p53 protein, an active form of p53, were measured in the cochlear tissues by western blots. We found that cisplatin treatment increased phosphorylated p53 protein levels in a time dependent manner (Figure 3-11G). These results suggest that p53-dependent apoptosis may be involved in cisplatin-induced cochlear hair cell death.

To further investigate how cisplatin treatment affects the expression of apoptotic and anti-apoptotic genes, we measured mRNA expression levels of 96 apoptosis related genes by focused apoptosis gene microarrays performed on RNA extracted from cochlear tissues from rat pups at postanal day 3 cultured in control conditions or cisplatin-treated for 3 or 12 hours [5,36,37,47]. First, to identify apoptotic genes involved in an early stage of cisplatin-induced hair cell death, cochlear explants were treated with 0.2 mM cisplatin for 3 hours, and then mRNA expression of apoptotic or anti-apoptotic genes were measured by PCR arrays. Cisplatin treatment for 3 hours induced up-regulation of 10 apoptotic or anti-apoptotic genes, while no apoptotic or anti-apoptotic genes were down-regulated by cisplatin (Figure 3-12A). The up-regulated genes include CASP2 and RIPK1 domain containing adaptor with death domain (*Gadd45a),* myeloid differentiation primary response gene 88 (*Myd88*), Ras-related associated with diabetes (*Rrad*), tumor necrosis factor alpha-induced protein 2 (*Tnfaip2*), tumor necrosis factor receptor superfamily member 12a (*Tnfrsfl2a*), and tumor necrosis factor receptor superfamily member 1a (*Tnfrsf1a*) (Figure 3-12A) that are considered as pro-apoptotic genes and involved in multiple apoptotic pathways or families, including the p53-mediated signaling, TNF receptor family, death domain family, BCL-2 family, CARD family, and GTP signaling pathways [5,36,37,47]. The remaining 4 genes were B-cell CLL/lymphoma 10 (*Bcl10*), Inhibitor of apoptosis protein 3 (*Birc3*), BCL2/adenovirus E1B 19 kDa-interacting protein 3 (*Bnip3*), and myeloid cell leukemia

Figure 3-12.

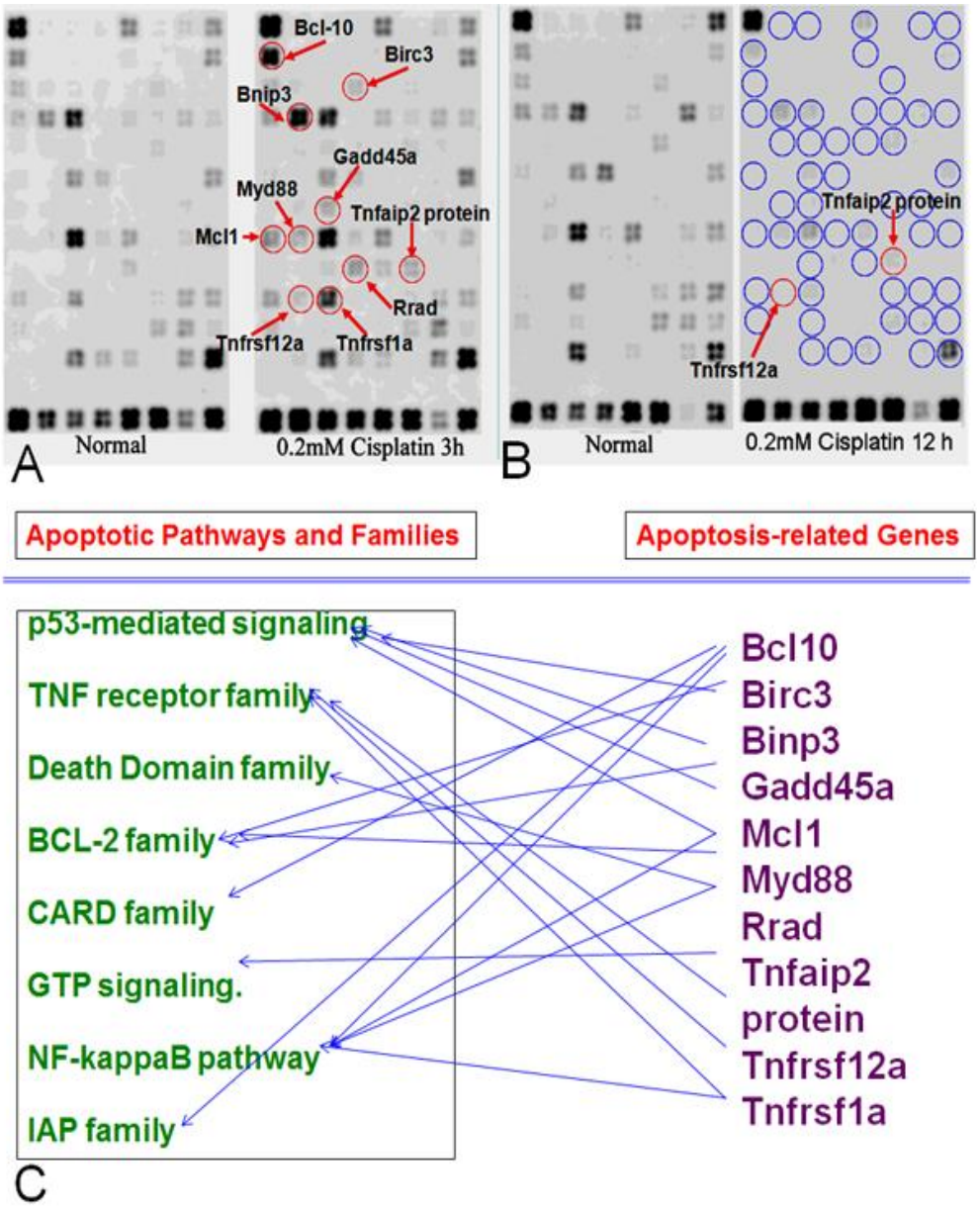

Figure 3-12. List of up-regulated or down-regulated apoptotic and anti-apoptotic genes induced by cisplatin. (A) Focused apoptosis gene microarrays showing increased expression (red circles) of 10 apoptotic or anti-apoptotic genes 3 hours after cisplatin treatment. (B) Focused apoptosis gene microarrays showing increased expression (red circles) of 2 apoptotic genes and decreased expression (blue circles) of over 50% of apoptotic and anti-apoptotic genes 12 hours after cisplatin treatment. (C) Ten apoptotic and anti-apoptotic genes were involved in multiple apoptotic pathways and families under cisplatin treatment.

sequence 1 (*Mcl1)*, members of the anti-apoptotic genes, involved in the NF-kappaB pathway, CARD family, IAP family, Bc -2 family, and P53 signaling (Figure 3-12C), [5,36,37,47]. We then found that cochlear explants treated with 0.2 mM cisplatin for 12 hours induced up-regulation of only tumor necrosis factor alpha-induced protein 2 **(*Tnfaip2*)** and tumor necrosis factor receptor superfamily member 12a (*Tnfrsf12a*)(Figure 3-12B), members of the tumor necrosis factor receptor super family that are known to interact with caspase-8 (Figure 3-12B) [5,36,37,47]. Cisplatin treatment for 12 hours also resulted in down-regulation of over 50% of the apoptotic and anti-apoptotic genes tested (Figure 3-12B), consistent with the previous pathological observations that cisplatin treatment causes severe degeneration of cochlear hair cells (Figure 3-11A and B). Together, these results indicate the following 10 genes, *Gadd45a, Myd88, Rrad, Tnfaip2, Tnfrsfl2a, Tnfrsf1a, Bcl10, Birc3, Bnip3,* and *Mcl1* respond to cisplatin and play roles in p53 and caspase apoptotic pathways in cisplatin-induced hair cell death in cochlear tissues.

8. Roles of apoptotic cell death in acute ototoxicity by co-administration of cisplatin and ethacrynic acid

Previous studies have shown that intravenous injection of ethacrynic acid effectively breaks the blood-cochlea barrier and enhances the entry of cisplatin into the cochlea [4,5,9,23,29,30,33,36,126,278]. To investigate whether or how co-administration of cisplatin and ethacrynic acid causes cell death in cochleae, chinchillas were co-administrated cisplatin (0.8 mg/kg, I.P.) and ethacrynic acid (40 mg/kg, I.V.) and euthanized after 6, 12, 24, or 48 hours. Cochlear tissue were double stained with phalloidin (green) for the cuticular plates of hair cells and propidium iodine (red) for nuclei. I first confirmed that there was no hair cell degeneration (bracket, arrow)

and that PI-labeled nuclei appeared large, round, and normal in the control cochleas (Figure 3-13A). Although supporting cells appeared normal, the nuclei of the outer hair cells (arrows) were shrunken 24 hours after combined treatment with cisplatin and ethacrynic acid (Figure. 3-13B). Caspase-8 and caspase-9 are two important initiator caspases that activate downstream executioner caspases, caspase-3 and caspase-6 [7,9,28,33,36,41,48]. Caspase-8 is activated by death receptors on the cell membrane, whereas caspase-9 is activated by cytochrome *c* from the mitochondria[4,9,28]. Next, to investigate whether caspases-8 or caspases-9 play a role to initiate the cell death signals after cisplatin and ethacrynic acid co-administration, fluorescence-labeled caspase-8 or caspase-9 were observed 24 hours after a single injection of cisplatin and ethacrynic acid [5,28,33,35,36,48,195]. Strong caspase-8 staining (green, arrows) was detected in the outer hair cells 24 hours following cisplatin and ethacrynic acid treatment (Figure. 3-13C). In contrast, caspase-9 staining (green) was not detected in the hair cells with condensed or fragmented nuclei 24 hours after cisplatin/ethacrynic acid treatment (Figure. 3-13D). These results suggest that cisplatin-initiated cell death signal may be released from the cell death receptors on the cell membrane, but mitochondrial apoptosis may not play a role in cisplatin-induced hair cell death. Next, strong staining of the executioner caspase-3 (green, arrows) (Figure 3-13E) and caspase-6 (green, arrows) (Figure 3-13F) was detected in the outer hair cells with condensed or fragmented nuclei 24 hours after cisplatin and ethacrynic acid treatment. These results suggest that because strong caspase-8 staining (green, arrows) had already appeared in the outer hair cells 24 hours following cisplatin/ethacrynic acid treatment (Figure. 3-13C) and caspase-8 is known to act upstream of casspase-3 and caspase-6 [5,28,33,35,36,48,195], cisplatin and ethacrynic acid treatment likely triggered caspase-8 activation, which in turn activated caspase-6 and caspase-3 in cochlear hair cells.

Figure 3-13.

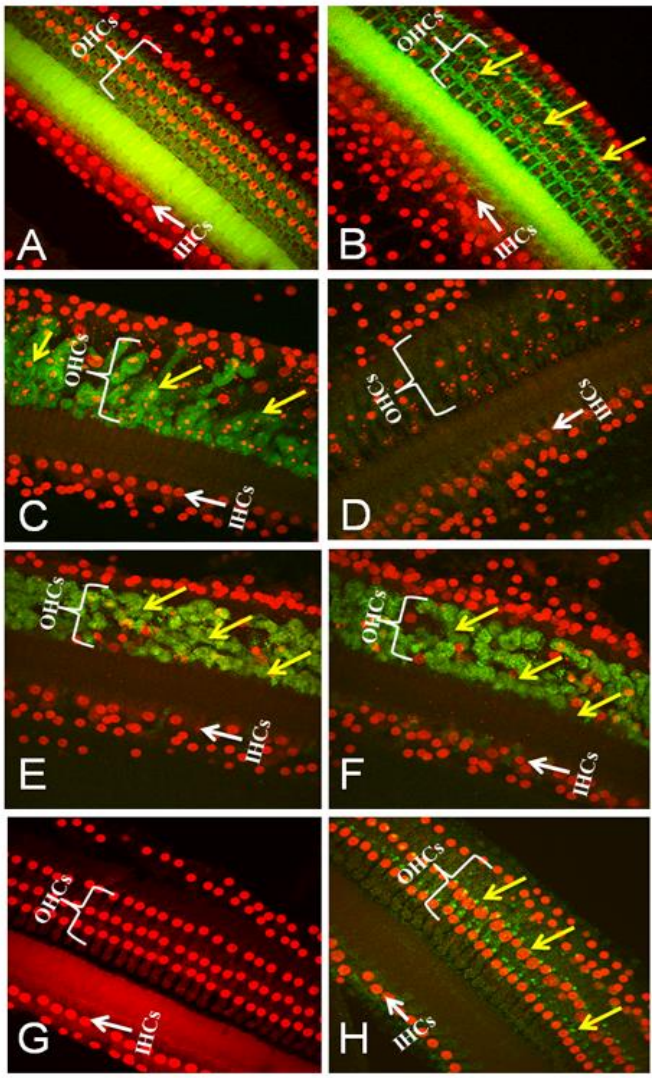

Figure 3-13. Roles of caspase-8, cassase-6, caspase-3, and TRADD in cisplatin and ethacrynic acid-induced hair cell death. (A) The cuticular plates of the cochlear hair cells were stained with phalloidin (green) while the nuclei of the hair cells were stained with propidium iodine (red). There was no hair cell degeneration in the control cochleas. Bracket and arrow indicate outer and inner hair cells respectively. (B) Nuclear shrinkage (yellow arrows) was detected in the outer hair cells after cisplatin and ethacrynic acid injection. (C) Caspase-8 staining (yellow arrow, green) was detected in the outer hair cells after cisplatin and ethacrynic acid injection. (D) Caspase-9 staining (green) was not detected in the hair cells with nuclear fragmentation after cisplatin and ethacrynic acid treatment. (E) Caspase-3 staining (yellow arrows, green) was detected 24 hours after cisplatin/ethacrynic acid treatment. (F) Caspase-6 staining (yellow arrows, green) was detected after cisplatin and ethacrynic acid treatment. (G) TRADD staining (green) was absent in the control cochlear hair cells. (H) TRADD staining (yellow arrows, green) was detected 6 hours after cisplatin and ethacrynic acid treatment.

Tumor necrosis factor associated death domain (TRADD) is a death domain adaptor protein that interacts with tumor necrosis factor receptors in the plasma membrane, which in turn causes apoptotic cell death through NFkB [5,28,33,35,36,48,195]. To investigate whether TRADD plays a role in hair cell death under treatment with cisplatin and ethacrynic acid, cochleas under treatment with cisplatin and ethacrynic acid for 6 hours were stained with antibodies for TRADD (green). I first confirmed that TRADD immunostaining (arrows) was absent in the control cochlea (Figure. 3-13G). However, TRADD staining (green, arrows) was detected in the outer hair cells 6 hours after cisplatin and ethacrynic acid treatment (Figure. 3-13H). These results suggest that TRADD activates caspase-8, which in turn activates caspase-6 and caspase-3 in cisplatin and ethacrynic acid-mediated hair cell death in cochlear tissues.

9. Mefloquine-induced apoptosis in organotypic culture system of the inner ear

Malaria is one of the leading causes of death and diseases in developing countries worldwide and mefloquine is one of the most widely used antimalarial drugs [7,41-43,196-198]. However, mefloquine causes multiple side effects, including hearing and balance disturbances [204,279]. To investigate whether and how mefloquine causes hair cell death, cochlear organotypic cultures from rat pups at postnatal day 3 were treated with 10 – 200 μM mefloquine for 24 hours, and then cochleograms were performed. Under treatment with 10 μM mefloquine for 24 hours, there was little or no hair cell loss in the cochlea cultures (Figure 3-14A). Under treatment with 25 – 35 μM mefloquine for 24 hours, severe cochlear outer hair cell loss was confirmed in the basal region of the cochlea (Figure. 3-14B and C). Nearly all the cochlear outer hair cells were lost under treatment with ≥50 μM mefloquine for 24 hours (Figure. 3-14D, E, F). Together, these results show that mefloquine causes cochlear hair cell loss in a dose-dependent manner, and the

Figure 3-14.

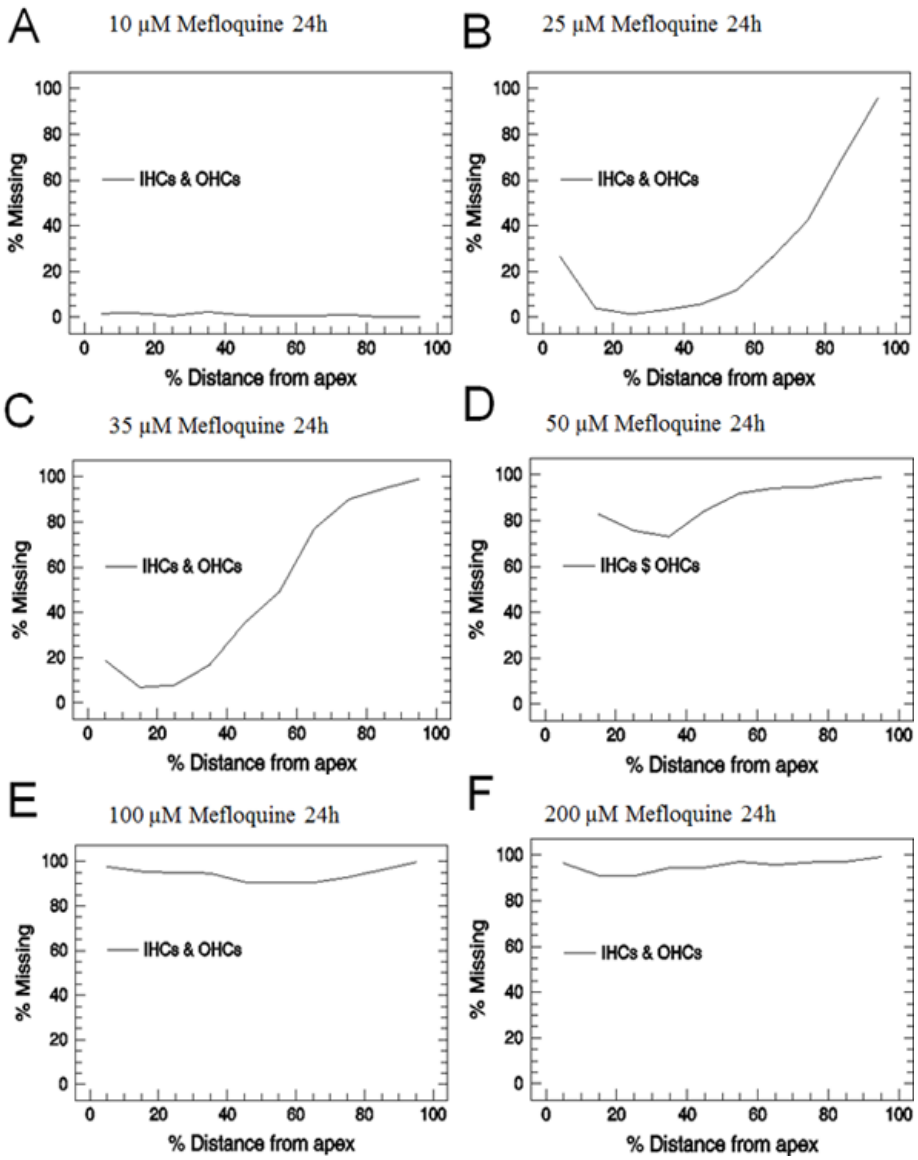

Figure 3-14. Mefloquine induces hair cell damage in a dose-dependent manner in cochlear organotypic cultures. Averaged (n=6/group) cochleograms showing percent missing hair cells as a function of percent distance from the apex 24 hours after treatment with different doses of mefloquine. Since the inner hair cells and outer hair cells were disarranged after mefloquine treatment, the inner hair cells and outer hair cells were not counted separately. (A) Little or no outer hair cell loss was detected under 10 µM mefloquine treatment. (B-C) Severe cochlear outer hair cell loss was confirmed in the basal region of the cochlea under 25-35 µM mefloquine treatment. (D-F) Nearly all the cochlear outer hair cells were lost under treatment with mefloquine at concentrations of 50 µM and higher.

sensory cell loss in the cochlea occurs in a stereotypic pattern; damage begins at the base of the cochlea and progresses toward the apex. To investigate whether and how mefloquine causes vestibular hair cell death, vestibular organotypic cultures from rat pups at postnatal day 3 were also treated with 10 – 200 μM mefloquine for 24 hours. Vestibular hair cells were stained with TRITC-conjugated phalloidin (red). I first confirmed that there was no hair cell (red, arrows) damage in the vestibular cultures in the standard culture condition without mefloquine (Figure 3-15A). However, hair cell density (arrows) was slightly reduced in the vestibular cultures treated with 10 μM mefloquine for 24 hours (Figure 3-15B). Disarrayed or disorganized stereocilia tufts (red, arrows) were observed in the vestibular cultures treated with 100 μM mefloquine (Figure 3-15C). Nearly all the hair cells (arrows) were lost under treatment with 200 μM mefloquine (Figure 3-15D). To validate these histological observations, vestibular hair cell numbers were counted in the vestibular utricles treated with 0, 10, 50, 100, or 200 μM mefloquine for 24 hours. We found that the utricles treated with 50, 100, or 200 μM mefloquine displayed significantly more hair cell loss compared to those of controls ($P<0.05$), while utricles treated with 10 μM mefloquine displayed significantly less hair cell loss compared to those of the utricles treated with 50, 100, or 200 μM mefloquine (Figure 3-15E) ($P<0.05$). Furthermore, utricles treated with 200 μM mefloquine displayed significantly more hair cell loss compared to those of the utricles treated with 50 to 100 μM mefloquine treatment ($P<0.05$). Together, these results show that mefloquine treatment causes vestibular hair cell loss in a dose-dependent manner.

To investigate whether and how mefloquine causes auditory nerve fiber denervation, cochlear organotypic cultures from rat pups were treated with 35-200 μM mefloquine for 24 hours. After fixation, cochlear explants were double stained with antibody against neurofilament

Figure 3-15.

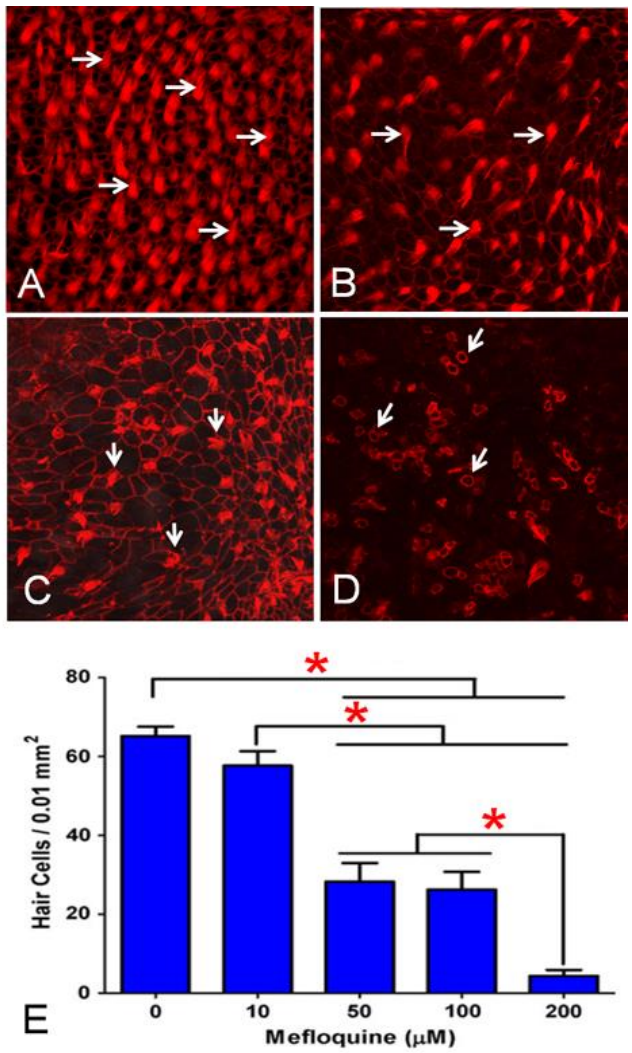

Figure 3-15. Mefloquine-induced hair cell damage in vestibular cultures. (A) There was no hair cell (red) damage in the control macula of utricle in the vestibular cultures. Arrows indicate stereocilia tufts and hexagonal ring of the hair cells (red). (B) Hair cell density (red) was slightly reduced in the vestibular cultures treated with 10 μM mefloquine for 24 hours. (C) Disarrayed or disorganized stereocilia tufts (arrows) were observed in the vestibular cultures treated with 100 μM mefloquine. (D) Nearly all hair cells were lost under 200 μM mefloquine treatment for 24 hours. Note that the circumferential ring on the remaining hair cells appeared shrunken (arrow). (E) Mean numbers of hair cells per 0.01 mm^2 in the maculae of utricle as a function of mefloquine dose. The utricles treated with 50, 100, or 200 μM mefloquine displayed significantly more hair cell loss compared to those of controls ($P<0.05$), while utricles treated with 10 μM mefloquine displayed significantly less hair cell loss compared to those of the utricles treated with 50, 100, or 200 μM mefloquine ($P<0.05$). Furthermore, utricles treated with 200 μM mefloquine displayed significantly more hair cell loss compared to those of the utricles treated with 50 to 100 μM mefloquine treatment ($P<0.05$). *significantly different. S.D.=standard deviation.

200 (red) and FITC-conjugated phalloidin (green). I first confirmed that there was no auditory nerve fiber (red, arrows) damage in the control cochlear cultures: thick bands of the auditory nerve fibers projecting towards the hair cells (red, arrows) were confirmed. (Figure 3-16A). Severe disintegration of the auditory nerve fibers (arrows, red) into small beads or puncta were observed in the basal region of the cochlear cultures treated for 24 hours with 50 μM (Figure 3-16B), 100 μM (Figure 3-16C), or 200 μM (Figure 3-16D) mefloquine treatment. Minor damage to the auditory nerve fibers (arrows, red) was observed in the apical region (Figure 3-16E), but severe damage was found in the basal region (Figure 3-16F) of the cochlear cultures treated for 24 hours with 35 μM mefloquine. Furthermore, under 50 μM mefloquine treatment for 24 hours, nearly complete destruction of the hair cells and auditory nerve fibers in the apical region (Figure 3-16G) and basal region (Figure 3-16H) was observed.

To investigate whether caspases play a role in cochlear and vestibular hair cell death induced by mefloquine, cochlear explants under treatment with 35-200 μM mefloquine for 24 hours were stained with fluorescently-labeled caspase-8, caspase-9, or caspase-3 inhibitors, phalloidin for the cuticular plates of hair cells or propidium iodide for nuclei. I first confirmed that caspase-3 staining (green) was absent in the control cochlear hair cells (Figure 3-17A). Under treatment with 35 μM mefloquine for 24 hours, caspase-8 staining (green, arrows) was detected in the damaged cochlear hair cells and surrounding supporting cells (Figure 3-17B). Caspase-9 staining (green, arrows) was also detected in the damaged cochlear hair cells and surrounding supporting cells under 35 μM mefloquine treatment for 24 hours (Figure 3-17C). Moreover, caspase-3 staining (green, arrows) was detected in the damaged cochlear hair cells and surrounding supporting cells under 35 μM mefloquine treatment for 24 hours (Figure 3-

17D). In spiral ganglion neurons, I first confirmed that caspase-3 staining (green) was absent in the

Figure 3-16.

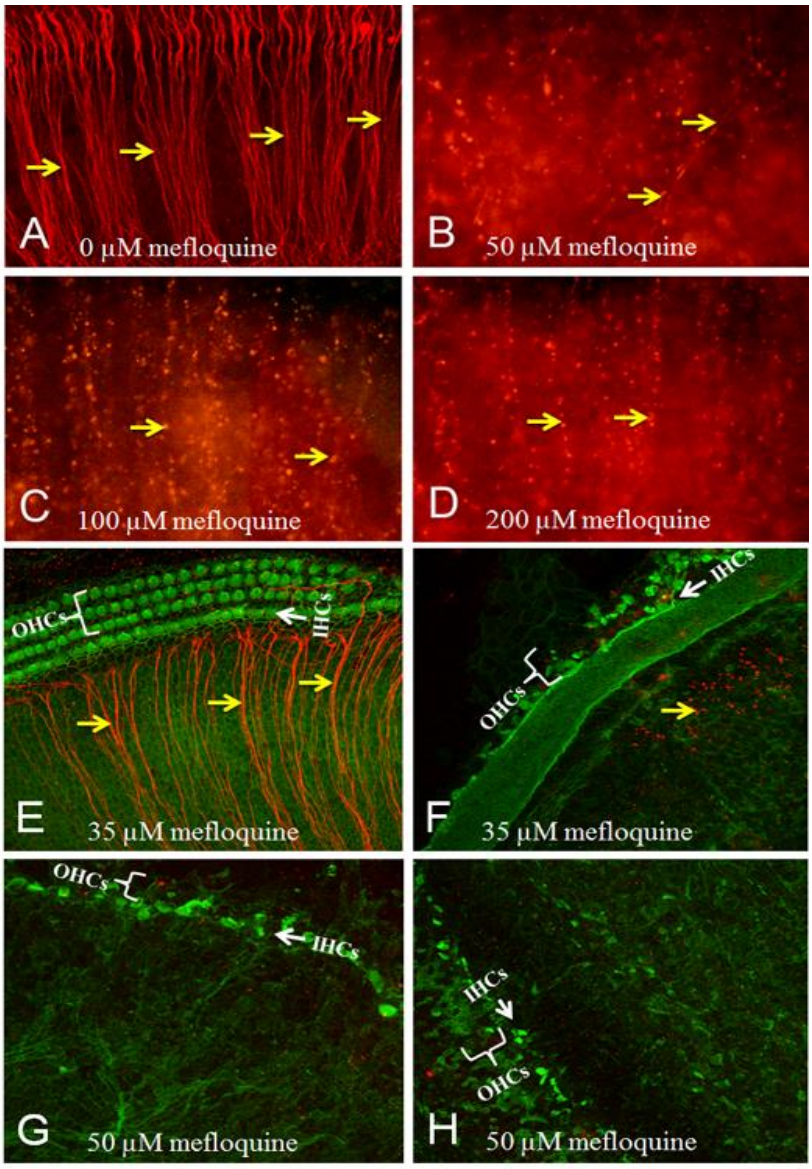

Figure 3-16. Mefloquine induces auditory nerve fiber degeneration. (A) There was no auditory nerve fiber (red) damage in the control cochlear cultures: thick bands of the auditory nerve fibers projecting towards the hair cells were observed (yellow arrows). Severe degeneration of the auditory nerve fibers into small beads or puncta (yellow arrows) were observed in the basal region of the cochlear cultures under treatment with 50 µM (B), 100 µM (C), or 200 µM (D) mefloquine. Auditory nerve fibers (yellow arrows) were intact in the apical region (E), but damaged auditory nerve fibers were detected in the basal region (yellow arrows) (F) of the cochlear cultures treated with 35 µM. Under 50 µM mefloquine treatment, nearly complete

destruction in the apical region (G) and basal region (H) of the hair cells and auditory nerve fibers were observed. Bracket and arrow indicate outer and inner hair cells respectively.

Figure 3-17.

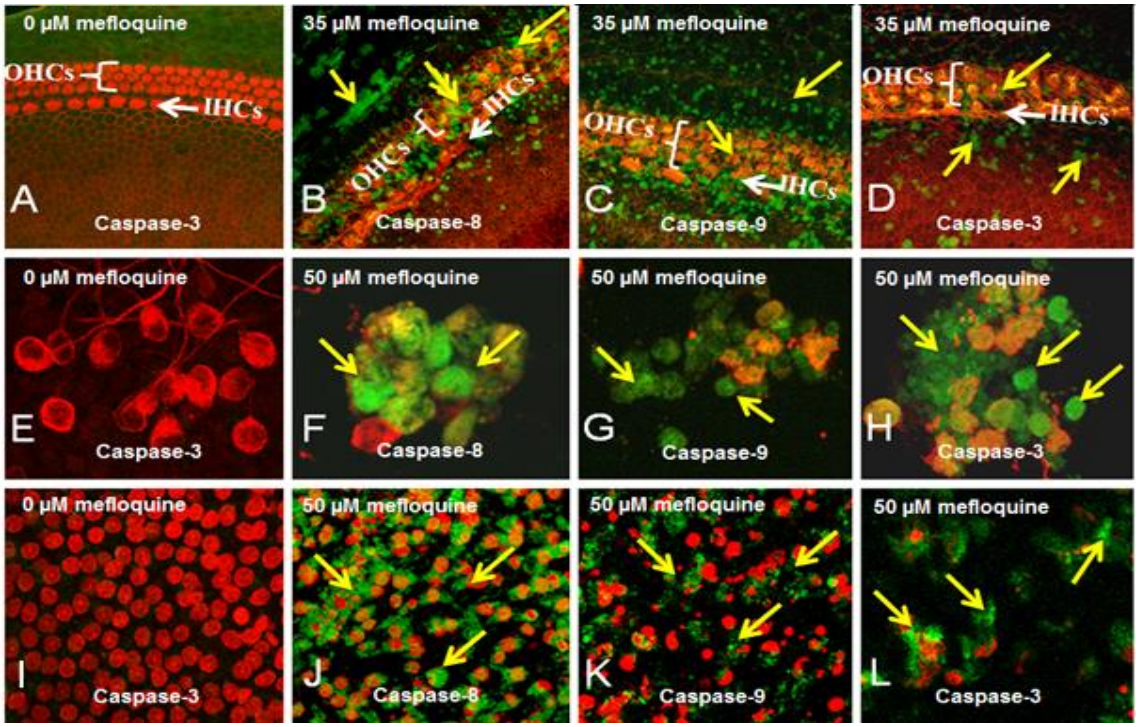

Figure 3-17. Roles of caspases-mediated apoptosis in mefloquine-induced cochlear and vestibular cell death. (A) Caspase-3 (green) staining was absent in the control cochlear hair cells (red). (B) Under treatment with 35 μM mefloquine, caspase-8 staining (yellow arrows, green) was detected in the damaged cochlear hair cells and surrounding supporting cells. (C) Caspase-9 staining (yellow arrows, green) was detected in the damaged cochlear hair cells and surrounding supporting cells under 35 μM mefloquine treatment. (D) Caspase-3 staining (yellow arrows, green) was detected in the damaged cochlear hair cells and surrounding supporting cells under 35 μM mefloquine treatment. (E) Caspase-3 staining (green) was absent in the control spiral ganglion neurons. (F) Under treatment with 50 μM mefloquine, caspase-8 staining (yellow arrows, green) was detected in the damaged spiral ganglion neurons. (G) Caspase-9 staining (yellow arrows, green) was detected in the damaged spiral ganglion neurons under 50 μM mefloquine treatment. (H) Caspase-3 (yellow arrows, green) staining was detected in the damaged cochlear spiral ganglion neurons under 50 μM mefloquine treatment. (I) In vestibular cultures, caspase-3 staining (green) was absent in the control hair cells. (J) Under treatment with 50 μM mefloquine, caspase-8 staining (yellow arrows, green) was detected in the damaged vestibular hair cells. (K) Caspase-9 staining (yellow arrows, green) was also detected in the damaged vestibular hair cells under 50 μM mefloquine treatment. (L) Caspase-3 staining (yellow arrows, green) was detected in the damaged vestibular hair cells under 50 μM mefloquine treatment.

control (Figure 3-17E). However, under treatment with 50 μM mefloquine for 24 hours, caspase-8 staining (green, arrows) was detected in the damaged spiral ganglion neurons (Figure 3-17F). Caspase-9 staining (green, arrows) was also detected in the damaged spiral ganglion neurons under 50 μM mefloquine treatment for 24 hours (Figure 3-17G). Moreover, caspase-3 staining (green, arrows) was detected in the damaged cochlear spiral ganglion neurons under 50 μM mefloquine treatment for 24 hours (Figure 3-17H).

In vestibular cultures, I fist confirmed that caspase-3 staining (green) was absent in the control hair cells (Figure 3-17I). However, under treatment with 50 μM mefloquine for 24 hours, caspase-8 staining (green, arrows) was detected in the damaged vestibular hair cells (Figure 3-17J). Caspase-9 staining (green, arrows) was also detected in the damaged vestibular hair cells under 50 μM mefloquine treatment for 24 hours (Figure 3-17K). Moreover, caspase-3 staining (green, arrows) was detected in the damaged vestibular hair cells under 50 μM mefloquine treatment for 24 hours (Figure 3-17L). Lastly, I investigated whether mefloquine increases DNA fragmentation, a key feature of apoptosis, in the spiral ganglion neurons cells under 35 μM mefloquine treatment for 6 hours by TUNEL staining. I first confirmed that no TUNEL-positive cells (green, arrows) were detected in the spiral ganglion neurons in the control cochleas (Figure 3-18A). However, under treatment with 35 μM mefloquine for 6 hours, TUNEL-positive nuclei (green) were detected in the damaged spiral ganglion cells with nuclear DNA fragmentation (Figure. 3-18B). Together, these observations indicate that mefloquine treatment induces apoptotic cell death in the hair cells or spiral ganglion neurons of the vestibular and cochlear tissues through the caspases-8, caspases-9, and/or caspases-3-mediated apoptosis pathways.

To further investigate how mefloquine treatment affects the expression of apoptotic and

anti-apoptotic genes, we measured mRNA expression levels of 84 apoptotic or anti-apoptotic

Figure 3-18.

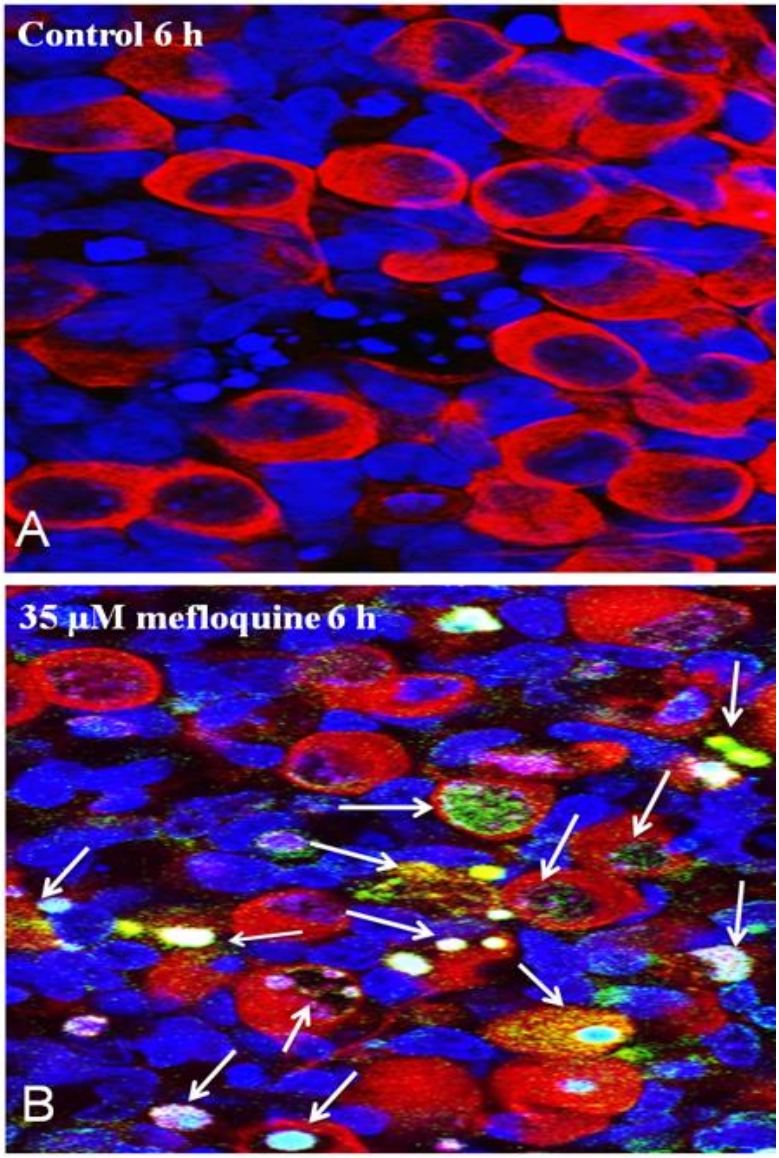

Figure 3-18. Mefloquine causes DNA fragmentation in the cochlear spiral ganglion neurons. (A) No TUNEL-positive cells (green) were detected in the spiral ganglion neurons in the control cochlea without mefloquine treatment. (B) Under treatment with 35 μM mefloquine treatment for 6 hours, TUNEL-positive nuclei (arrows, green) were detected in the damaged spiral ganglion cells with nuclear DNA fragmentation.

genes in the epithelium of cochlear basilar membranes containing hair cells and supporting cells, or spiral ganglion neurons with or without 100 μM mefloquine treatment for 3 hours using qRT-PCR arrays [42,125]. The custom-made qRT-PCR array contained 84 key apoptosis related genes in a 96-well plate as previously described [42,125]. Mefloquine treatment resulted in up-regulation or down-regulation of 23 apoptotic or anti-apoptotic genes in the cochlear epithelium (Figure 3-19A), and up-regulation or down-regulation of 32 apoptotic or anti-apoptotic genes in the spiral ganglion neurons in comparison with controls (Figure. 3-19B). Those mefloquine-induced gene names, gene symbols, gene function categories, and fold changes are listed in Table 1 and 2.

Three hours after 100 μM mefloquine treatment, mefloquine induced changes in mRNA expression of 23 of the 84 studied genes from cochlear epitheliums. Mefloquine upregulated 10 genes and down-regulated 13 genes (Table 1). The remaining 61 genes showed no significant change in comparison with untreated cochlear tissues. The 10 up-regulated genes were *Bcl2a1, Birc3, Gadd45a, Il10, Mcl1, Nfkb1, Prok2, Pycard, Tnf,* and *Tnfsf6,* and those showing decreased expression were *Bid3, Birc4, Bnip1, Casp1, Casp7, Casp9, Cradd, Faim, Prlr, Sphk2, Tnfsf10, Tnfsf12,* and *Tradd*. These genes are relevant to multiple apoptotic signaling pathways, including the Bcl-2 (*Bcl2a1, Bid3, Bnip1, Mcl1*), caspase (*Casp1, Casp7, Casp9*), TNF ligand/receptor (*Faim, Tnf, Tnfsf6, Tnfsf10, Tnfsf12, Il10, Prok2, Sphk2, Tradd*), IAP (*Birc3, Birc4*), death domain/death effector domain (*Cradd, Tradd*), p53, DNA damage-induced apoptosis (*Casp7, Casp9, Cradd, Gadd45a, Mcl1, Nfkb1, Pycard, Tnf, Tnfsf6, Tradd*), NF-kappa B (*Bcl2a1, Il10, Nfkb1, TNF, Tnfsf6, Tnfsf10, Tradd*), Card (*Birc3, Birc4, Casp1, Casp9, Cradd, Pycard*), and cytokine receptor families (*Prlr*). These are either pro-apoptotic (*Bid3, Casp1, Casp7, Casp9, Cradd, Gadd45a, Pycard, Tnfsf6, Tnfsf10, Tnfsf12, Tradd*) or anti-apoptotic genes (*Bcl2a1, Birc3, Birc4, Bnip1, Faim, Il10, Mcl1, Nfkb1, Prlr, Prok2, Sphk2, Tnf*) (Table 1).

Figure 3-19.

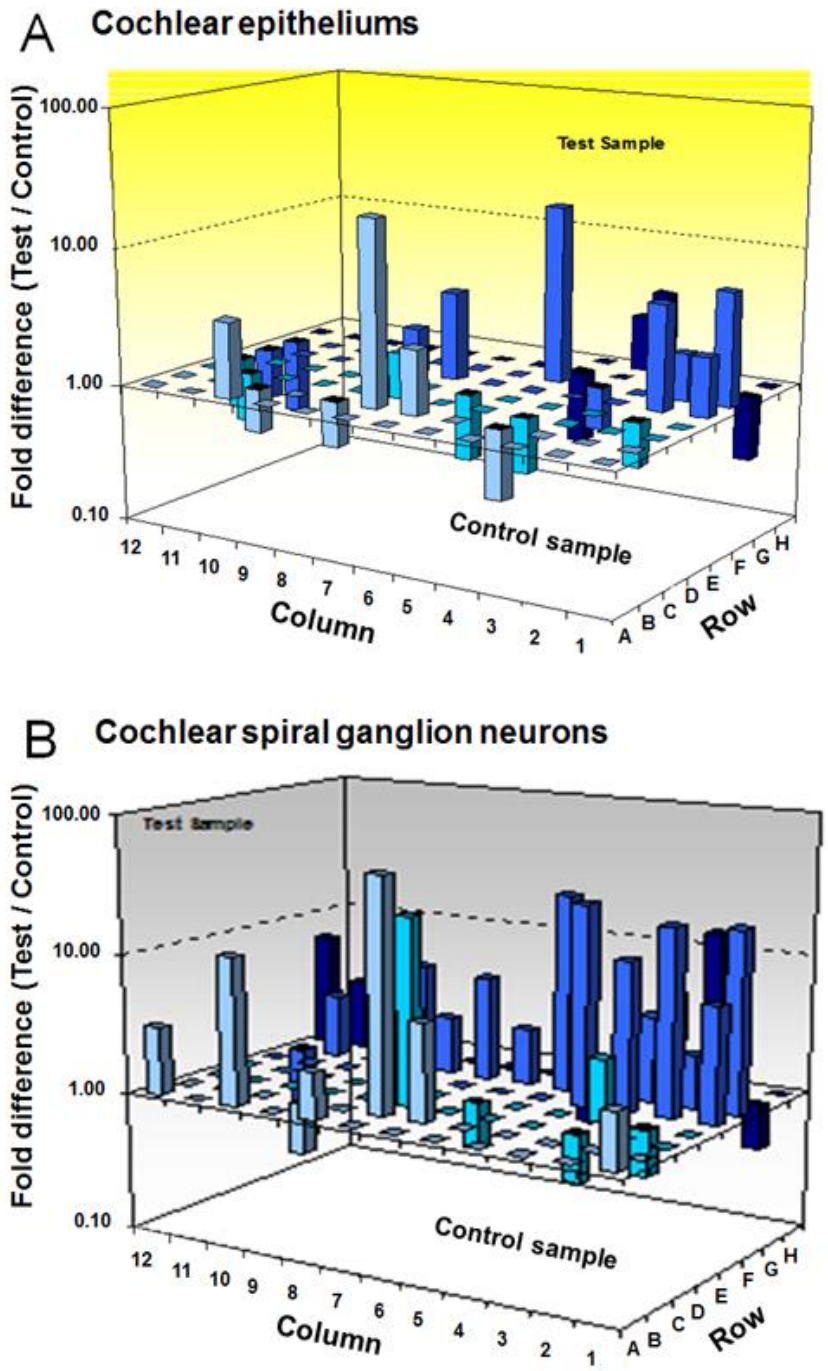

Figure 3-19. Mefloquine-induced changes in apoptosis related genes. Typical photographs showing altered apoptosis related genes in cochlear epitheliums (A) and in spiral ganglion neurons (B) under treatment with 100 μM mefloquine for 3 hours.

Table 1. List of up-regulated or down-regulated genes in cochlear epitheliums under mefloquine treatment.

Gene	Description	Functional Gene Grouping	Fold changes	p value
Bcl2a1	B-cell leukemia/lymphoma 2 related protein A1	Bcl-2 family	3.63	<0.0001
Bid3	BH3 interacting (with BCL2 family) domain, apoptosis agonist	Bcl-2 family	-3.14	<0.0001
Birc3	Inhibitor of apoptosis protein 1	IAP family	21.86	<0.0001
Birc4	Baculoviral IAP repeat-containing 4	IAP family	-2.14	0.0004
Bnip1	BCL2/adenovirus E1B 19kDa-interacting protein 1	Bcl-2 family	-2.09	0.0005
Casp1	Caspase 1	Caspase family / Card family	-2.43	<0.0001
Caps7	Caspase 7	Caspase family / p53 family	-2.28	0.0119
Casp9	Caspase 9	Caspase family / p53 family / Card family	-2.08	0.0193
Cradd	CASP2 and RIPK1 domain containing adaptor with death domain (predicted)	Death domain family / Card family / p53 family	-2.96	<0.0001
Faim	Fas apoptotic inhibitory molecule	TNF ligand / receptor family	-2.37	0.0017
Gadd45a	Growth arrest and DNA-damage-inducible 45 alpha	p53 family	2.69	<0.0001
Il10	Interleukin 10	NF-kappa B family	5.68	0.0078
Mcl1	Myeloid cell leukemia sequence 1	Bcl-2 family / p53 family	4.37	0.0143
Nfkb1	Nuclear factor of kappa light chain gene enhancer in B-cells 1, p105	p53 family / NF-kappa B family	2.15	0.0002
Prlr	Prolactin receptor	Cytokine receptor family	-2.34	0.0098
Prok2	Homolog of mouse Bv8 (Bombina variegata 8 kDa); prokineticin 2 precursor	TNF ligand / receptor family	6.6	0.018
Pycard	Apoptosis-associated speck-like protein containing a CARD	Death domain family / p53 family	2.18	<0.0001
Sphk2	Sphingosine kinase 2	TNF ligand / receptor family	-2.01	<0.0001
Tnf	Tumor necrosis factor superfamily, member 2	TNF ligand family / NF-kappa B family	19.08	<0.0001
Tnfsf10	Tumor necrosis factor (ligand) superfamily, member 10	TNF ligand family / NF-kappa B family	-3.55	0.0002
Tnfsf12	Tumor necrosis factor ligand superfamily member 12	TNF ligand family / NF-kappa B family	-2.83	0.0012
Tnfsf6	Tumor necrosis factor (ligand) superfamily, member 6	TNF ligand family / p53 family / NF-kappa B family	4.6	0.0058
Tradd	TNFRSF1A-associated via death domain	TNF ligand /p53 / NF-kappa B / Death domain	-3.32	<0.0001

In the tissue of spiral ganglion neurons, mefloquine treatment induced changes in mRNA expression of 32 genes: mefloquinine up-regulated 25 genes and down-regulated 7 genes. There was no expression change in the remaining 52 genes (Table 2). The 25 up-regulated genes were *Apaf1, Bcl10, Bcl2a1, Bcl2l11, Birc1b, Birc3, Casp14-predicted, Cflar, Gadd45a, Il10, Lhx4-predicated, Lta, Nfkb1, Prok2, Pycard, Ripk2, Tnf, Tnfrsf10b-predicted, Tnfrsf11b, Tnfrsf1a, Tnfrsf6, Tnfsf5, Tnfsf6, Trp63,* and *Trp73-predicted*, while the down-regulated 7 genes were *Birc5, Card6-predicted, Casp9, Cradd, Tnfsf10, Tnfsf12, Tradd*. Nineteen of these genes are pro-apoptotic (*Apaf1, Bcl10, Bcl2l11, Card6-predicted, Casp14-predicted, Casp9, Cradd, Gadd45a, Lta, Pycard, Tnfrsf10b-predicted, Tnfrsf11b, Tnfrsf1a, Tnfsf10, Tnfsf12, Tnfsf6, Tradd, Trp63, Trp73-predicted*) and the remaining 13 genes (*Bcl2a1, Birc1b, Birc3, Birc5, Cflar, Il10, Lhx4-predicated, Nfkb1, Prok2, Ripk2, Tnf, Tnfrsf6, Tnfsf5*) are anti-apoptotic genes. The multiple apoptotic signals are involved in the following pathways: the Bcl-2 family (*Bcl2a1, Bcl2l11*), caspase family (*Casp14-predicted, Casp9*), IAP family (*Birc1b, Birc3, Birc5*), TNF ligand/receptor family (*Lta, Prok2, Tnf, Tnfsf5, Tnfsf6, Tnfsf10, Tnfsf12, Tnfrsf10b-predicted, Tnfrsf11b, Tnfrsf1a, Tnfrsf6, Tradd*), Death domain/Death effector domain family (*Cflar, Cradd, Tnfrsf11b, Tnfrsf6, Tradd*), Card family (*Apaf1, Bcl10, Birc3, Card6-predicted, Casp9, Cradd, Pycard, Ripk2*), p53 family and DNA damage-induced apoptosis (*Apaf1, Casp9, Cradd, Gadd45a, Nfkb1, Pycard, Tnf, Tnfrsf10b-predicted, Tnfrsf6, Tnfsf6, Tradd, Trp63, Trp73*), NF-kappa B family (*Bcl10, Bcl2a1, Cflar, Il10, Lta, Nfkb1, Ripk2, Tnf, Tnfrsf1a, Tnfrsf10b-predicted, Tnfsf6, Tnfsf10, Tradd*), and LIM-homeobox gene family (*Lhx4-predicated*)(Table 2). Together, these RCR array results provide strong evidence that multiple apoptosis genes and pathways are involved in mefloquine-induced cochlear damage.

Table 2. List of up-regualted or down-regulated genes in cochlear spiral ganglion neurons under mefloquine treatment.

Gene	Description	Functional Gene Grouping	Fold changes	p value
Apaf1	Apoptotic peptidase activating factor 1	Card family	2.52	0.0021
Bcl10	B-cell CLL/lymphoma 10	Card family	2.18	0.0026
Bcl2a1	B-cell leukemia/lymphoma 2 related protein A1	Bcl-2 family	11.75	<0.0001
Bcl2l11	BCL2-like 11 (apoptosis facilitator)	Bcl-2 family	3.07	0.0053
Birc1b	Baculoviral IAP repeat-containing 1b	IAP family	5.07	<0.0001
Birc3	Inhibitor of apoptosis protein 1	IAP family	47.5	<0.0001
Birc5	Baculoviral IAP repeat-containing 5	IAP family	-2.3	0.004
Card6-predicted	Caspase recruitment domain, member 6	Caspase family / Card family	-2.2	0.0114
Casp14-predicted	Caspase 14 (predicted)	Caspase family	22.35	<0.0001
Casp9	Caspase 9	Caspase family / p53 family / Card family	-2.13	0.0231
Cflar	CASP8 and FADD-like apoptosis regulator	Death domain / Death effector domain family	2.81	0.0002
Cradd	CASP2 and RIPK1 domain containing adaptor with death domain (predicted)	Death domain family / Card family / p53 family	-2.11	0.0009
Gadd45a	Growth arrest and DNA-damage-inducible 45 alpha	p53 familu	6.82	<0.0001
Il10	Interleukin 10	NF-kappa B family	21.65	<0.0001
Lhx4-predicted	LIM homeobox protein 4 (predicted)	LIM-homeobox gene family	11.7	<0.0001
Lta	Lymphotoxin A	TNF ligand family / NF-kappa B family	26.83	<0.0001
Nfkb1	Nuclear factor of kappa light chain gene enhancer in B-cells 1, p105	p53 family / NF-kappa B family	7.15	<0.0001
Prok2	Prokineticin 2 precursor	TNF ligand / receptor family	19.89	<0.0001
Pycard	Apoptosis-associated speck-like protein containing a CARD	Death domain family / p53 family / caspase family	2.42	<0.0001
Ripk2	Receptor (TNFRSF)-interacting serine-threonine kinase 2, anti-apoptotic	Card family	4.15	<0.0001
Tnf	Tumor necrosis factor superfamily, member 2	TNF ligand family / NF-kappa B family	25.71	<0.0001
Tnfrsf10b-predicted	Tumor necrosis factor receptor superfamily, member 10b (predicted)	TNF receptor family / p53 family / NF-kappa B	2.54	0.0017
Tnfrsf11b	Tumor necrosis factor receptor superfamily, member 11b (osteoprotegerin)	TNF receptor family / Death domain family	5.5	<0.0001
Tnfrsf1a	Tumor necrosis factor receptor superfamily, member 1a	TNF receptor family	2.55	0.0037
Tnfrsf6	Tumor necrosis factor receptor superfamily, member 6	TNF receptor family	2.84	0.0006
Tnfsf10	Tumor necrosis factor (ligand) superfamily, member 10	TNF ligand family	-3.83	<0.0001
Tnfsf12	Tumor necrosis factor (ligand) superfamily member 12	TNF ligand family	-2.09	0.0049
Tnfsf5	Tumor necrosis factor (ligand) superfamily, member 5	TNF ligand family	15.35	<0.0001
Tnfsf6	Tumor necrosis factor (ligand) superfamily, member 6	TNF ligand family	5.23	<0.0001
Tradd	TNFRSF1A-associated via death domain	p53 family / NF-kappa B family / Death domain	-2.06	0.0002
Trp63	Transformation related protein 63	p53 family	3.23	0.0005
Trp73-predicted	Transformation related protein 73 (predicted)	p53 family	6.68	0.0001

10. Mefloquine treatment results in increased oxidative stress

To investigate whether mefloquine treatment increases oxidative stress in cochlear hair cells and spiral ganglion neurons, we measured the levels of superoxide, one of the major ROS (reactive oxygen species), in the hair cells and spiral ganglion neurons of cultured cochlear organs from rat pups at postnatal day 3 treated with mefloquine using dihydroethidium to label superoxide as previously shown [7,9,23,43,224]. I first confirmed that little or no superoxide staining (red) was detected in the organ of Corti region (Figure 3-20A) and spiral ganglion neuron region (Figure 3-20E) in the control cochlear cultures. Under treatment with 50 μM mefloquine for 12 hours, superoxide staining (red) was detected in the cytosol of the hair cells (Figure 3-20B) and spiral ganglion neurons (Figure 3-20F). Strong superoxide staining (red) was detected in the nuclei of the damaged hair cells (Figure 3-20C) and spiral ganglion neurons (Figure 3-20G) under treatment with 50 μM mefloquine for 24 hours, (Figure 3-20C). To validate these observation results, we measured superoxide staining intensity levels in the hair cells and spiral ganglion neurons. We found that 50 μM mefloquine treatment increased superoxide staining levels in a time-dependent manner in the hair cells (Figure 3-21D) and spiral ganglion neurons (Figure 3-21H). These results suggest that mefloquine treatment increases oxidative stress, which in turn leads to apoptotic cell death of cochlear hair cells and/or spiral ganglion neurons.

Figure 3-20.

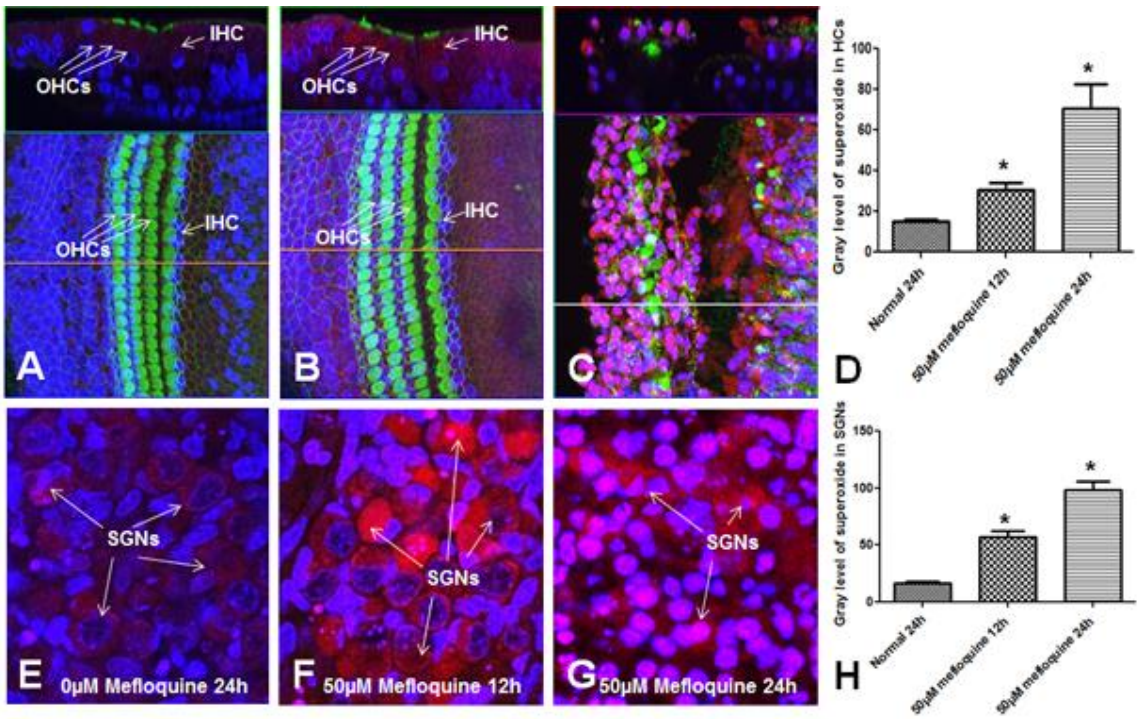

Figure 3-20. Mefloquine treatment increases superoxide levels in the cochlear hair cells and spiral ganglion neurons. (A) Little or no superoxide staining (red) was detected in the organ of Corti region in the control cochlear cultures. Arrows indicate outer and inner hair cells. (B) Under treatment with 50 μM mefloquine for 12 hours, superoxide staining (arrows, red) was detected in the cytosol of the hair cells. (C) Strong superoxide staining (red) was detected in the nuclei of the damaged hair cells under treatment with 50 μM mefloquine for 24 hours. (D) Treatment with 50 μM mefloquine increased superoxide staining (red) levels in a time-dependent manner in the hair cells. *significantly different from control. Error bars indicate S.D. (E) Little or no superoxide staining (red) was detected in the spiral ganglion neuron region in the control cochlear cultures. (F) Under treatment with 50 μM mefloquine for 12 hours, superoxide staining (arrows, red) was detected in the cytosol of the spiral ganglion neurons. (G) Strong superoxide staining (arrows, red) was detected in the nuclei of the degenerated spiral ganglion neurons under treatment with 50 μM mefloquine for 24 hours. (H) Treatment with 50 μM mefloquine increased superoxide staining (red) levels in a time-dependent manner in the spiral ganglion neurons. *significantly different from control. Error bars indicate S.D.

CHAPTER 4: DISCUSSION

1. Potential mechanisms by which aminoglycoside antibiotics lead to inner ear cell death

The ototoxic effects of aminoglycoside antibiotics have been linked to their antibacterial mechanisms [9,23,77,92,93,280,281]. Aminoglycoside antibiotics target the prokaryotic ribosomes or 70s ribosomes. In bacteria, aminoglycosides preferentially bind to the prokaryotic ribosomes at the A (adenosine) decoding region of the 16S ribosomal RNA (rRNA), a subunit of the 70s ribosomes. This in turn results in codon misreading and translation suppression, leading to cell death. In contrast, eukaryotic cells have 80S ribosomes in the cytoplasm and nucleus, which cannot be affected by aminoglycoside antibiotics[92,119,120,282,283]. However, eukaryotic mitochondria have 70S ribosomes, and hence, aminoglycoside antibiotics can damage eukaryotic cells by targeting the mitochondrial 70S ribosomes. Because eukaryotic mitochondria morphologically resemble those of prokaryotic cells, it was suggested that mitochondria might be descendants of the ancient prokaryotic organisms[9,23,284]. The Endosymbiosis Theory also postulates that eukaryotic cells acquired mitochondria as a result of invasion by prokaryotic cells because of the following suggestive evidence [9,23,285-287]: both eukaryotic mitochondria and prokaryotic cells: 1) are similar in dimensions, structure, and mass, 2) replicate in the same manner, 3) contain circular DNA which does not combine with histidine, 4) contain a protein synthesis "factory," 5) are targeted by a number of antibiotics due to the presence of 70S ribosomes, and 6) are insensitive to cycloheximide. Previous studies also found that under treatment with an antibiotic agent, levels of the antibiotic in a prokaryotic cell were 4-250 times higher than that of the extracellular space *in vitro*, indicating that the 70S ribosomes in a prokaryotic cell are the target of the antibiotic agent [288,289].

Organs with high energy demands, such as heart and liver, are known to have a relatively large number of mitochondria[290,291]. Cochlear hair cells also have a high demand for energy to transduce sound information and have a relatively large number of mitochondria [4,9,10,274,292,293]. A number of studies identified mitochondria as the first organelle damage site in aminoglycoside-induced ototoxicity[4,9,23,239,241]. Hence, one potential explanation as to why hair cells, but not the other cochlear cell types with low energy demands, are more vulnerable to aminoglycosides might be that hair cells have more mitochondria. In the current study of acute cochlear damage by co-administration of gentamicin and ethacrynic acid, the well-established mitochondrial function markers succinate dehydrogenase activity and mitochondrial membrane potential, rapidly decreased 4 hours after gentamicin and ethacrynic acid injection despite the fact that the hair cells were morphologically intact (Figure 3-6). We have also demonstrated that gentamicin treatment leads to increased levels of cytochrome *c*, caspases-9, and caspases-3, resulting in apoptotic hair cell death (Figure 3-7). Collectively, these results suggest that mitochondria are the earliest site in the hair cell damaged by gentamicin. I also postulate that gentamicin triggers cytochrome *c* release from the impaired mitochondria membrane into the cytoplasm, where it binds to the cytosolic protein Apaf-1. This in turn leads to the activation of intrinsic apoptosis pathway initiator caspase-9, which subsequently activates caspase-3, resulting in apoptotic hair cell death (Figure 4-1).

Since the cell death process occurs rapidly in the acute damage model, most cells likely die through apoptosis. However, in contrast, results of our long-term kanamycin treatment tests show that hair cell damage by kanamycin injection for 7 consecutive days occurs through necrosis (Figure 3-1, 3-2). One explanation for necrosis in chronic ototoxicity by kanamycin is that the lysosomes of cochlear cells may be able to detoxify antibiotics or digest impaired

Figure 4-1.

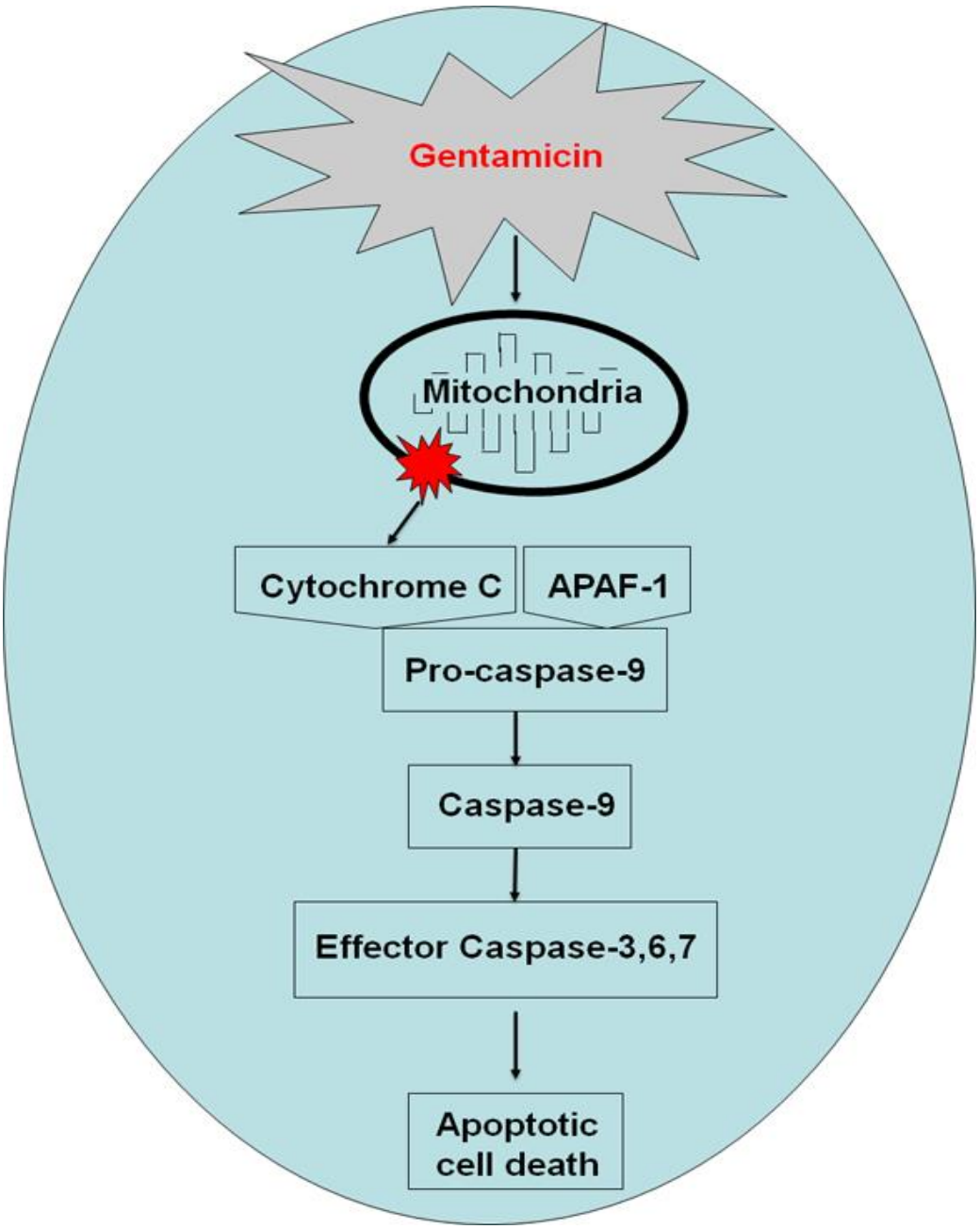

Figure 4-1. A model for mitochondrial apoptosis in gentamicin-induced cochlear hair cell death. Aminoglycoside antibiotics, such as gentamicin, trigger cytochrome *c* release from the impaired mitochondrial membrane into the cytoplasm, where it binds to the cytosolic protein Apaf-1. This in turn leads to the activation of intrinsic initiator caspase-9, which subsequently activates caspase-3, resulting in apoptotic hair cell death.

mitochondria at a lower concentration of kanamycin. However, as seen in our studies with increasing concentrations of kanamicin in organotypic cultures (Figure 3-3), at higher concentrations of kanamycin, damaged organelles may overload the lysosomes. Hence, I postulate that the lysosomal membranes would be expanded and ruptured, leading to necrotic cell death by autolysis (Figure 3-2, 4-2).

We have also demonstrated that reactive oxygen species (ROS) play important roles in hair cell degeneration induced by aminoglycoside antibiotics (Figure 3-5), cisplatin, or mefloquine (Figure 3-20). A free radical is an atom, molecule or ion that has an unpaired electron, while ROS are reactive molecules that contain oxygen such as superoxide and hydrogen peroxide[15,294,295]. In a biological system, free radicals or ROS can have a dual role, beneficial in some situations and harmful in others: at low levels or under normal conditions, free radicals are thought to play a role in cellular signaling pathways, but when over-generated, unstable free radicals can cause oxidative damage or degeneration of cellular components such as DNA, protein/enzymes, and membranes [15,294,295]. Interestingly, a high level of reactive oxygen species is thought to cause necrotic injury, while a lower or mild level of reactive oxygen species usually induces apoptosis [296,297].To prevent oxidative damage by free radicals, cells have developed an elaborate series of antioxidant enzymes that counteract oxidative stress induced by free radicals, protect cells by decomposing free radicals, and maintain the proper balance of oxidation and anti-oxidation [15,224,294]. These antioxidants or antioxidant enzymes are also capable of preventing apoptosis through the reduction of oxidative stress [256,298,299]. It is thought that during aging or under ototoxic compound exposure, there is an increase in free radical levels or an imbalance in oxidation and anti-oxidation [7,9,23,43,295,300]. This in turn leads to oxidative damage to DNA, proteins, and/or lipids, causing apoptotic or necrotic cell death. In agreement with these reports,

Figure 4-2.

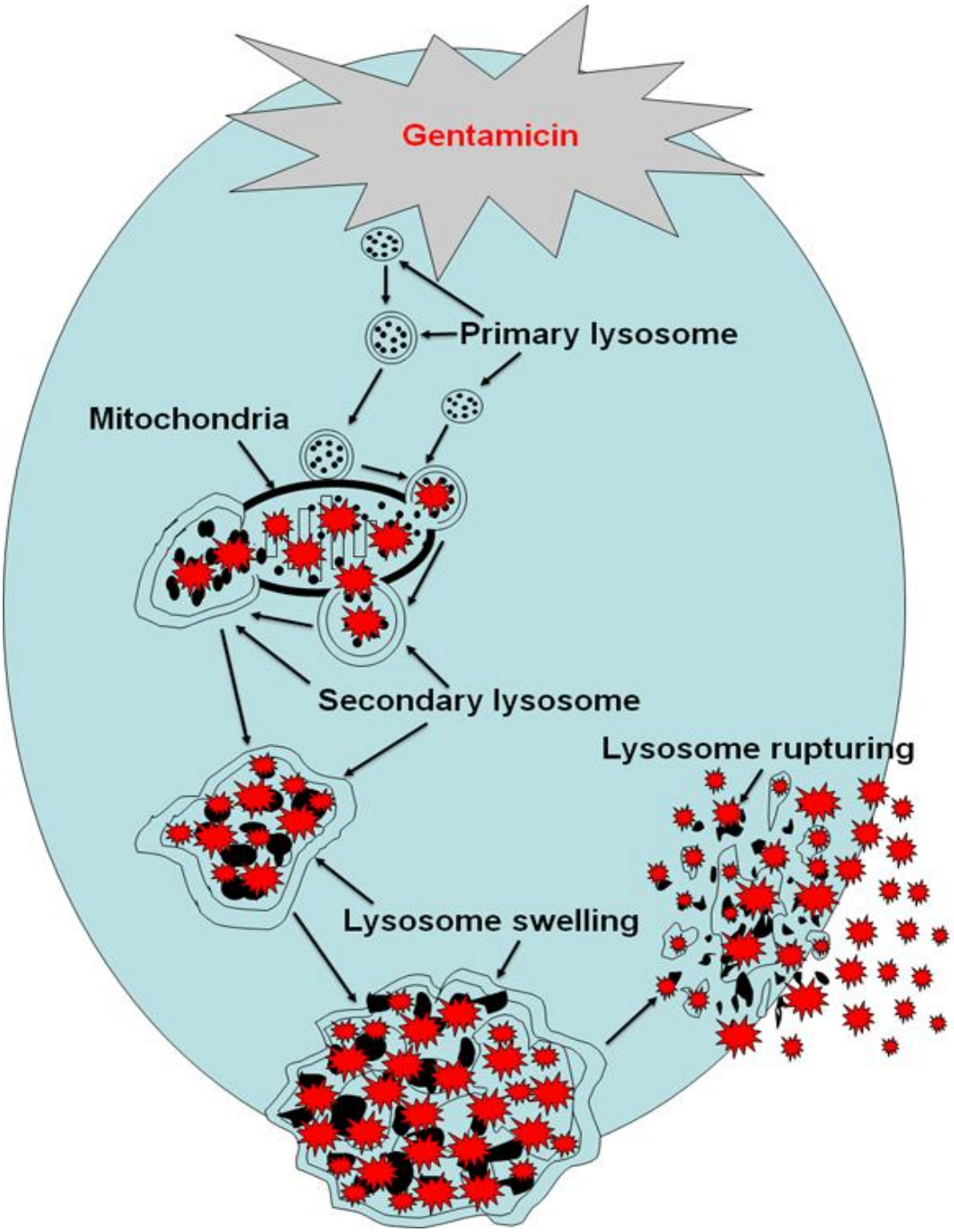

Figure 4-2. A model for necrosis in hair cell death under long term treatment with gentamicin. When lysosmes become overloaded with damaged organelles, the lysosome membranes could be expanded and rupture, leading to necrotic cell death by autolysis.

free radicals are known to interact with a number of apoptotic proteins: oxidative stress can trigger the activation of the anti-apoptotic bcl-2 family members [300], while Fas-induced apoptosis is triggered by reactive oxygen species [301]. A decline in antioxidant activities can also trigger apoptosis [302], suggesting that a decline in the intracellular redox environment could drive the apoptotic cell death process.

2. Potential mechanisms by which cisplatin leads to inner ear cell death

Because the blood-cochlea barrier can efficiently block cisplatin from entering the cochlea, the molecular mechanisms by which cisplatin treatment damages cochlear cells remained unclear until the new approaches to deliver cisplatin into the cochlear cells were developed [3,5,28,33,36,39,195]. The first approach developed was to deliver cisplatin into the cochlea directly through the round window membrane, which causes rapid apoptotic cell death in the cochlea (acute damage model) [3,31,33]. The second method was to deliver cisplatin into the cochlea by treating animals concurrently with cisplatin and a diuretic drug agent [28,31,33,48] because diuretic drugs such as ethacrynic acid and furosemide can reduce blood flow in the blood vessels of the cochlear lateral wall, which in turn causes ischemia and anoxia in the stria vascularis, breaking the blood-cochlea barrier in the cochlear lateral wall. Consistent with these reports, co-administration of cisplatin, kanamycin, or gentamicin with diuretic drugs has been shown to cause rapid cell death in the cochlea [4,9,23,28,30,31,33,36,48,162,278]. In the current study, we have demonstrated that co-administration of cisplatin and ethacrynic acid results in increased levels of the apoptosis initiator caspase-8, but not caspase-9, the apoptosis initiator activated by cytochrome c release from mitochondria (Figure 3-13C and D). This was followed by activation of the apoptosis executioners, caspase-3 and caspase-6 (Figure 3-13E and F). We have also

demonstrated that co-administration of cisplatin and ethacrynic acid results in increased levels of tumor necrosis factor associated death domain (TRADD) (Figure 3-13H) and TNF receptor gene expression (Figure 3-12). Since caspase-8 is activated in response to an extrinsic signal through the transmembrane cell death receptor and TRADD acts as a cell death ligand and induces extrinsic apoptosis by binding to the transmembrane cell death receptor, I postulate that extrinsic apoptosis likely plays a key role in acute cisplatin ototoxicity.

DNA is thought to be a major site of cisplatin damage and cisplatin is thought to damage DNA though forming inter/intra-strand DNA-links when activated by conversion into aquated species. [303-305]. Once DNA is damaged, the cell repairs the damaged DNA or destroys itself through p53-mediated apoptosis [37,47,68]. Consistent with these reports, our PCR array analyses found that gene expression of members of the p53/DNA damage family was induced in response to cisplatin treatment (Figure 3-12). We also found that gene expression of members of the NF-kappaB family, a transcription factor family that is known to be activated in response to DNA damage[37,47,68,306], was also induced by cisplatin treatment (Figure 3-12). Cisplatin treatment also increased mRNA expression levels of the Bcl -2 family, CARD family, death domain family, and TRAF family members (Figure 3-12). The Bcl-2 family members such as Bak and Bax are known to interact with the p53 signaling pathway [37,47,68]. Moreover, members in the CARD, death domain family, and TRAF family also interact with the p53 signaling pathway[37,47,68,307-309]. These findings suggest that in response to DNA damage, p53 induces a broad network of the apoptosis program, including the TNF receptor family that triggers the activation of caspase-mediated apoptosis[3,33,36,37]. This hypothesis is supported by previous studies which found that the p53 inhibitor, pifithrin-α, protected hair cells from cisplatin injury [3,33,36,37,68]. Therefore, I

postulate that, the p53, TNF death receptor, and/or TRAF families are likely involved in cisplatin-induced ototocity (Figure 4-3).

3. Potential mechanisms by which mefloquine causes cochlear cell death

The anti-malarial drug mefloquine damages cochlear hair cells in a manner similar to that of gentamycin or cisplatin; cochlear damage usually begins in the basal region of the cochlea and progresses toward the apex region [3,9,23,33,36,39]. Mefloquine, gentamicin, and cisplatin also cause hair cell death through the apoptotic program. However, our studies found that mefloquine caused hair cell death through an apoptosis pathway different from that of gentamicin or cisplatin: gentamicin treatment triggered cytochrome *c* release from the mitochondrial membranes (Figure 3-7B)[9,23], while cisplatin treatment triggered the activation of TRADD or FADD that was released from the transmembrane cell death receptors (Figure 3-13) [3,28,33,36]. Interestingly, mefloquine treatment increased the two major caspase initiators, caspase-8 and caspase-9 at an early stage of mefloquine-induced cell death (Figure 3-17), suggesting that mefloquine damages hair cells and spiral ganglion neurons by activating both the intrinsic and extrinsic apoptosis pathways[7,40-42].

Our PCR array studies found that of the 84 apoptosis-related genes examined (55 pro-apoptotic genes and 29 anti-apoptotic genes) in cochlear epithelium and spiral ganglion neurons, the genes that were induced early in response to mefloquine treatment were members of the Bcl-2 family, caspase family, Card family, TNF ligand and TNF receptor family, IAP family, death domain and death effector domain family, DNA damage and p53 family, and NF-kappa B family (Figure 3-19)(Table 1, 2) These results provide evidence that multiple apoptotic pathways are

Figure 4-3.

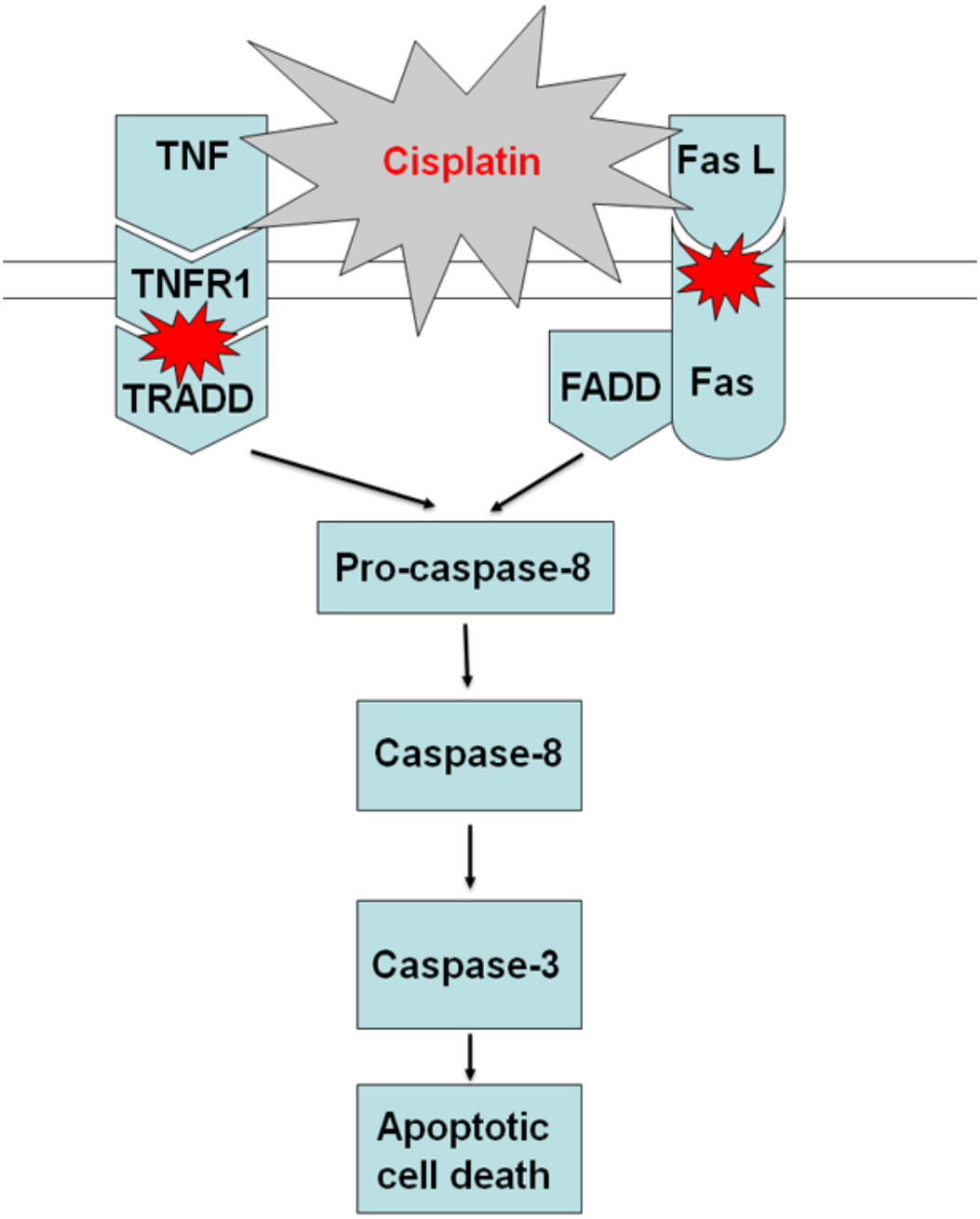

Figure 4-3. Following cisplatin and ethacrynic acid co-treatment we found increased expression of TNF receptor and p53 signaling gene family members (Figure 3-12), strong TRADD expression, activation of caspase 8 (Figure 3-13), increased expression of phophorylated p53 protein and caspase 3 activation (Figure 3-11). We propose a model for extrinsic apoptosis in cisplatin-induced hair cell death. Cisplatin triggers the cell death receptors on the cell membrane, and activates TRADD and FADD, which when induce caspase-8 activations. Finally, a wide network of p53 signals is stimulated leading to cell apoptosis.

involved in mefloquine-induced apoptosis in both cochlear epithelium and spiral ganglion neurons (Figure 3-19)(Table 1, 2). I note that the TNF ligand/TNF receptor family member genes That were induced by mefloquine are also members of or involved in the DNA damage/p53 family, death domain/death effector domain family, and NF-kappa B family [42,125,306]. All the members of the Card (caspase activation and recruitment domain) family possess the caspase recruitment domain and are members of the daspase family while all the members of the IAP family serve as endogenous inhibitors of programmed cell death, specifically binding and inhibiting activation of caspases and prevent apoptosis. Therefore, up-regulation of the IAP family genes not only indicates an anti-apoptotic cellular response to an apoptotic signal induced by mefloqunine, but also indicates caspase activation [42,125,310,311]. Because the Bcl-2 family governs a mitochondrial apoptosis program[42,125,312], the Bcl-2 family members are thought to play a major role in mitochondrial degeneration or dysfunction. Members of the Bcl-2 family also interact with the p53 signaling pathway[313-319]. DNA damage, death receptor stimuli, and/or stimuli from the TNF ligand/receptor family are also known to trigger mitochondrial apoptosis that is regulated by the Bcl-2 family members[313-319]. The activation of mitochondrial apoptosis in turn leads to the activation of a caspase cascade.

In the current study, we have demonstrated that mefloquine damages rat cochlear hair cells and spiral ganglion neurons in a dose-dependent manner (Figure 3-14). Mefloquine treatment also upregulated or down regulated mRNA expression of mitochondrial apoptosis related genes such as *Apaf1, Bcl2a1, BCl2l11, Bid3, Birc1b, Birc3, Birc4, Bnip1, Casp1, Casp7, Casp9, Cradd, Mcl1*, and *TNF* (Table 1, 2) and cell death receptors related apoptotic genes such as *Ripk2, Tnf, Tnfsf10, Tnfrf10b, Tnfrsf11b, Tnfrsf1a, Tnfrsf6, Tnfsf5, Tnfsf10, Tnfsf12, Tnfsf6, Tradd, Trp63*, and *Trp73* (Table 1, 2) [42,125]. These results were consistent with the

immunostaining results that mefloquine treatment increased immunostaining levels of caspase-9, cytochrome *c*, caspase-8, and caspase-3 (Figure 3-17). Together, I speculate that mefloquine can trigger both extrinsic apoptotic signals and intrinsic apoptotic signals which lead to apoptotic cell death (Figure 3-17) (Figure 4-4).

Previous studies indicate that nicotinamide adenine dinucleotide (NAD^+) supplementation can suppress the development of axonal degeneration in traumatic injury, ischemia damage, autoimmune encephalomyelitis, p53-induced neuron apoptosis, and radiation-induced immunosuppression[320-322]. Our recent study also revealed that NAD^+ can protect cochlear hair cells and spiral ganglion neurons against mefloquine and oxaliplatin [7,43,186,323]. Since apoptosis and associated oxidative stress likely plays a key role in mefloquine-induced cochlear damage, the reduction of axonal degeneration by NAD^+ may occur through the reduction of oxidative stress or apoptosis [7,43]. Another potential explanation for the protective role of NAD^+ in mefloquine-induced damage is that NAD^+ might activate NAD^+-dependent deacetylase Sirt1 that is known to regulate cell survival by inhibiting p53 apoptosis in mammalian cells [321,324-326]. Indeed, as a cofactor of Sirt1, NAD^+ has been implicated in diverse biological pathways/functions, including DNA damage repair and life span extension[321,324-330]. Those NAD^+ study results strongly support our finding that an apoptosis program plays a major role in mefloquine-induced cochlear cell death.

Figure 4-4.

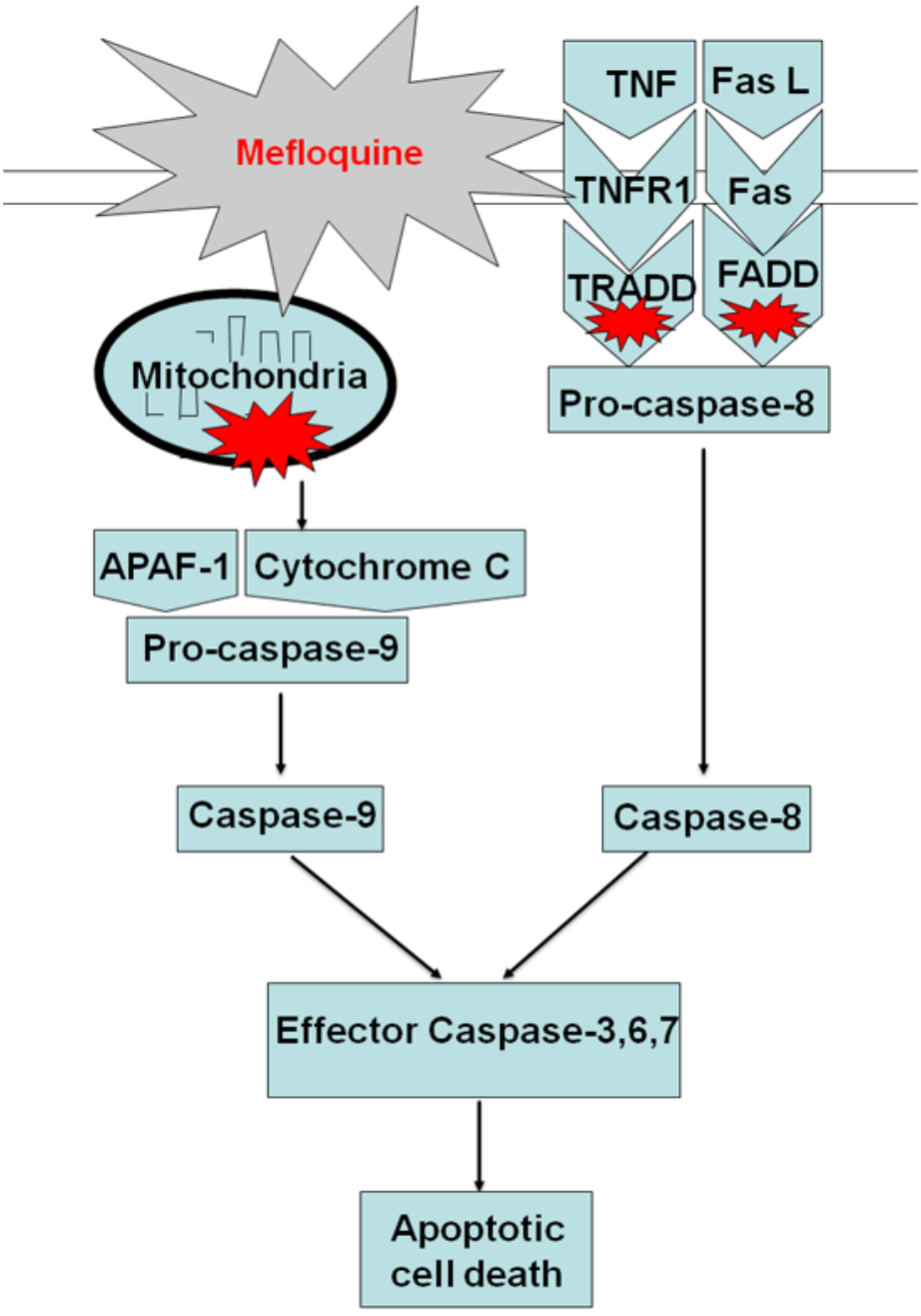

Figure 4-4. A model for extrinsic and intrinsic apoptosis in antimalarial, mefloquine-induced cochlear cell apoptosis. Mefloquine increases expression of the Fas (Tnfrsf6) and TNFR1 receptors activating FADD, TRADD and caspase 8 in the extrinsic apoptotic pathway, and also inceaseases Apaf1 expression, triggers cytochrome c release, and activates caspase 9 in the intrinsic apoptotic pathway (Figure 3-17, Table 2). Therefore mefloquine-induced cell apoptotic signals activate cell death signaling pathways on the cell membrane and in mitochondria.

CONCLUSION

A number of publications have shown that aminoglycoside antibiotics, anti-tumor platinum agents, and antimalarial chemicals are ototoxic and can cause severe damage to the cochlear hair cells and/or spiral ganglion neurons. When those ototoxic drugs are used, sensory hair cell loss/damage usually occurs in the basal turn of the cochlea first and then progresses toward the apex [9,12,23,31,48,219,220], and such cochlear cell damage increases in a dose-dependent matter both *in vitro* or *in vivo* [9,12,23,31,48,219,220]. How those major ototoxic chemicals damage cochlear hair cells and spiral ganglion neurons at the molecular levels remained unclear until our studies identified several apoptosis proteins that are involved the cochlear damage induced by gentamicin [4,9,23], cisplatin [3,27,28,33,36,37,195], or mefloquine [7,40-43,125].

In the current *in vitro* laboratory animal studies, we found that cisplatin-induced hair cell damage begins and progresses along the cochlear basilar membrane, rather than progressing from the basal region toward the apex region *in vivo*. This suggests the mechanism by which cisplatin damages cochlear hair cells in culture conditions is different from that of hair cell damage induced by aging or noise. Interestingly, while at a low concentration, cisplatin extensively destroyed cochlear hair cells and spiral ganglion neurons, at a high dose of cisplatin if the concentration of cisplatin was over 400 μM, it could not damage cochlear hair cells and spiral ganglion neurons [3,27,33,38]. Similar results were also found in other studies using the platinum agents, carboplatin and oxaliplatin in both cochlear and vestibular systems [3,36,74,154,236,237,323,331]. It is thought that the platinum-based antitumor reagent cisplatin enters the cell through the copper transporters [3,27,33,35,36,38,74,236,237,260,323,332-339]. Since extracellular cisplatin is not toxic, cisplatin must be transported from the bloodstream into cochlear hair cells, neurons

and supporting cells via copper transporters to damage the cochlear cell. Hence, when a high level of extracellular platinum exists, the cell might develop an intrinsic resistance by regulating the copper transporters to reduce the platinum influx and enhance the platinum efflux [3,27,28,33,35,36,38,154,195,236,237,260]. In the vestibular system, the platinum agents cisplatin and carboplatin selectively destroy the type I hair cells, but not the type II hair cells [11,34,36,74,153,168,340]. These observations also suggest that cisplatin or carboplatin damages sensory hair cells in the inner ear through targeting a specific cell type and/or specific region of the inner ear.

Previous studies have shown that aquated cisplatin generates highly toxic free radicals and reactive oxygen species (ROS) such as superoxide and hydroxyl radicals, hydrogen peroxide, nitric oxide synthase and peroxynitrite which can damage cellular components such as DNA [341-344]. When cisplatin enters into the cytoplasm, it can also damage key antioxidant enzymes such as glutathione peroxidase, glutathione reductase, catalase, copper/zinc superoxide dismutase through generating ROS, thereby reducing the ability of the cell to combat oxidative stress [345,346]. Moreover, because cisplatin turns into an active form once it enters the cytoplasm and its chloride atoms are displaced by water molecules, the aquated cisplatin itself can react with and damage DNA [33,38]. Intracellular platinum-glutathione conjugates such as cisplatin-glutathione-conjugates, cisplatin-cysteinyl-glycine-conjugates, and cisplatin-cysteine-conjugates are thought to be toxic[347,348] [349]. These reports suggest that when cisplatin is transported into the cell, it can bind to glutathione to form a cisplatin-glutathione complex to exert toxic effects. Indeed, the formation of the glutathione-cisplatin complex is known to trigger the release of an apoptotic signal from the cell death transmembrane receptor, which in turn leads to the activation of caspase-8, followed by the induction of a p53-mediated apoptosis program [3,28,33,36,37,68,195,349].

Based on these observations and our findings, I speculate that a p53-mediated extrinsic apoptotic program may play a key role in cisplatin-induced apoptotic cell death within the cochlea.

We also identified mitochondria as a target organelle for the aminoglycoside antibiotics kanamycin and gentamicin. As discussed earlier, both kanamycin and gentamicin selectively inhibit the protein synthesis in a bacterial cell by binding to the prokaryotic 70S ribosomal RNA [77,119,120]. Because mammalian mitochondria also have 70S ribosomal RNA (identical to the prokaryotic 70S ribosomal RNA), mitochondria are likely the initial target of kanamycin or gentamicin and the site first damaged in cochlear cells following administration of the drugs (Figure 3-4). Moreover, we showed that under a short term treatment or acute ototoxicity conditions, kanamycin-or gentamicin-induced damage led to energy decline and associated mitochondrial dysfunction. This in turn led to cytochrome *c* release; resulting in the activation of initiator caspase-9 and associated induction of mitochondrial apoptosis (Figure 3-6). Interestingly, under a long-term treatment or chronic ototoxicity conditions, kanamycin or gentamicin treatment also caused mitochondrial dysfunction, resulting in lysosome rupture and associated necrotic cell death (Figure 3-2). Hence, I speculate that both apoptotic and necrotic cell death play a role in kanamycin- or gentamicin-induced chronic ototoxicity.

We have also demonstrated that the antimalarial reagent, mefloquine, causes apoptotic cell death in the sensory hair cells and peripheral neurons in both the cochlear and vestibular systems (Figure 3-17). Our PCR array analysis found that mefloquine treatment up-regulated a number of Bcl-2 family and tumor necrosis factor super family genes in the cochlear basilar membrane and spiral ganglion neurons (Table 1, 2).These results were confirmed by the immunostaining analyses. Based on those results, I speculate that the mitochondrial apoptosis and tumor necrosis

factor/death receptor-mediated apoptosis are the major cell death programs in mefloquine-induced cell death in the cochlea.

An important conclusion derived from our studies of the roles of apoptosis in ototoxic chemical-induced cochlear cell death is that each ototoxic compound damages cochlear cells by targeting a specific cell type and specific region of the cochlea through a defined and specific apoptotic pathway. Thus, the cell loss induced by kanamycin, gentamicin, cisplatin, and/or mefloquine is a regulated process that can be blocked by inhibiting the activity of one or more of the apoptosis proteins identified in the current studies. If this hypothesis is correct, a significant component of the side-effect process by: 1) cisplatin may be pharmacologically blocked by suppressing the p53-mediated or caspases-8-mediated extrinsic apoptosis pathway, 2) kanamycin or gentamicin may be blocked by suppressing cytochrome c release or caspases-9 activity, and 3) mefloquine-induced cell degeneration may be pharmacologically suppressed by coenzyme nicotinamide adenine dinucleotide (NAD^+). In summary, the findings from my dissertation studies undoubtedly strengthen understanding of the mechanisms inducing apoptosis and necrosis, in ototoxic compound-induced cochlear cell death in experimental animals and in humans. Future studies to expand on the results from each ototoxic compound study will provide further insight to increase fundamental knowledge about the degenerating process of cochlear sensory hair cells or neurons induced by multiple ototoxic drugs.

REFERENCES

1. Engelberg-Kulka H, Amitai S, Kolodkin-Gal I, Hazan R. Bacterial programmed cell death and multicellular behavior in bacteria. PLoS genetics 2006;2:e135.

2. Green DR. The end and after: how dying cells impact the living organism. Immunity 2011;35:441-4.

3. Ding D, Allman A, Salvi RJ. Review: Ototoxic characteristics of platinum antitumor drugs. THE ANATOMICAL RECORD 2012;295:1851-67.

4. Ding D, Jiang H, Salvi RJ. Mechanisms of rapid sensory hair-cell death following co-administration of gentamicin and ethacrynic acid. Hearing research 2010;259:16-23.

5. Ding D, Jiang T, Qu Y, Qi W, Salvi R. Science of the inner ear. Chinese Science and Technology Publishing Company 2010.

6. Barceloux DG. Cobalt. Journal of toxicology Clinical toxicology 1999;37:201-6.

7. Ding D, Qi W, Yu D, et al. NAD+ Prevents Mefloquine-induced Neuroaxonal and Hair Cell Degeneration through Reduction of Caspase-3-mediated Apoptosis. PloS one 2013.

8. Ding D, Roth J, Salvi R. Manganese is toxic to spiral ganglion neurons and hair cells in vitro. Neurotoxicology 2011;32:233-41.

9. Ding D, Salvi R. Review of cellular changes in the cochlea due to aminoglycoside antibiotics. The Volta Review 2005;105:407-38.

10. Ding DL, McFadden SL, Wang J, Hu BH, Salvi RJ. Age- and strain-related differences in dehydrogenase activity and glycogen levels in CBA and C57 mouse cochleas. Audiology & neuro-otology 1999;4:55-63.

11. Ding DL, Wang J, Salvi R, et al. Selective loss of inner hair cells and type-I ganglion neurons in carboplatin-treated chinchillas. Mechanisms of damage and protection. Annals of the New York Academy of Sciences 1999;884:152-70.

12. Fu Y, Ding D, Wei L, Jiang H, Salvi R. Ouabain-induced apoptosis in cochlear hair cells and spiral ganglion neurons in vitro. BioMed research international 2013;2013:628064.

13. McFadden SL, Ding D, Reaume AG, Flood DG, Salvi RJ. Age-related cochlear hair cell loss is enhanced in mice lacking copper/zinc superoxide dismutase. Neurobiology of aging 1999;20:1-8.

14. McFadden SL, Ding D, Salvi R. Anatomical, metabolic and genetic aspects of age-related hearing loss in mice. Audiology : official organ of the International Society of Audiology 2001;40:313-21.

15. McFadden SL, Ohlemiller KK, Ding D, Shero M, Salvi RJ. The Influence of Superoxide Dismutase and Glutathione Peroxidase Deficiencies on Noise-Induced Hearing Loss in Mice. Noise Health 2001;3:49-64.

16. Salvi RJ, Ding D, Wang J, Jiang HY. A review of the effects of selective inner hair cell lesions on distortion product otoacoustic emissions, cochlear function and auditory evoked potentials. Noise Health 2000;2:9-26.

17. Salvi RJ, Wang J, Ding D, Stecker N, Arnold S. Auditory deprivation of the central auditory system resulting from selective inner hair cell loss: animal model of auditory neuropathy. Scandinavian audiology Supplementum 1999;51:1-12.

18. Ding D, Jin X. The changes of cochlear bioelectric potential in guinea pigs during brief anoxia. Acta Otorhinolaryngology 1998;12:4-6.

19. Qi W, Ding D, Salvi RJ. Cytotoxic effects of dimethyl sulphoxide (DMSO) on cochlear organotypic cultures. Hearing research 2008;236:52-60.

20. Wang J, Ding D, Shulman A, Stracher A, Salvi RJ. Leupeptin protects sensory hair cells from acoustic trauma. Neuroreport 1999;10:811-6.

21. Wu X, Ding D, Sun H, Liu H, Jiang H, Salvi R. Lead neurotoxicity in rat cochlear organotypic cultures. Journal of Otology 2011;6:45-52.

22. Liu H, Ding D, Sun H, et al. Cadmium-Induced Ototoxicity in Rat Cochlear Organotypic Cultures. Neurotoxicity research 2014.

23. Ding D, Salvi R. Experiences in ototoxic investigations in aminoglycoside antibiotics Journal of Otology 2007;2:125-31.

24. Luo D, Ding D, Huangfu M. [Ultracytochemical observation on lysosome of hair cells in kanamycin ototoxic guinea pigs]. Zhonghua Er Bi Yan Hou Ke Za Zhi 1990;25:281-2, 318.

25. Ding D, Stracher A, Salvi RJ. Leupeptin protects cochlear and vestibular hair cells from gentamicin ototoxicity. Hearing research 2002;164:115-26.

26. Cech TR, Damberger SH, Gutell RR. Representation of the secondary and tertiary structure of group I introns. Nature structural biology 1994;1:273-80.

27. Ding D, He J, Allman BL, et al. Cisplatin ototoxicity in rat cochlear organotypic cultures. Hearing research 2011;282:196-203.

28. Ding D, Jiang H, Wang P, Salvi R. Cell death after co-administration of cisplatin and ethacrynic acid. Hear Res 2007;226:129-39.

29. Ding D, McFadden SL, Browne RW, Salvi RJ. Late dosing with ethacrynic acid can reduce gentamicin concentration in perilymph and protect cochlear hair cells. Hearing research 2003;185:90-6.

30. Ding D, McFadden SL, Woo JM, Salvi RJ. Ethacrynic acid rapidly and selectively abolishes blood flow in vessels supplying the lateral wall of the cochlea. Hearing research 2002;173:1-9.

31. Li Y, Ding D, Jiang H, Fu Y, Salvi R. Co-administration of cisplatin and furosemide causes rapid and massive loss of cochlear hair cells in mice. Neurotoxicity research 2011;20:307-19.

32. Liu H, Ding DL, Jiang HY, Wu XW, Salvi R, Sun H. Ototoxic destruction by co-administration of kanamycin and ethacrynic acid in rats. Journal of Zhejiang University Science B 2011;12:853-61.

33. Ding D, Allman A, Yin S, Sun H, Salvi RJ. Cisplatin ototoxicity Nova Science Publishers, Inc 2011;Chapter 2:39-63.

34. Ding D, Wang J, Hofstatter P, Salvi RJ, Li M. Effects of carboplatin on the vestibular system of chinchilla. Otorhinolaryngological Journal of Integrated Traditional and Western Medicine in China 1998;6:1-5.

35. Ding D, He J, Yu D, Jiang H, Li Y, Salvi RJ. New insights on cisplatin ototoxicity. Canadian Hearing Report 2013;8:29-31.

36. Ding D, Qi W, Zhang M, Wang P, Jiang H, Salvi R. Cisplatin and its ototoxicity. Chinese Journal of Otology 2008;6:125-33.

37. Ding D, Wang P, Jiang H, Coling D, Salvi R. Gene expression in cisplatin ototoxicity and protection with p53 inhibitor. Journal of Otology 2009;4:15-24.

38. He J, Ding D, Yu D, Jiang H, Yin S, Salvi R. Modulation of copper transporters in protection against cisplatin-induced cochlear hair cell damage. Journal of Otology 2011;6:53-61.

39. He J, Yin S, Wang J, Ding D, Jiang H. Effectiveness of different approaches for establishing cisplatin-induced cochlear lesions in mice. Acta oto-laryngologica 2009;129:1359-67.

40. Ding D, Qi W, Jiang H, Salvi R. Mefloquine induced apoptosis in hair cells and spiral ganglion neurons in cochlear organotypic cultures. Abstr Assoc Res Otolaryngol 2007.

41. Ding D, Qi W, Yu D, Jiang H, Salvi R. Ototoxic effects of mefloquine in cochlear organotypic cultures. Journal of Otology 2009;4:29-38.

42. Ding D, Someya S, Jiang H, et al. Detection of apoptosis by RT-PCR array in mefloquine-induced cochlear damage. Journal of Otology 2011;6:1-9.

43. Ding D, Someya S, Tanokura M, Jiang H, Salvi R. NAD attenuates mefloquine-induced cochlear damage from reactive oxygen species. Abstr Assoc Res Otolaryngol 2013.

44. Adams JD, Mukherjee SK, Klaidman LK, Chang ML, Yasharel R. Apoptosis and oxidative stress in the aging brain. Annals of the New York Academy of Sciences 1996;786:135-51.

45. Devarajan P, Savoca M, Castaneda MP, et al. Cisplatin-induced apoptosis in auditory cells: role of death receptor and mitochondrial pathways. Hear Res 2002;174:45-54.

46. Huang T, Cheng AG, Stupak H, et al. Oxidative stress-induced apoptosis of cochlear sensory cells: otoprotective strategies. International journal of developmental neuroscience : the official journal of the International Society for Developmental Neuroscience 2000;18:259-70.

47. Jiang H, Ding D, Qi W, Salvi R. Cisplatin-induced changes in apoptotic gene expression in sensory versus neural subdivisions of rat cochlear cultures. . Abstr Assoc Res Otolaryngol 2007.

48. Ding D, Allman BL, Salvi R. Review: ototoxic characteristics of platinum antitumor drugs. Anat Rec (Hoboken) 2012;295:1851-67.

49. Grutter MG. Caspases: key players in programmed cell death. Current opinion in structural biology 2000;10:649-55.

50. Haupt S, Berger M, Goldberg Z, Haupt Y. Apoptosis - the p53 network. J Cell Sci 2003;116:4077-85.

51. Jokay I, Soos G, Repassy G, Dezso B. Apoptosis in the human inner ear. Detection by in situ end-labeling of fragmented DNA and correlation with other markers. Hear Res 1998;117:131-9.

52. Kaji A, Zhang Y, Nomura M, et al. Pifithrin-alpha promotes p53-mediated apoptosis in JB6 cells. Mol Carcinog 2003;37:138-48.

53. McDonald ES, Randon KR, Knight A, Windebank AJ. Cisplatin preferentially binds to DNA in dorsal root ganglion neurons in vitro and in vivo: a potential mechanism for neurotoxicity. Neurobiol Dis 2005;18:305-13.

54. McDonald ES, Windebank AJ. Cisplatin-induced apoptosis of DRG neurons involves bax redistribution and cytochrome c release but not fas receptor signaling. Neurobiol Dis 2002;9:220-33.

55. Park SA, Park HJ, Lee BI, Ahn YH, Kim SU, Choi KS. Bcl-2 blocks cisplatin-induced apoptosis by suppression of ERK-mediated p53 accumulation in B104 cells. Brain Res Mol Brain Res 2001;93:18-26.

56. Seth R, Yang C, Kaushal V, Shah SV, Kaushal GP. p53-dependent caspase-2 activation in mitochondrial release of apoptosis-inducing factor and its role in renal tubular epithelial cell injury. J Biol Chem 2005;280:31230-9.

57. Simon HU, Haj-Yehia A, Levi-Schaffer F. Role of reactive oxygen species (ROS) in apoptosis induction. Apoptosis 2000;5:415-8.

58. Someya S, Xu J, Kondo K, et al. Age-related hearing loss in C57BL/6J mice is mediated by Bak-dependent mitochondrial apoptosis. Proceedings of the National Academy of Sciences of the United States of America 2009;106:19432-7.

59. Van De Water TR, Lallemend F, Eshraghi AA, et al. Caspases, the enemy within, and their role in oxidative stress-induced apoptosis of inner ear sensory cells. Otology & neurotology : official publication of the American Otological Society, American Neurotology Society [and] European Academy of Otology and Neurotology 2004;25:627-32.

60. Wang J, Pabla N, Wang CY, Wang W, Schoenlein PV, Dong Z. Caspase-mediated cleavage of ATM during cisplatin-induced tubular cell apoptosis: inactivation of its kinase activity toward p53. Am J Physiol Renal Physiol 2006;291:F1300-7.

61. Watanabe K, Inai S, Jinnouchi K, Baba S, Yagi T. Expression of caspase-activated deoxyribonuclease (CAD) and caspase 3 (CPP32) in the cochlea of cisplatin (CDDP)-treated guinea pigs. Auris Nasus Larynx 2003;30:219-25.

62. Wilson MR. Apoptosis: unmasking the executioner. Cell Death Differ 1998;5:646-52.

63. Wilson MR. Apoptotic signal transduction: emerging pathways. Biochemistry and cell biology = Biochimie et biologie cellulaire 1998;76:573-82.

64. Wyllie AH, Arends MJ, Morris RG, Walker SW, Evan G. The apoptosis endonuclease and its regulation. Seminars in immunology 1992;4:389-97.

65. Yang C, Kaushal V, Shah SV, Kaushal GP. Mcl-1 is downregulated in cisplatin-induced apoptosis, and proteasome inhibitors restore Mcl-1 and promote survival in renal tubular epithelial cells. Am J Physiol Renal Physiol 2007;292:F1710-7.

66. Yao X, Panichpisal K, Kurtzman N, Nugent K. Cisplatin nephrotoxicity: a review. Am J Med Sci 2007;334:115-24.

67. Yu D, Ding D, Jiang H, Stolzberg D, Salvi R. Mefloquine damage vestibular hair cells in organotypic cultures. Neurotoxicity research 2011;20:51-8.

68. Zhang M, Liu W, Ding D, Salvi R. Pifithrin-alpha suppresses p53 and protects cochlear and vestibular hair cells from cisplatin-induced apoptosis. Neuroscience 2003;120:191-205.

69. Ding D, Jiang H, McFadden SL, Salvi R. Quantitative analysis of hair cells, spiral ganglion neurons and nerve fibers in knockout mice lacking SOD1 gene. Acta Otorhinolaryngology 1999;13:1-3.

70. Proskuryakov SY, Konoplyannikov AG, Gabai VL. Necrosis: a specific form of programmed cell death? Experimental cell research 2003;283:1-16.

71. Majno G, Joris I. Apoptosis, oncosis, and necrosis. An overview of cell death. Am J Pathol 1995;146:3-15.

72. Trump BF, Berezesky IK, Chang SH, Phelps PC. The pathways of cell death: oncosis, apoptosis, and necrosis. Toxicol Pathol 1997;25:82-8.

73. Ding D, Zhu X, Chen H, Zhao J, Huangfu M. A study of acidphosphatase in the cochlea of kanamycin deafened guinea pigs. Chinese Journal of Otorhinolaryngology 1986;9:121-2.

74. Ding D, Qi W, Qu Y, Jiang H, Salvi R. Carboplatin and its ototoxicity. Chinese Journal of Otology 2008;6:134-44.

75. Wei L, Ding D, Salvi R. Salicylate-induced degeneration of cochlea spiral ganglion neurons-apoptosis signaling. Neuroscience 2010;168:288-99.

76. Deng L, Ding D, Su J, Manohar S, Salvi R. Salicylate Selectively Kills Cochlear Spiral Ganglion Neurons by Paradoxically Up-regulating Superoxide. Neurotoxicity research 2013.

77. Recht MI, Douthwaite S, Puglisi JD. Basis for prokaryotic specificity of action of aminoglycoside antibiotics. The EMBO journal 1999;18:3133-8.

78. Jamesdaniel S, Hu B, Kermany MH, et al. Noise induced changes in the expression of p38/MAPK signaling proteins in the sensory epithelium of the inner ear. Journal of proteomics 2011;75:410-24.

79. Ahmed RM, Hannigan IP, MacDougall HG, Chan RC, Halmagyi GM. Gentamicin ototoxicity: a 23-year selected case series of 103 patients. The Medical journal of Australia 2012;196:701-4.

80. Walker PD, Barri Y, Shah SV. Oxidant mechanisms in gentamicin nephrotoxicity. Renal failure 1999;21:433-42.

81. Duff P. The aminoglycosides. Obstetrics and gynecology clinics of North America 1992;19:511-7.

82. Walker EM, Jr., Fazekas-May MA, Bowen WR. Nephrotoxic and ototoxic agents. Clinics in laboratory medicine 1990;10:323-54.

83. Kumin GD. Clinical nephrotoxicity of tobramycin and gentamicin. A prospective study. JAMA : the journal of the American Medical Association 1980;244:1808-10.

84. Forge A, Schacht J. Aminoglycoside antibiotics. Audiol Neurootol 2000;5:3-22.

85. Barton-Davis ER, Cordier L, Shoturma DI, Leland SE, Sweeney HL. Aminoglycoside antibiotics restore dystrophin function to skeletal muscles of mdx mice. J Clin Invest 1999;104:375-81.

86. Bidou L, Hatin I, Perez N, Allamand V, Panthier JJ, Rousset JP. Premature stop codons involved in muscular dystrophies show a broad spectrum of readthrough efficiencies in response to gentamicin treatment. Gene Ther 2004;11:619-27.

87. Howard MT, Anderson CB, Fass U, et al. Readthrough of dystrophin stop codon mutations induced by aminoglycosides. Ann Neurol 2004;55:422-6.

88. Kerem E. Pharmacologic therapy for stop mutations: how much CFTR activity is enough? Curr Opin Pulm Med 2004;10:547-52.

89. Kerem E. Pharmacological induction of CFTR function in patients with cystic fibrosis: mutation-specific therapy. Pediatr Pulmonol 2005;40:183-96.

90. Mulherin D, Fahy J, Grant W, Keogan M, Kavanagh B, FitzGerald M. Aminoglycoside induced ototoxicity in patients with cystic fibrosis. Irish J Med Sci 1991;160:173-5.

91. Wilschanski M, Famini C, Blau H, et al. A pilot study of the effect of gentamicin on nasal potential difference measurements in cystic fibrosis patients carrying stop mutations. Am J Respir Crit Care Med 2000;161:860-5.

92. Moazed D, Noller HF. Interaction of antibiotics with functional sites in 16S ribosomal RNA. Nature 1987;327:389-94.

93. Recht MI, Douthwaite S, Dahlquist KD, Puglisi JD. Effect of mutations in the A site of 16 S rRNA on aminoglycoside antibiotic-ribosome interaction. J Mol Biol 1999;286:33-43.

94. Wilhelm JM, Pettitt SE, Jessop JJ. Aminoglycoside antibiotics and eukaryotic protein synthesis: structure--function relationships in the stimulation of misreading with a wheat embryo system. Biochem 1978;17:1143-9.

95. Barth AD, Wood MR. The effect of streptomycin, oxytetracycline, tilmicosin and phenylbutazone on spermatogenesis in bulls. Can Vet J 1998;39:103-6.

96. Carew DP, Patterson BD. The effect of antibiotics on the growth of Catharanthus roseus tissue cultures. Lloydia 1970;33:275-7.

97. Chakravarti BP, Anilkumar TB. In vitro development of resistance to streptomycin in Erwinia carotovora and Pseudomonas lapsa causal organisms of bacterial stalk rot of maize in India. Hindustan Antibiot Bull 1970;12:73-4.

98. Daniels MJ. Possible adverse effects of antibiotic therapy in plants. Rev Infect Dis 1982;4 Suppl:S167-70.

99. Edgar R, Friedman N, Molshanski-Mor S, Qimron U. Reversing bacterial resistance to antibiotics by phage-mediated delivery of dominant sensitive genes. Applied and environmental microbiology;78:744-51.

100. Heuer H, Schmitt H, Smalla K. Antibiotic resistance gene spread due to manure application on agricultural fields.

101. Lopez M, Tejera NA, Lluch C. Validamycin A improves the response of Medicago truncatula plants to salt stress by inducing trehalose accumulation in the root nodules. Journal of plant physiology 2009;166:1218-22.

102. Martinez JL. Antibiotics and antibiotic resistance genes in natural environments. Science 2008;321:365-7.

103. Matsuhashi M, Shindo A, Ohshima H, et al. Cellular signals regulating antibiotic sensitivities of bacteria. Microb Drug Resist 1996;2:91-3.

104. McGlinchey TA, Rafter PA, Regan F, McMahon GP. A review of analytical methods for the determination of aminoglycoside and macrolide residues in food matrices. Analytica chimica acta 2008;624:1-15.

105. McManus PS, Stockwell VO, Sundin GW, Jones AL. Antibiotic use in plant agriculture. Annual review of phytopathology 2002;40:443-65.

106. Misato T, Ko K, Yamaguchi I. Use of antibiotics in agriculture. Adv Appl Microbiol 1977;21:53-88.

107. Moffat AS. Finding new ways to fight plant diseases. Science 2001;292:2270-3.

108. Morar M, Wright GD. The genomic enzymology of antibiotic resistance. Annu Rev Genet;44:25-51.

109. Padilla IM, Burgos L. Aminoglycoside antibiotics: structure, functions and effects on in vitro plant culture and genetic transformation protocols. Plant Cell Rep;29:1203-13.

110. Paulin JP, Ride M, Prunier JP. [Discovery of phytopathogenic bacteria 100 years ago: transatlantic controversies and polemics]. C R Acad Sci III 2001;324:905-14.

111. Peng D, Li S, Wang J, Chen C, Zhou M. Integrated biological and chemical control of rice sheath blight by Bacillus subtilis NJ-18 and jinggangmycin. Pest Manag Sci;70:258-63.

112. Rezzonico F, Stockwell VO, Duffy B. Plant agricultural streptomycin formulations do not carry antibiotic resistance genes. Antimicrobial agents and chemotherapy 2009;53:3173-7.

113. Stockwell VO, Duffy B. Use of antibiotics in plant agriculture. Rev Sci Tech;31:199-210.

114. Sundin GW. Antibiotic resistance affects plant pathogens. Science 2001;291:2551.

115. Vidaver AK. Uses of antimicrobials in plant agriculture. Clinical infectious diseases : an official publication of the Infectious Diseases Society of America 2002;34 Suppl 3:S107-10.

116. Walsh F, Ingenfeld A, Zampicolli M, Hilber-Bodmer M, Frey JE, Duffy B. Real-time PCR methods for quantitative monitoring of streptomycin and tetracycline resistance genes in agricultural ecosystems. Journal of microbiological methods;86:150-5.

117. Weber DJ, Rutala WA. Use of germicides in the home and the healthcare setting: is there a relationship between germicide use and antibiotic resistance? Infection control and hospital

epidemiology : the official journal of the Society of Hospital Epidemiologists of America 2006;27:1107-19.

118. Woegerbauer M, Burgmann H, Davies J, Graninger W. DNase I induced DNA degradation is inhibited by neomycin. The Journal of antibiotics 2000;53:276-85.

119. Lynch SR, Puglisi JD. Structural origins of aminoglycoside specificity for prokaryotic ribosomes. J Mol Biol 2001;306:1037-58.

120. Lynch SR, Puglisi JD. Structure of a eukaryotic decoding region A-site RNA. J Mol Biol 2001;306:1023-35.

121. Gutell RR. Collection of small subunit (16S- and 16S-like) ribosomal RNA structures: 1994. Nucleic Acids Res 1994;22:3502-7.

122. Vellai T, Takacs K, Vida G. A new aspect to the origin and evolution of eukaryotes. J Mol Evol 1998;46:499-507.

123. Ding D, Li M, Zheng X, Wang J, Salvi RJ. [Cochleogram for assessing hair cells and efferent fibers in carboplatin-treated ear]. Lin chuang er bi yan hou ke za zhi = Journal of clinical otorhinolaryngology 1999;13:510-2.

124. Ding D, Li M, Zheng XY, Wang J, Salvi R. Cochleogram for assessing hair cells and efferent fibers in carboplatin-treated ear. Journal of Clinical Otorhinolaryngology 1999;13:510-2.

125. Jiang H, Ding D, Salvi R. Mefloquine-induced changes in apoptotic gene expression in cochlear basilar membrane and spiral ganglion neurons Abstr Assoc Res Otolaryngol 2008.

126. Ding D, Zhang Z, Zhu Q. Experimental study of concurrent ototoxicity between ethacrynic acid and gentamycin. Journal of Audiology and Speech Disorder 1995;3:76-9.

127. Ding D, Jin X, Zhang Z, Zhu Q. Different susceptibility in gentamycin ototoxicity between red and black eye guinea pigs. Acta Otorhinolaryngology 1995;9:70-4.

128. Ding D, Li M, Jiang S, Salvi R. Morphology of the inner ear. Heilongjiang Science & Technology Publishing Company 2001.

129. Beck C. Protein and Ribonucleic Acid Metabolism in the Cochlea. Arch Otolaryngol 1965;81:548-52.

130. Ding D, Jin X, Huangfu M. Functional and morphological changes of the cochlea in guinea pigs during anoxia. Chinese Journal of Otorhinolaryngology 1993;28:265-7.

131. Rozencweig M, Abele R, von Hoff DD, Muggia FM. Cisplatin: impact of a new anticancer agent on current therapeutic strategies. Anticancer research 1981;1:199-204.

132. Biedermann B, Landmann C, Kann R, et al. Combined chemoradiotherapy with daily low-dose cisplatin in locally advanced inoperable non-small cell lung cancer. Radiotherapy and oncology : journal of the European Society for Therapeutic Radiology and Oncology 2000;56:169-73.

133. Aggarwal SK, Fadool JM. Cisplatin and carboplatin induced changes in the neurohypophysis and parathyroid, and their role in nephrotoxicity. Anticancer Drugs 1993;4:149-62.

134. Bertolini P, Lassalle M, Mercier G, et al. Platinum compound-related ototoxicity in children: long-term follow-up reveals continuous worsening of hearing loss. J Pediatr Hematol Oncol 2004;26:649-55.

135. Chaney SG, Campbell SL, Bassett E, Wu Y. Recognition and processing of cisplatin- and oxaliplatin-DNA adducts. Crit Rev Oncol Hematol 2005;53:3-11.

136. Holmes J, Stanko J, Varchenko M, et al. Comparative neurotoxicity of oxaliplatin, cisplatin, and ormaplatin in a Wistar rat model. Toxicol Sci 1998;46:342-51.

137. Uehara T, Miyoshi T, Tsuchiya N, et al. Comparative analysis of gene expression between renal cortex and papilla in nedaplatin-induced nephrotoxicity in rats. Hum Exp Toxicol 2007;26:767-80.

138. Uehara T, Watanabe H, Itoh F, et al. Nephrotoxicity of a novel antineoplastic platinum complex, nedaplatin: a comparative study with cisplatin in rats. Arch Toxicol 2005;79:451-60.

139. Supalkova V, Beklova M, Baloun J, et al. Affecting of aquatic vascular plant Lemna minor by cisplatin revealed by voltammetry. Bioelectrochemistry 2008;72:59-65.

140. Sures B, Zimmermann S, Messerschmidt J, von Bohlen A, Alt F. First report on the uptake of automobile catalyst emitted palladium by European eels (Anguilla anguilla) following experimental exposure to road dust. Environ Pollut 2001;113:341-5.

141. Zimmermann S, Messerschmidt J, von Bohlen A, Sures B. Uptake and bioaccumulation of platinum group metals (Pd, Pt, Rh) from automobile catalytic converter materials by the zebra mussel (Dreissena polymorpha). Environmental research 2005;98:203-9.

142. Moldovan M, Rauch S, Gomez M, Palacios MA, Morrison GM. Bioaccumulation of palladium, platinum and rhodium from urban particulates and sediments by the freshwater isopod Asellus aquaticus. Water research 2001;35:4175-83.

143. Wang W, Freemark K. The use of plants for environmental monitoring and assessment. Ecotoxicology and environmental safety 1995;30:289-301.

144. Fairchild JF, Ruessler DS, Haverland PS, Carlson AR. Comparative sensitivity of Selenastrum capricornutum and Lemna minor to sixteen herbicides. Archives of environmental contamination and toxicology 1997;32:353-7.

145. Gonzalez VM, Fuertes MA, Perez-Alvarez MJ, et al. Induction of apoptosis by the bis-Pt(III) complex [Pt(2)(2-mercaptopyrimidine)(4)Cl(2)]. Biochem Pharmacol 2000;60:371-9.

146. Kartalou M, Essigmann JM. Mechanisms of resistance to cisplatin. Mutat Res 2001;478:23-43.

147. Kartalou M, Essigmann JM. Recognition of cisplatin adducts by cellular proteins. Mutat Res 2001;478:1-21.

148. Trimmer EE, Essigmann JM. Cisplatin. Essays Biochem 1999;34:191-211.

149. Chu G. Cellular responses to cisplatin. The roles of DNA-binding proteins and DNA repair. J Biol Chem 1994;269:787-90.

150. Laurent G, Erickson LC, Sharkey NA, Kohn KW. DNA cross-linking and cytotoxicity induced by cis-diamminedichloroplatinum(II) in human normal and tumor cell lines. Cancer Res 1981;41:3347-51.

151. Cepero V, Garcia-Serrelde B, Moneo V, et al. Trans-platinum(II) complexes with cyclohexylamine as expectator ligand induce necrosis in tumour cells by inhibiting DNA synthesis and RNA transcription. Clin Transl Oncol 2007;9:521-30.

152. Moroso MJ, Blair RL. A review of cis-platinum ototoxicity. J Otolaryngol 1983;12:365-9.

153. Ding D, Wang J, Salvi RJ. Early damage in the chinchilla vestibular sensory epithelium from carboplatin. Audiology & neuro-otology 1997;2:155-67.

154. Ding D, Fu Y, Jiang H, Salvi R. Oxaliplatin ototoxicity in rat cochlear organotypic cultures. Abstr Assoc Res Otolaryngol 2010:247.

155. Al-Batran SE, Hartmann JT, Probst S, et al. Phase III trial in metastatic gastroesophageal adenocarcinoma with fluorouracil, leucovorin plus either oxaliplatin or cisplatin: a study of the Arbeitsgemeinschaft Internistische Onkologie. J Clin Oncol 2008;26:1435-42.

156. Ta LE, Espeset L, Podratz J, Windebank AJ. Neurotoxicity of oxaliplatin and cisplatin for dorsal root ganglion neurons correlates with platinum-DNA binding. Neurotoxicology 2006;27:992-1002.

157. Zhang S, Lovejoy KS, Shima JE, et al. Organic cation transporters are determinants of oxaliplatin cytotoxicity. Cancer Res 2006;66:8847-57.

158. Ding D, Allman BL, Salvi R. Review: Ototoxic Characteristics of Platinum Antitumor Drugs. Anat Rec (Hoboken) 2012.

159. Laurell G, Engstrom B, Hirsch A, Bagger-Sjoback D. Ototoxicity of cisplatin. Int J Androl 1987;10:359-62.

160. Ding D, Qi, W., Qu, Y., Jiang, H., Salvi, R. Carboplatin and its ototoxicity. Chinese Journal of Otology 2008;6:134-44.

161. Ding D, Wang, P., Jiang, H., Coling, D., Salvi, R. Gene expression in cisplatin ototoxicity and protection with p53 inhibitor. Chinese Journal of Otology 2009;4:15-24.

162. Ding D, Jiang H, MeFadden S, Salvi RJ. Ethacrinic acid is the key for opening of the blood-labyrinth barrier. Chinese Journal of Otology 2004;2:42-7.

163. Ding D, Jiang H, Salvi R. Local application of copper sulfate protects cochlear hair cells against carboplatin in chinchillas. Abstr Assoc Res Otolaryngol 2012:56.

164. Ding D, Jiang H, Wang J, Salvi R. Quantitative observation of carboplatin induced early damage in chinchilla hair cells and nerve fibers. Chinese Journal of Otorhinolaryngology-Skull Base Surgery 2002;8:241-3.

165. Ding D, Wang J, Zheng XY, Salvi R. Early damage of spiral ganglion caused by carboplatin in chinchilla. Journal of Audiology and Speech Pathology 1998;6:65-7.

166. Ding D, Wang J, Zheng XY, Sun H, Salvi R. Quantitative analysis of hair cells, spiral ganglion neurons and nerve fibers in the same cochlea. Chinese Journal of Otorhinolaryngology-Skull Base Surgery 1998;4:200-4.

167. Ding D, Zheng XY, Wang J, Hosfstetter P, Salvi R. Quantitative analysis of nerve fibers in habenular perforata in chinchilla. Chinese Journal of Otorhinolaryngology 1998;33:30-1.

168. Ding L, McFadden SL, Salvi RJ. Calpain immunoreactivity and morphological damage in chinchilla inner ears after carboplatin. Journal of the Association for Research in Otolaryngology : JARO 2002;3:68-79.

169. Anniko M, Sobin A. Cisplatin: evaluation of its ototoxic potential. Am J Otolaryngol 1986;7:276-93.

170. Hinojosa R, Riggs LC, Strauss M, Matz GJ. Temporal bone histopathology of cisplatin ototoxicity. Am J Otol 1995;16:731-40.

171. Laurell G, Bagger-Sjoback D. Dose-dependent inner ear changes after i.v. administration of cisplatin. J Otolaryngol 1991;20:158-67.

172. Schweitzer VG, Rarey KE, Dolan DF, Abrams G, Litterst CJ, Sheridan C. Ototoxicity of cisplatin vs. platinum analogs CBDCA (JM-8) and CHIP (JM-9). Otolaryngol Head Neck Surg 1986;94:458-70.

173. Laurell G, Bagger-Sjoback D. Degeneration of the organ of Corti following intravenous administration of cisplatin. Acta Otolaryngol 1991;111:891-8.

174. Ding D, Jiang H, Wang J, Yang J, McFadden SL, Salvi R. Carboplatin-induced vestibular damage: Quantitative measurement of type I hair cell loss and ganglion cell loss. Journal of Audiology and Speech Pathology 2002;10:170-3.

175. Jiang H, Ding D, Salvi R. Carboplatin induced cochlear hair cell lesion in organotypic cultures. Association for Research in Otolaryngology Abstract book 2006:193.

176. Ding D, Jiang H, Wang J, Yang J, Salvi R. Carboplatin induced vestibular hair cell lesion in the adult chinchilla organotypic cultures. Journal of Audiology and Speech Pathology 2003;11:281-3.

177. Hofstetter P, Ding D, Powers N, Salvi RJ. Quantitative relationship of carboplatin dose to magnitude of inner and outer hair cell loss and the reduction in distortion product otoacoustic emission amplitude in chinchillas. Hear Res 1997;112:199-215.

178. Hofstetter P, Ding D, Salvi R. Magnitude and pattern of inner and outer hair cell loss in chinchilla as a function of carboplatin dose. Audiology 1997;36:301-11.

179. Lockwood DS, Ding DL, Wang J, Salvi RJ. D-Methionine attenuates inner hair cell loss in carboplatin-treated chinchillas. Audiol Neurootol 2000;5:263-6.

180. McFadden SL, Kasper C, Ostrowski J, Ding D, Salvi RJ. Effects of inner hair cell loss on inferior colliculus evoked potential thresholds, amplitudes and forward masking functions in chinchillas. Hear Res 1998;120:121-32.

181. Wake M, Takeno S, Ibrahim D, Harrison R. Selective inner hair cell ototoxicity induced by carboplatin. Laryngoscope 1994;104:488-93.

182. Wake M, Takeno S, Ibrahim D, Harrison R, Mount R. Carboplatin ototoxicity: an animal model. J Laryngol Otol 1993;107:585-9.

183. Wang J, Ding D, Salvi RJ. Carboplatin-induced early cochlear lesion in chinchillas. Hear Res 2003;181:65-72.

184. Salvi RJ, Wang J, Ding D. Auditory plasticity and hyperactivity following cochlear damage. Hear Res 2000;147:261-74.

185. Cavaletti G, Tredici G, Petruccioli MG, et al. Effects of different schedules of oxaliplatin treatment on the peripheral nervous system of the rat. Eur J Cancer 2001;37:2457-63.

186. Jiang H, Ding D, Li Y, Salvi R. Nicotinamide adenine dinucleotide protects cochlea against ototoxic effects of oxaliplatin in vitro Abstr Assoc Res Otolaryngol 2011:302.

187. Hellberg V, Wallin I, Eriksson S, et al. Cisplatin and oxaliplatin toxicity: importance of cochlear kinetics as a determinant for ototoxicity. Journal of the National Cancer Institute 2009;101:37-47.

188. Comis SD, Rhys-Evans PH, Osborne MP, Pickles JO, Jeffries DJ, Pearse HA. Early morphological and chemical changes induced by cisplatin in the guinea pig organ of Corti. J Laryngol Otol 1986;100:1375-83.

189. Boheim K, Bichler E. Cisplatin-induced ototoxicity: audiometric findings and experimental cochlear pathology. Archives of oto-rhino-laryngology 1985;242:1-6.

190. Estrem SA, Babin RW, Ryu JH, Moore KC. Cis-diamminedichloroplatinum (II) ototoxicity in the guinea pig. Otolaryngol Head Neck Surg 1981;89:638-45.

191. Kohn S, Fradis M, Pratt H, et al. Cisplatin ototoxicity in guinea pigs with special reference to toxic effects in the stria vascularis. Laryngoscope 1988;98:865-71.

192. Komune S, Snow JB, Jr. Potentiating effects of cisplatin and ethacrynic acid in ototoxicity. Arch Otolaryngol 1981;107:594-7.

193. Ding D, Jiang H, Wang J, Yang J, McFadden S, Salvi R. Carboplatin-induced vestibular damage: Quantitative measurement of type I hair cell loss and ganglion cell loss. Journal of Audiology and Speech Pathology 2002;10:170-3.

194. Jamesdaniel S, Coling D, Hinduja S, et al. Cisplatin-induced ototoxicity is mediated by nitroxidative modification of cochlear proteins characterized by nitration of Lmo4. The Journal of biological chemistry 2012;287:18674-86.

195. Ding D, Jiang H, Salvi R. Machanisms of rapid hair cell death induced by co-administration of cisplatin and ethacrynic acid. Abstr Assoc Res Otolaryngol 2005:133.

196. Sogunro R. Malaria. Sante Salud 1993:5-6.

197. Crawley J, Nahlen B. Prevention and treatment of malaria in young African children. Seminars in pediatric infectious diseases 2004;15:169-80.

198. Snow RW, Guerra CA, Mutheu JJ, Hay SI. International funding for malaria control in relation to populations at risk of stable Plasmodium falciparum transmission. PLoS medicine 2008;5:e142.

199. Angus BJ. Malaria on the World Wide Web. Clinical infectious diseases : an official publication of the Infectious Diseases Society of America 2001;33:651-61.

200. Russell PF. World-wide malaria distribution, prevalence, and control. The American journal of tropical medicine and hygiene 1956;5:937-65.

201. Dow GS, Koenig ML, Wolf L, et al. The antimalarial potential of 4-quinolinecarbinolamines may be limited due to neurotoxicity and cross-resistance in mefloquine-resistant Plasmodium falciparum strains. Antimicrobial agents and chemotherapy 2004;48:2624-32.

202. Dow G. BR, Caridha D., Cabezas M., Du F., Gomer-Lobo R. Mefloquine induces dose-related neurological effects in a rat model. Antimicrobial Agents and Chemotherapy 2006;50:1045-53.

203. Phillips-Howard PA, ter Kuile FO. CNS adverse events associated with antimalarial agents. Fact or fiction? Drug Saf 1995;12:370-83.

204. Gutell RR. Collection of small subunit (16S- and 16S-like) ribosomal RNA structures: 1994. Nucleic acids research 1994;22:3502-7.

205. Barrett PJ, Emmins PD, Clarke PD, Bradley DJ. Comparison of adverse events associated with use of mefloquine and combination of chloroquine and proguanil as antimalarial prophylaxis: postal and telephone survey of travellers. Bmj 1996;313:525-8.

206. Croft AM, World MJ. Neuropsychiatric reactions with mefloquine chemoprophylaxis. Lancet 1996;347:326.

207. Hennequin C, Bouree P, Bazin N, Bisaro F, Feline A. Severe psychiatric side effects observed during prophylaxis and treatment with mefloquine. Archives of internal medicine 1994;154:2360-2.

208. Pous E, Gascon J, Obach J, Corachan M. Mefloquine-induced grand mal seizure during malaria chemoprophylaxis in a non-epileptic subject. Trans R Soc Trop Med Hyg 1995;89:434.

209. Sturchler D, Handschin J, Kaiser D, et al. Neuropsychiatric side effects of mefloquine. N Engl J Med 1990;322:1752-3.

210. Weinke T, Trautmann M, Held T, et al. Neuropsychiatric side effects after the use of mefloquine. The American journal of tropical medicine and hygiene 1991;45:86-91.

211. Roland P, Rutka. Ototoxicity. BC Decker, Hamilton, ON 2004.

212. Yu D, Ding D, Salvi. R. Ototoxicity of mefloquine in vestibular organotypic cultures Abstr Assoc Res Otolaryngol 2008.

213. Vendittoli PA, Ganapathi M, Lavigne M. Blood and urine metal ion levels in young and active patients after Birmingham hip resurfacing arthroplasty. The Journal of bone and joint surgery British volume 2007;89:989; author reply -90.

214. Deng L, Ding D, Su J, Manohar S, Salvi R. Salicylate selectively kills cochlear spiral ganglion neurons by paradoxically up-regulating superoxide. Neurotoxicity research 2013;24:307-19.

215. Wei L, Ding D, Sun W, Xu-Friedman MA, Salvi R. Effects of sodium salicylate on spontaneous and evoked spike rate in the dorsal cochlear nucleus. Hear Res 2010.

216. Wang L, Ding D, Salvi R, Roth JA. Nicotinamide adenine dinucleotide prevents neuroaxonal degeneration induced by manganese in cochlear organotypic cultures. Neurotoxicology 2014;40:65-74.

217. Watanabe A, Taniguchi F, Izawa M, et al. The role of survivin in the resistance of endometriotic stromal cells to drug-induced apoptosis. Hum Reprod 2009;24:3172-9.

218. Consignment purchasers forge new buying group. Hospital purchasing news : HPN 1984;8:1, 17.

219. Fu Y, Ding D, Jiang H, Salvi R. Ouabain-induced cochlear degeneration in rat in vitro and in vivo. Abstr Assoc Res Otolaryngol 2010.

220. Fu Y, Ding D, Jiang H, Salvi R. Ouabain-induced cochlear degeneration in rat. Neurotoxicity research 2012;22:158-69.

221. Zheng XY, Salvi RJ, McFadden SL, Ding DL, Henderson D. Recovery of kainic acid excitotoxicity in chinchilla cochlea. Annals of the New York Academy of Sciences 1999;884:255-69.

222. Sun H, Hashino E, Ding DL, Salvi RJ. Reversible and irreversible damage to cochlear afferent neurons by kainic acid excitotoxicity. The Journal of comparative neurology 2001;430:172-81.

223. Sun H, Salvi RJ, Ding DL, Hashino DE, Shero M, Zheng XY. Excitotoxic effect of kainic acid on chicken otoacoustic emissions and cochlear potentials. The Journal of the Acoustical Society of America 2000;107:2136-42.

224. Nicotera TM, Ding D, McFadden SL, Salvemini D, Salvi R. Paraquat-induced hair cell damage and protection with the superoxide dismutase mimetic m40403. Audiology & neuro-otology 2004;9:353-62.

225. Deng L, Ding D, Su J, Manohar S, Salvi R. Salicylate selectively kills cochlear spiral ganglion neurons by paradoxically up-regulating superoxide. Abstr Assoc Res Otolaryngol 2013.

226. Ding D, Mcfadden S, Salvemini D, Nicotera T, Salvi R. Paraquat-induced hair cell damage and protective effect of M40403 Abstr Assoc Res Otolaryngol 2003.

227. Jiang H, Ding D, Manohar S, Prolla T, Salvi RJ. Paraquat induces different damage pattern to cochlear hair cells between mice and rats in neonatal cochlear cultures. Abstr Assoc Res Otolaryngol, 2014.

228. Finkler AD, Silveira AF, Munaro G, Zanrosso CD. Otoprotection in guinea pigs exposed to pesticides and ginkgo biloba. Brazilian journal of otorhinolaryngology 2012;78:122-8.

229. Korbes D, Silveira AF, Hyppolito MA, Munaro G. Organophosphate-related ototoxicity: Description of the vestibulocochlear system ultrastructural aspects of guinea pigs. Brazilian journal of otorhinolaryngology 2010;76:238-44.

230. Moshi NH, Minja BM, Ole-Lengine L, Mwakagile DS. Bacteriology of chronic otitis media in Dar es Salaam, Tanzania. East African medical journal 2000;77:20-2.

231. Ozdemir S, Tuncer U, Tarkan O, Akar F, Surmelioglu O. Effects of topical oxiconazole and boric acid in alcohol solutions to rat inner ears. Otolaryngology--head and neck surgery : official journal of American Academy of Otolaryngology-Head and Neck Surgery 2013;148:1023-7.

232. Zhao J, Ding D, Huangfu M. The influence of enthacrynic acid on the activity of enzyme in the stria vascularis in guinea pigs. Journal of Clinical Otorhinolaryngology 1988;2:65-7.

233. Zhao J, Ding D, Wang J, Huangfu M. Influence of ethacrynic acid on microcirculation of stria vascularis of cochlea in guinea pigs. Acta Universitates Medicinalis Secondae Shanghai 1988;8:34-7.

234. Hangfu M, Zhao J, Din D. The prophylactic effect of thyroxin on kanamycin ototoxicity in guinea pigs. Hearing research 1992;61:132-6.

235. Ding D, Guo Y, Luo D, Huangfu M. The silver nitrate staining technique for the inner ear end-organs of guinea pigs. Acta Universitatis Medicinalis Secondae Shanghai 1989;9:326-7.

236. Ding D, Jiang H, Fu Y, Salvi R, Someya S, Tanokura M. Ototoxic effects of carboplatin in cochlear organotypic cultures in chinchillas and rats. Journal of Otology 2012;7:92-101.

237. Ding D, Wu X, Liu H, Jiang H, Salvi R. Ototoxicity and neurotoxicity of nedaplatin in cochlear organotypic cultures Abstr Assoc Res Otolaryngol 2011:208.

238. Wang L, Ding D, Salvi RJ, Roth J. Nicotinamide adenine dinucleotide prevents neuroaxonal degeneration induced by manganese in cochlear organotypic cultures. Neurotoxicology 2014;40:65-74.

239. Ding D, Jin X, Zhao J. Accumulative sites of kanamycin in cochlea basal membrane cells Chinese Journal of Otorhinolaryngology 1995;30:323-5.

240. Ding D, Jin X, Zhao J. Different binding sites of kanamycin and streptomycin in the organs of Corti Journal of Clinical Otorhinolaryngology 1995;9:346-7.

241. Ding D, Jin X, Zhao J. Accumulative sites of kanamycin in the organ of Corti by microautoradiography Chinese Journal of Otorhinolaryngology 1997;32:438-349.

242. Chen Y, Heeg MJ, Braunschweiger PC, Xie W, Wang PG. A carbohydrateline cisplatin analogue having antitumor activity. Angew Chem Int 1999;Edition 38:1768-9.

243. Ding D, Jiang S. Handbook of inner ear anatomy and the experimental technique in guinea pigs. Xuelin Publishing House 1989.

244. Ding D, Wang J, He Y. Surface preparation technique of the spiral ligament of the cochlea in guinea pig. Shanghai Medical Journal 1984;7:657-8.

245. Ding D, Zhao J, Huangfu M, He Y. Modified technique for surface preparation of the cochlea. Chinese Journal of Otorhinolaryngology 1981;16:207-9.

246. Ding D, Zhao J, Huangfu M, Jin X. Dissection of membranous labyrinth of the inner ear in guinea pigs. Journal of Clinical Otorhinolaryngology 1987;1:173-4.

247. Ding D, McFadden SL, Wang J, Hu BH, Salvi R. Age-and strain-related differences in dehydrogenase activity and glycogen level in CBA and C57 mouse cochleas. Audiology and Neuro-Otology 1999;4:55-63.

248. Ding D, Huangfu M, Jin X. The technique of frozen section in the inner ear of guinea pigs. Acta Academiae Medicinae Bengbu 1987;12:222.

249. McFadden SL, Ding D, Jiang H, Salvi RJ. Time course of efferent fiber and spiral ganglion cell degeneration following complete hair cell loss in the chinchilla. Brain research 2004;997:40-51.

250. Ding D, McFadden S, Salvi RJ, eds. Cochlear hair cell densities and inner ear staining techniques. Boca Raton: CRC Press; 2001.

251. Ding D, Jiang T, Qu Y, Qi W, Salvi R. Science of the inner ear. Chinese Science and Technology Publishing Company 2010.

252. Zheng QY, Ding D, Yu H, Salvi RJ, Johnson KR. A locus on distal chromosome 10 (ahl4) affecting age-related hearing loss in A/J mice. Neurobiology of aging 2009;30:1693-705.

253. Ding D, Wang J, Yu Z, Jiang H, Wang P, Salvi R. Spontaneous proliferation in organotypic cultures of mouse cochleae. Journal of Otology 2008;3:76-83.

254. Li M, Ding D, Zheng XY, Salvi R. Vestibular destruction by slow infusion of gentamicin into semicircular canals. Acta oto-laryngologica 2004;552:1-7.

255. Gavrieli Y, Sherman Y, Ben-Sasson SA. Identification of programmed cell death in situ via specific labeling of nuclear DNA fragmentation. The Journal of cell biology 1992;119:493-501.

256. Hockenbery DM, Oltvai ZN, Yin XM, Milliman CL, Korsmeyer SJ. Bcl-2 functions in an antioxidant pathway to prevent apoptosis. Cell 1993;75:241-51.

257. Oltvai ZN, Milliman CL, Korsmeyer SJ. Bcl-2 heterodimerizes in vivo with a conserved homolog, Bax, that accelerates programmed cell death. Cell 1993;74:609-19.

258. Korsmeyer SJ, Shutter JR, Veis DJ, Merry DE, Oltvai ZN. Bcl-2/Bax: a rheostat that regulates an anti-oxidant pathway and cell death. Seminars in cancer biology 1993;4:327-32.

259. Kane DJ, Sarafian TA, Anton R, et al. Bcl-2 inhibition of neural death: decreased generation of reactive oxygen species. Science 1993;262:1274-7.

260. He J, Ding D, Salvi R, Coling D. Extracellular copper modulates cisplatin ototoxicity. Abstr Assoc Res Otolaryngol 2009.

261. Bradford MM. A rapid and sensitive method for the quantitation of microgram quantities of protein utilizing the principle of protein-dye binding. Anal Biochem 1976;72:248-54.

262. Aran JM, Dulon D, Hiel H, Erre JP, Aurousseau C. [Ototoxicity of aminosides: recent results on uptake and clearance of gentamycin by sensory cells of the cochlea]. Revue de laryngologie - otologie - rhinologie 1993;114:125-8.

263. Hashino E, Shero M, Salvi RJ. Lysosomal augmentation during aminoglycoside uptake in cochlear hair cells. Brain research 2000;887:90-7.

264. Oda Y, Harada Y, Kasuga S, Hirakawa K, Yajin K. Effect of streptomycin on the supporting cells of the utricular macula. Acta oto-laryngologica Supplementum 1995;519:238-43.

265. Bandyopadhyay D, Cyphersmith A, Zapata JA, Kim YJ, Payne CK. Lysosome transport as a function of lysosome diameter. PloS one 2014;9:e86847.

266. Williams R, Ryves WJ, Dalton EC, et al. A molecular cell biology of lithium. Biochemical Society transactions 2004;32:799-802.

267. Benov L, Sztejnberg L, Fridovich I. Critical evaluation of the use of hydroethidine as a measure of superoxide anion radical. Free radical biology & medicine 1998;25:826-31.

268. Bindokas VP, Jordan J, Lee CC, Miller RJ. Superoxide production in rat hippocampal neurons: selective imaging with hydroethidine. The Journal of neuroscience : the official journal of the Society for Neuroscience 1996;16:1324-36.

269. McFadden SL, Ding D, Jiang H, Woo JM, Salvi RJ. Chinchilla models of selective cochlear hair cell loss. Hearing research 2002;174:230-8.

270. Hou Q, Zhao T, Zhang H, et al. Granzyme H induces apoptosis of target tumor cells characterized by DNA fragmentation and Bid-dependent mitochondrial damage. Mol Immunol 2008;45:1044-55.

271. Iglesias-Guimarais V, Gil-Guinon E, Sanchez-Osuna M, et al. Chromatin collapse during caspase-dependent apoptotic cell death requires DNA fragmentation factor, 40-kDa subunit-/caspase-activated deoxyribonuclease-mediated 3'-OH single-strand DNA breaks. The Journal of biological chemistry 2013;288:9200-15.

272. Jacobson MD, Burne JF, Raff MC. Programmed cell death and Bcl-2 protection in the absence of a nucleus. The EMBO journal 1994;13:1899-910.

273. Lu Z, Zhang C, Zhai Z. Nucleoplasmin regulates chromatin condensation during apoptosis. Proceedings of the National Academy of Sciences of the United States of America 2005;102:2778-83.

274. Ding D, Wang J, Hu BH, Salvi R. Age-induced alterations of succinic dehydrogenase activity in the organ of Corti in mice. Journal of Clinical Otorhinolaryngology 1998;12:78-80.

275. Zheng JL, Gao WQ. Differential damage to auditory neurons and hair cells by ototoxins and neuroprotection by specific neurotrophins in rat cochlear organotypic cultures. Eur J Neurosci 1996;8:1897-905.

276. Zheng JL, Stewart RR, Gao WQ. Neurotrophin-4/5, brain-derived neurotrophic factor, and neurotrophin-3 promote survival of cultured vestibular ganglion neurons and protect them against neurotoxicity of ototoxins. J Neurobiol 1995;28:330-40.

277. Zheng JL, Stewart RR, Gao WQ. Neurotrophin-4/5 enhances survival of cultured spiral ganglion neurons and protects them from cisplatin neurotoxicity. J Neurosci 1995;15:5079-87.

278. Ding D, Jin X, Zhao J. The changes of cochlear bioelectric potential on guinea pigs deafened with ethacrynic acid. Journal of Clinical Otorhinolaryngology 1996;10:330-2.

279. Fusetti M, Eibenstein A, Corridore V, Hueck S, Chiti-Batelli S. [Mefloquine and ototoxicity: a report of 3 cases]. La Clinica terapeutica 1999;150:379-82.

280. Wilhelm JM, Jessop JJ, Pettitt SE. Aminoglycoside antibiotics and eukaryotic protein synthesis: stimulation of errors in the translation of natural messengers in extracts of cultured human cells. Biochemistry 1978;17:1149-53.

281. Wilhelm JM, Pettitt SE, Jessop JJ. Aminoglycoside antibiotics and eukaryotic protein synthesis: structure--function relationships in the stimulation of misreading with a wheat embryo system. Biochemistry 1978;17:1143-9.

282. Walter F, Vicens Q, Westhof E. Aminoglycoside-RNA interactions. Current opinion in chemical biology 1999;3:694-704.

283. Ryu DH, Rando RR. Aminoglycoside binding to human and bacterial A-Site rRNA decoding region constructs. Bioorganic & medicinal chemistry 2001;9:2601-8.

284. Vellai T, Takacs K, Vida G. A new aspect to the origin and evolution of eukaryotes. Journal of molecular evolution 1998;46:499-507.

285. Williams TA, Foster PG, Cox CJ, Embley TM. An archaeal origin of eukaryotes supports only two primary domains of life. Nature 2013;504:231-6.

286. Jiang JH, Davies JK, Lithgow T, Strugnell RA, Gabriel K. Targeting of Neisserial PorB to the mitochondrial outer membrane: an insight on the evolution of beta-barrel protein assembly machines. Molecular microbiology 2011;82:976-87.

287. Szklarczyk R, Huynen MA. Mosaic origin of the mitochondrial proteome. Proteomics 2010;10:4012-24.

288. Price KE, DeFuria MD, Pursiano TA. Amikacin, an aminoglycoside with marked activity against antibiotic-resistant clinical isolates. The Journal of infectious diseases 1976;134 SUPPL:S249-61.

289. Bryan LE, Van Den Elzen HM. Gentamicin accumulation by sensitive strains of Escherichia coli and Pseudomonas aeruginosa. The Journal of antibiotics 1975;28:696-703.

290. Alam MA, Kauter K, Withers K, Sernia C, Brown L. Chronic l-arginine treatment improves metabolic, cardiovascular and liver complications in diet-induced obesity in rats. Food & function 2013;4:83-91.

291. Boveris A, Costa LE, Poderoso JJ, Carreras MC, Cadenas E. Regulation of mitochondrial respiration by oxygen and nitric oxide. Annals of the New York Academy of Sciences 2000;899:121-35.

292. Nakai Y, Hilding D. Oxidative enzymes in the cochlea. An electron microscopic and histochemical study of succinic dehydrogenase and dihydronicotinamide adenine dinucleotide diaphorase. Acta oto-laryngologica 1968;65:459-67.

293. Spector GJ. The ultrastructural cytochemistry of lactic dehydrogenase, succinic dehydrogenase, dihydro-nicotinamide adenine dinucleotide diaphorase and cytochrome oxidase activities in hair cell mitochondria of the guinea pig cochlea. The journal of histochemistry and cytochemistry : official journal of the Histochemistry Society 1975;23:216-34.

294. McFadden SL, Ding D, Burkard RF, et al. Cu/Zn SOD deficiency potentiates hearing loss and cochlear pathology in aged 129,CD-1 mice. The Journal of comparative neurology 1999;413:101-12.

295. McFadden SL, Ding D, Salvemini D, Salvi RJ. M40403, a superoxide dismutase mimetic, protects cochlear hair cells from gentamicin, but not cisplatin toxicity. Toxicol Appl Pharmacol 2003;186:46-54.

296. Finkel T. Oxidant signals and oxidative stress. Current opinion in cell biology 2003;15:247-54.

297. Lennon SV, Martin SJ, Cotter TG. Dose-dependent induction of apoptosis in human tumour cell lines by widely diverging stimuli. Cell proliferation 1991;24:203-14.

298. Lafon C, Mathieu C, Guerrin M, Pierre O, Vidal S, Valette A. Transforming growth factor beta 1-induced apoptosis in human ovarian carcinoma cells: protection by the antioxidant N-acetylcysteine and bcl-2. Cell growth & differentiation : the molecular biology journal of the American Association for Cancer Research 1996;7:1095-104.

299. Mates JM. Effects of antioxidant enzymes in the molecular control of reactive oxygen species toxicology. Toxicology 2000;153:83-104.

300. Kern JC, Kehrer JP. Free radicals and apoptosis: relationships with glutathione, thioredoxin, and the BCL family of proteins. Frontiers in bioscience : a journal and virtual library 2005;10:1727-38.

301. Um HD, Orenstein JM, Wahl SM. Fas mediates apoptosis in human monocytes by a reactive oxygen intermediate dependent pathway. J Immunol 1996;156:3469-77.

302. Slater AF, Stefan C, Nobel I, van den Dobbelsteen DJ, Orrenius S. Signalling mechanisms and oxidative stress in apoptosis. Toxicology letters 1995;82-83:149-53.

303. Kasparkova J, Brabec V. Recognition of DNA interstrand cross-links of cis-diamminedichloroplatinum(II) and its trans isomer by DNA-binding proteins. Biochemistry 1995;34:12379-87.

304. Olivova R, Kasparkova J, Vrana O, et al. Unique DNA binding mode of antitumor trinuclear tridentate platinum(II) compound. Molecular pharmaceutics 2011;8:2368-78.

305. Sundquist WI, Lippard SJ, Stollar BD. Binding of cis- and trans-diamminedichloroplatinum(II) to deoxyribonucleic acid exposes nucleosides as measured immunochemically with anti-nucleoside antibodies. Biochemistry 1986;25:1520-4.

306. Wang Y, Sun X, Wu J, et al. Casein kinase 1alpha interacts with RIP1 and regulates NF-kappaB activation. Biochemistry 2008;47:441-8.

307. Park HH, Wu H. Crystal structure of RAIDD death domain implicates potential mechanism of PIDDosome assembly. J Mol Biol 2006;357:358-64.

308. Tong QS, Zheng LD, Wang L, et al. Downregulation of XIAP expression induces apoptosis and enhances chemotherapeutic sensitivity in human gastric cancer cells. Cancer Gene Ther 2005;12:509-14.

309. Sax JK, El-Deiry WS. Identification and characterization of the cytoplasmic protein TRAF4 as a p53-regulated proapoptotic gene. J Biol Chem 2003;278:36435-44.

310. Simons M, Beinroth S, Gleichmann M, et al. Adenovirus-mediated gene transfer of inhibitors of apoptosis protein delays apoptosis in cerebellar granule neurons. Journal of neurochemistry 1999;72:292-301.

311. Silverstein H, Yules RB. The effect of diuretics on cochlear potentials and inner ear fluids. The Laryngoscope 1971;81:873-88.

312. Zhang H, Holzgreve W, De Geyter C. Bcl2-L-10, a novel anti-apoptotic member of the Bcl-2 family, blocks apoptosis in the mitochondria death pathway but not in the death receptor pathway. Human molecular genetics 2001;10:2329-39.

313. D'Sa-Eipper C, Leonard JR, Putcha G, et al. DNA damage-induced neural precursor cell apoptosis requires p53 and caspase 9 but neither Bax nor caspase 3. Development 2001;128:137-46.

314. Kotipatruni RR, Dasari VR, Veeravalli KK, Dinh DH, Fassett D, Rao JS. p53- and Bax-mediated apoptosis in injured rat spinal cord. Neurochemical research 2011;36:2063-74.

315. Mancini F, Di Conza G, Pellegrino M, et al. MDM4 (MDMX) localizes at the mitochondria and facilitates the p53-mediated intrinsic-apoptotic pathway. The EMBO journal 2009;28:1926-39.

316. Mihara M, Erster S, Zaika A, et al. p53 has a direct apoptogenic role at the mitochondria. Mol Cell 2003;11:577-90.

317. Moll UM, Marchenko N, Zhang XK. p53 and Nur77/TR3 - transcription factors that directly target mitochondria for cell death induction. Oncogene 2006;25:4725-43.

318. Palacios G, Moll UM. Mitochondrially targeted wild-type p53 suppresses growth of mutant p53 lymphomas in vivo. Oncogene 2006;25:6133-9.

319. Yu Z, Wang H, Zhang L, et al. Both p53-PUMA/NOXA-Bax-mitochondrion and p53-p21cip1 pathways are involved in the CDglyTK-mediated tumor cell suppression. Biochemical and biophysical research communications 2009;386:607-11.

320. Klaidman L, Morales M, Kem S, Yang J, Chang ML, Adams JD, Jr. Nicotinamide offers multiple protective mechanisms in stroke as a precursor for NAD+, as a PARP inhibitor and by partial restoration of mitochondrial function. Pharmacology 2003;69:150-7.

321. Luo J, Nikolaev AY, Imai S, et al. Negative control of p53 by Sir2alpha promotes cell survival under stress. Cell 2001;107:137-48.

322. Sadanaga-Akiyoshi F, Yao H, Tanuma S, et al. Nicotinamide attenuates focal ischemic brain injury in rats: with special reference to changes in nicotinamide and NAD+ levels in ischemic core and penumbra. Neurochemical research 2003;28:1227-34.

323. Ding D, Jiang H, Fu Y, Li Y, Salvi R. Ototoxic model of oxaliplatin and protection from nicotinamide adenine dinucleotide. Journal of Otology 2013;8 22-30.

324. Vaziri H, Dessain SK, Ng Eaton E, et al. hSIR2(SIRT1) functions as an NAD-dependent p53 deacetylase. Cell 2001;107:149-59.

325. Brunet A, Sweeney LB, Sturgill JF, et al. Stress-dependent regulation of FOXO transcription factors by the SIRT1 deacetylase. Science 2004;303:2011-5.

326. Motta MC, Divecha N, Lemieux M, et al. Mammalian SIRT1 represses forkhead transcription factors. Cell 2004;116:551-63.

327. Sakamoto J, Miura T, Shimamoto K, Horio Y. Predominant expression of Sir2alpha, an NAD-dependent histone deacetylase, in the embryonic mouse heart and brain. FEBS Lett 2004;556:281-6.

328. Smith J. Human Sir2 and the 'silencing' of p53 activity. Trends in cell biology 2002;12:404-6.

329. Smith JS, Avalos J, Celic I, Muhammad S, Wolberger C, Boeke JD. SIR2 family of NAD(+)-dependent protein deacetylases. Methods in enzymology 2002;353:282-300.

330. Tanno M, Sakamoto J, Miura T, Shimamoto K, Horio Y. Nucleocytoplasmic shuttling of the NAD+-dependent histone deacetylase SIRT1. The Journal of biological chemistry 2007;282:6823-32.

331. Jiang H, Ding D, Fu Y, Salvi R. Ototoxic effects of carboplatin in organotypic cultures in rats and chinchillas. Abstr Assoc Res Otolaryngol 2010.

332. Holzer AK, Howell SB. The internalization and degradation of human copper transporter 1 following cisplatin exposure. Cancer Res 2006;66:10944-52.

333. Holzer AK, Katano K, Klomp LW, Howell SB. Cisplatin rapidly down-regulates its own influx transporter hCTR1 in cultured human ovarian carcinoma cells. Clin Cancer Res 2004;10:6744-9.

334. Holzer AK, Samimi G, Katano K, et al. The copper influx transporter human copper transport protein 1 regulates the uptake of cisplatin in human ovarian carcinoma cells. Mol Pharmacol 2004;66:817-23.

335. More SS, Akil O, Ianculescu AG, Geier EG, Lustig LR, Giacomini KM. Role of the copper transporter, CTR1, in platinum-induced ototoxicity. The Journal of neuroscience : the official journal of the Society for Neuroscience 2010;30:9500-9.

336. Pabla N, Murphy RF, Liu K, Dong Z. The copper transporter Ctr1 contributes to cisplatin uptake by renal tubular cells during cisplatin nephrotoxicity. Am J Physiol Renal Physiol 2009;296:F505-11.

337. Safaei R. Role of copper transporters in the uptake and efflux of platinum containing drugs. Cancer Lett 2006;234:34-9.

338. Safaei R, Howell SB. Copper transporters regulate the cellular pharmacology and sensitivity to Pt drugs. Crit Rev Oncol Hematol 2005;53:13-23.

339. Safaei R, Otani S, Larson BJ, Rasmussen ML, Howell SB. Transport of cisplatin by the copper efflux transporter ATP7B. Mol Pharmacol 2007.

340. Wu X, Ding D, Liu H, Salvi R. Oxaliplatin induced lesions of the vestibular sensory epithelium in organotypic cultures. Abstr Assoc Res Otolaryngol 2011.

341. Clerici WJ, Yang L. Direct effects of intraperilymphatic reactive oxygen species generation on cochlear function. Hearing research 1996;101:14-22.

342. Dehne N, Lautermann J, Petrat F, Rauen U, de Groot H. Cisplatin ototoxicity: involvement of iron and enhanced formation of superoxide anion radicals. Toxicol Appl Pharmacol 2001;174:27-34.

343. Hsu DZ, Chen KT, Lin TH, Li YH, Liu MY. Sesame oil attenuates Cisplatin-induced hepatic and renal injuries by inhibiting nitric oxide-associated lipid peroxidation in mice. Shock 2007;27:199-204.

344. Jung M, Hotter G, Vinas JL, Sola A. Cisplatin upregulates mitochondrial nitric oxide synthase and peroxynitrite formation to promote renal injury. Toxicol Appl Pharmacol 2009;234:236-46.

345. Gabaizadeh R, Staecker H, Liu W, et al. Protection of both auditory hair cells and auditory neurons from cisplatin induced damage. Acta Otolaryngol 1997;117:232-8.

346. Rybak LP, Husain K, Whitworth C, Somani SM. Dose dependent protection by lipoic acid against cisplatin-induced ototoxicity in rats: antioxidant defense system. Toxicol Sci 1999;47:195-202.

347. Ishikawa T, Ali-Osman F. Glutathione-associated cis-diamminedichloroplatinum(II) metabolism and ATP-dependent efflux from leukemia cells. Molecular characterization of glutathione-platinum complex and its biological significance. The Journal of biological chemistry 1993;268:20116-25.

348. Mistry P, Loh SY, Kelland LR, Harrap KR. Effect of buthionine sulfoximine on PtII and PtIV drug accumulation and the formation of glutathione conjugates in human ovarian-

carcinoma cell lines. International journal of cancer Journal international du cancer 1993;55:848-56.

349. Hanigan MH, Gallagher BC, Townsend DM, Gabarra V. Gamma-glutamyl transpeptidase accelerates tumor growth and increases the resistance of tumors to cisplatin in vivo. Carcinogenesis 1999;20:553-9.